

73

CR 73445
Available to the Public

NASA

STUDY OF ASTRONAUT'S ABILITY TO DETECT STARS
THROUGH A CONTAMINATED SPACECRAFT WINDOW

Final Report

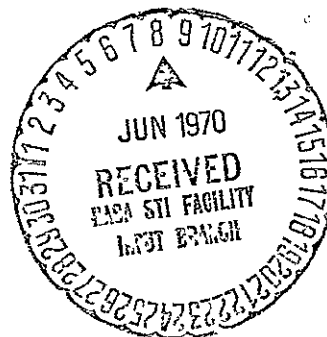
Distribution of this report is provided in
the interest of information exchange.
Responsibility for the contents resides in
the author or organization that prepared it.

May 1970

Prepared under Contract NAS 2-5015

Honeywell Inc.
Systems and Research Center
Minneapolis, Minnesota

for



NATIONAL AERONAUTICS AND SPACE ADMINISTRATION

FACILITY FORM 602	N70-28416	
	(ACCESSION NUMBER)	(THRU)
	156	1
	(PAGES)	(CODE)
	CR-73445	31
	(NASA CR OR TMX OR AD NUMBER)	(CATEGORY)

Reproduced by
NATIONAL TECHNICAL
INFORMATION SERVICE
US Department of Commerce
Springfield VA 22151

156P

NASA

STUDY OF ASTRONAUT'S ABILITY TO DETECT STARS
THROUGH A CONTAMINATED SPACECRAFT WINDOW

Final Report

by

R. P. Heinisch
R. N. Schmidt

Distribution of this report is provided in
the interest of information exchange.
Responsibility for the contents resides in
the author or organization that prepared it.

May 1970

Prepared under Contract NAS 2-5015

Honeywell Inc.
Systems and Research Center
Minneapolis, Minnesota

for

NATIONAL AERONAUTICS AND SPACE ADMINISTRATION

PRECEDING PAGE BLANK NOT FILMED.

FOREWORD

This technical report documents the results of a study of the effects of window contamination on the ability of an astronaut to detect stars. The program was performed for the National Aeronautics and Space Administration under Ames Research Center direction on Contract NAS 2-5015, Mr. Bedford A. Lampkin, technical monitor. This study is the second of a two-part program to investigate the ability of astronauts to detect stars visually through spacecraft windows. The first part is reported in a separate document entitled, "An Experimental and Analytical Study of Visual Detection in a Spacecraft Environment."

Honeywell Inc., Systems and Research Division, performed this study under the direction of Mr. R. N. Schmidt during the period 1 July 1969 through 1 January 1970. Dr. Roger P. Heinisch was the principal investigator. Assistance of Mr. Robert Daggit for running the vacuum tests, Messrs. Bim Gupta and Bernard Leland for data taking, and Mr. Tein Chow for preparing computer codes is gratefully acknowledged.

PRECEDING PAGE BLANK NOT FILMED.

CONTENTS	Page
FOREWORD	iii
SUMMARY	1
INTRODUCTION	1
NOMENCLATURE	3
EXPERIMENTAL APPARATUS	5
Vacuum System	7
Mass Spectrometer	7
Outgassing Fixtures	7
RTV Specimens	8
Material Collectors	10
Apollo Glass Specimen Holder	11
Window Samples	11
EXPERIMENTAL TECHNIQUE	11
Cleaning Procedure	11
Apollo Glass Specimens	15
PREDICTION OF VISUAL THRESHOLDS FOR STAR MAGNITUDES	15
Premises for Stellar Threshold Model	15
Discussion of Star Threshold Model for Sextant Telescope	18
STAR THRESHOLD CALCULATIONS	19
DISCUSSION OF RESULTS	20
Introduction	20
Scatter Measurements	21
Outgassing Studies	26
Photographs of Windows Contaminated by RTV IN A	32
Vacuum Environment	
Detection Thresholds	32
Polymerization of Outgassing	34
CONCLUSIONS	39
Recommendations	39
APPENDIX A LITERATURE REVIEW	
APPENDIX B SAMPLE THRESHOLD CALCULATION	
APPENDIX C MEASURED DATA	
APPENDIX D INFRARED SCANS AND MASS SPECTROMETER DATA	
REFERENCES	

PRECEDING PAGE BLANK NOT FILMED.

LIST OF ILLUSTRATIONS

Figure		Page
1	Schematic of Experimental Apparatus	6
2	Schematic Diagram of RTV Outgassing Fixtures	8
3	Photograph of Vacuum System	9
4	Photograph of Apollo Window Holder	12
5	Definition of Angles Used	12
6	Apollo Glass Specimen	16
7	Star Magnitude Detection Threshold versus Background Luminance (in space)	17
8	Contrast Thresholds as a Function of Background Luminance for Stimulus Size of 0.01 Arc Minute	19
9	Scatter Distribution for Window 246 ($\psi = 60^\circ$) Contaminated with High-Temperature-Cured RTV	22
10	Scatter Distribution of Window 244 ($\psi = 60^\circ$) Contaminated with Room-Temperature-Cured RTV	23
11	Scatter Distribution of Window 246 ($\psi = 50^\circ$) Contaminated with High-Temperature-Cured RTV	24
12	Scatter Distribution of Window 244 ($\psi = 30^\circ$) Contaminated with Room-Temperature-Cured RTV	25
13	Gas Chromatogram of Gas-Off Products from Silicon, RTV 560 (60 days 25°C)	29
14	Weight Loss Data for RTV 560	30
15	Weight Loss Data with Successive Increasing Temperatures of RTV 560, ref. 7	30
16	Significant Mass Fragments of RTV 560 After 90 Hours at 40°C, ref. 7	31
17	Significant Mass Fragments of RTV 560 at 60, 90 and 120°C, ref. 7	31
18	Window Contaminated by Room Temperature Cured RTV	33
19	Window Contaminated by High Temperature Cured RTV	33

LIST OF TABLES

Table		Page
1	Gas-Off Products from Silicone, RTV 560	28
2	Typical Cured Properties of RTV 560	29
3	Star Magnitude Predictions, Single Windows	35
4	Star Magnitude Predictions, Multiple Windows, 244 and 246	36
5	Star Magnitude Predictions, Single Windows	37
6	Star Magnitude Predictions, Multiple Windows, 244 and 246	38

STUDY OF ASTRONAUTS' ABILITY TO DETECT STARS THROUGH CONTAMINATED SPACECRAFT WINDOWS

By Roger P. Heinisch and Roger N. Schmidt
Systems and Research Center
Honeywell Inc.

SUMMARY

Astronauts have experienced difficulty in seeing navigational stars through spacecraft windows on the illuminated side of the spacecraft. The objective of this investigation was to predict the star magnitude which can be seen with the naked eye or a sextant telescope through a contaminated spacecraft window. The effects of geometry and outgassing conditions on that objective were studied. In addition, a relative comparison was made between laboratory contaminated windows and a small specimen flown on an Apollo flight.

The results indicate that the RTV560 used to seal the windows severely contaminates the window by outgassing. High-temperature-cured RTV560 is much worse in that respect than room-temperature-cured RTV560. In general, it is evident that, using a telescope or the naked eye, an astronaut will have difficulty seeing usual navigational stars under background conditions caused by light scattered from the contaminated windows studied in this program.

INTRODUCTION

This study (part two of a two-part program) was initiated because of the concern for the degradation of an astronaut's visual navigation capacity due to contamination of the spacecraft's window. The specific concern is that window contaminants, introduced either on the launch pad or in flight, will cause light to be scattered in the plane of the spacecraft window. This scattered light will produce a veiling luminance in the astronaut's field of view and will reduce the visual detection threshold.

The following four possibilities have been suggested as primary contributors to the astronaut's reduced visual detection threshold.

- 1) A cloud of debris (dumped waste, spacecraft outgassants, and reaction jet exhausts) surrounds the craft reducing the transmission qualities of the medium as well as producing a luminance veil resulting from scattered light.
- 2) The windows become contaminated with condensates and vehicle outgassants which reduce the window transmission qualities.

- 3) The contaminated windows scatter energy from other sources, such as the sun, moon, and earth, which creates a luminance veil
- 4) The clean window itself scatters and reflects energy from other sources which creates a luminance veil

The initial program (ref. 1) studied (4) above, this portion of the program studied (3) contaminate scattered energy. This investigation attempts only a cursory evaluation of the contamination problem.

The objective of the first program (ref 1) was to study the effect of the geometry of the source light-window-viewing orientation, window coating and to predict the star magnitude which could be detected with the naked eye or a sextant telescope through a spacecraft window. An apparatus was built, instrumented, and used for measuring the scattering luminance of typical spacecraft windows. Window illumination from the sun, moon, and earth was computed for typical orbit conditions. Star magnitude detection thresholds were predicted from the scattering data and window illuminations by applying the classical Tiffany visual threshold data. The star detection thresholds were computed for both unaided vision and vision using a monocular telescope. The measurements indicated that window cleanliness is of paramount importance in reducing light scattering. When considering the light transport through the spacecraft windows, light reflected off the windows from inside the spacecraft cabin was found to dominate the scattered light caused by the externally incident flux.

The results of this study provide a guideline by which the severity of the outgassing effects on astronaut's vision can be assessed. Three independent studies were conducted.

- The effect of possible contaminants introduced by the Apollo on-pad cleaning procedure was evaluated
- Light scatter from a glass specimen flown on the Apollo 9 and exposed to a spacecraft environment was measured to determine scatter levels
- The effect of contaminants caused by outgassing RTV silicone rubber was studied

The effect of spacecraft window contamination on the ability of an astronaut to visually detect stars is predicted as a function of six parameters. These parameters are the characteristics of the human eye, the effect of the optical system used to view the star, orientation of the window with respect to the sun, moon, and earth, distance from the sun, moon and earth, viewing angle, and number of window panes. For the purpose of this investigation, the ability of an astronaut to detect stars is defined as the minimum star magnitude that can be detected through a window for specified values of the above parameters. The definition of the detection ability was accomplished by completing the following four tasks

- Contaminating the window by condensing outgassants of RTV560 in a vacuum environment or on-pad cleaning procedure
- Measuring the light-scatter from various window orientations
- Calculating the light incident on the window for each specified "source" (sun, moon, and earth)
- Calculating star magnitudes based on a stellar threshold model presented in ref 1 (see Figure 18, that document)

The results of the first program revealed that the quality of the antireflection coating on windows has more influence on the scattering level than the type of coating examined. The better windows had as low a scattering level as a highly-polished optical flat. Painting the edges of the window black reduced the light scattering. Light scattering created by multiple-window configurations was found to be equivalent to the sum of individual windows (superposition theory can be used). The star magnitude detection thresholds were obtained and presented for the situation where a sextant telescope or the naked eye is used at the location of maximum, minimum, and average scatter for each window configuration. In general, when using a telescope, an astronaut in a spacecraft distant from the earth or moon is able to see stars as bright as a magnitude 2.00 star. On the other hand, with the naked eye, an astronaut has difficulty seeing the usual navigational stars under background conditions created by the light scattered from windows used in this program.

The light scattering distribution of three window configurations was measured for visible light with approximately the solar spectrum incident at specified angles. The windows studied were HEA coated Vycor.

Although the results of this study are far from conclusive in some areas, the tentative conclusions drawn provide a substantial basis for clarifying the most important steps to be taken in further study.

NOMENCLATURE

English

B	constant
BP	angular position of photometer when blackbody is in transmitted beam
BR	angular position of photometer when specular reflex from window is incident on blackbody

E	illumination
F	shape factor
L	luminance
LD	diffuser luminance
M	molecular weight
m/e	mass to charge ratio from mass spectrometer scans
N	molecules/unit area of surface
n	molecules/cm ² /sec
\vec{n}	window normal
P	vapor pressure of material in torr
Q	heat of absorption
R	gas constant
T	temperature
TB	angular position of detector in transmitted beam
W	weight loss, gm/cm ² /sec
WR	angular position of photometer when specular reflex from window is incident on photometer
WE	angular position of photometer when photometer views window edge
Greek	
τ	average time
τ_o	time related to lattice vibrations of a solid surface
λ	wavelength
ψ	angle between window normal and incident light beam
θ	angle between window normal and line of sight
c	contrast limen
ρ	reflectance

Subscripts

B	background
s	sun
t	threshold
w	window

EXPERIMENTAL APPARATUS

During Phase One of this investigation a unique apparatus were developed to measure the magnitude and distribution of light scattered from typical windows. A detailed discussion of the apparatus and the concepts on which the experimental procedure is based is given in ref 1. Scattering data obtained with that apparatus is used in this report to determine star magnitude detection thresholds for use with unaided binocular vision and with a monocular telescope.

The main components of the experimental facility are shown in Figure 1 and they include the following

- A fixed, high-temperature light source that approximates the spectral distribution in the visible portion of the solar spectrum
- A collimating lens to provide a 6-inch diameter light beam with divergence less than or equal to the sun's rays.
- A fixture to hold and position the spacecraft windows with respect to the light beam.
- A detector with the same spectral response as the human eye to record light scattering in various directions (0 to 360 degrees in the horizontal plane about the window).
- Blackbodies to absorb light and thus reduce the background level for the experiment.
- A filter hood to continuously blow filtered air over the window during the measurements.

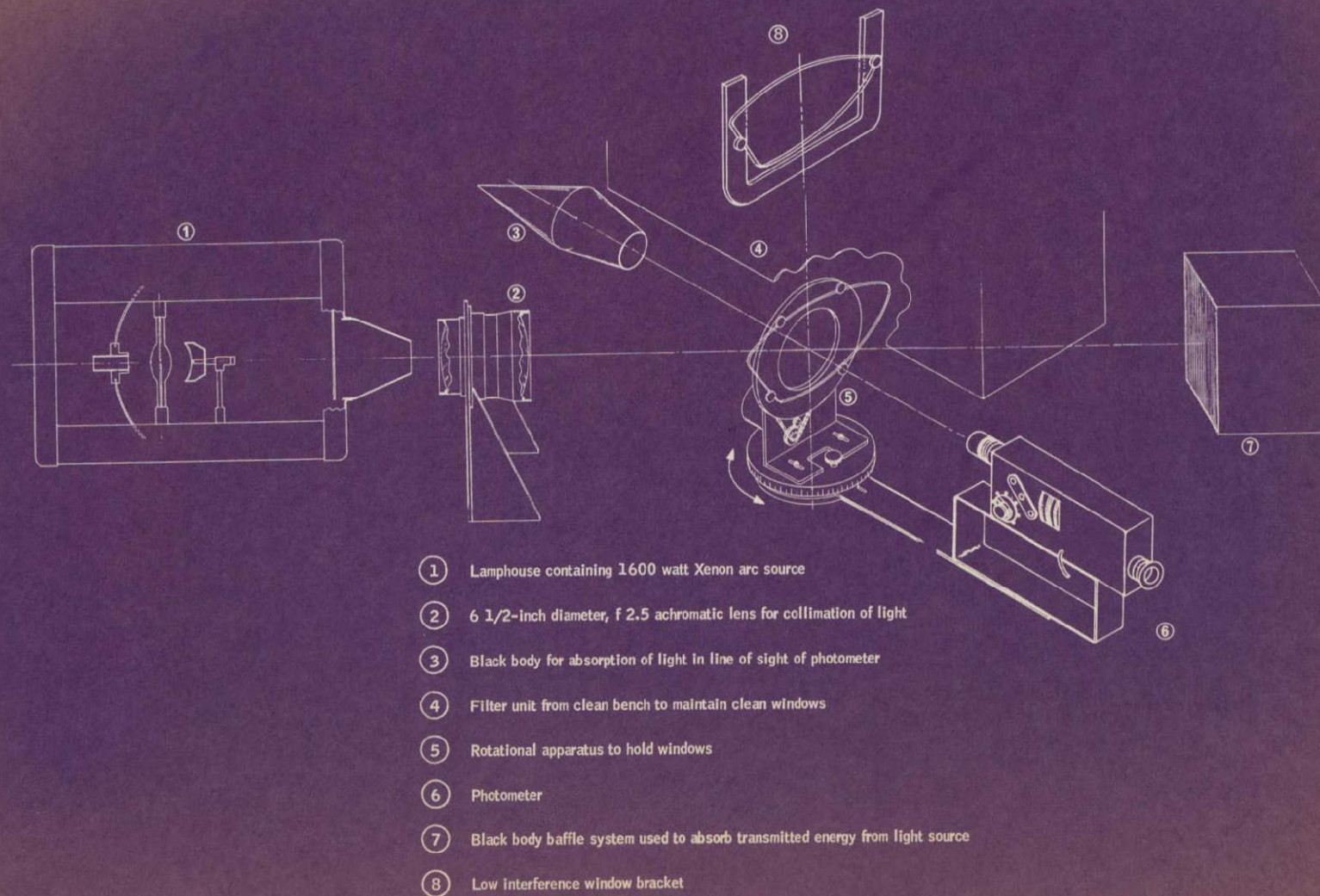


Figure 1. Schematic of Experimental Apparatus

So that the outgassing studies could be carried out in a vacuum environment, the following additional equipment was required for this investigation:

- Vacuum system
- Mass spectrometer which was connected to the vacuum system
- Fixtures used to hold the window and to heat RTV specimens in the vacuum chamber for the outgassing study
- Microscope slides and sodium chloride flats used in the vacuum system to collect the outgassing material.

Each of these components of the system is described in the following paragraphs.

VACUUM SYSTEM

The basic vacuum system used for the RTV outgassing study consisted of a standard 6-inch oil diffusion pump equipped with a liquid nitrogen trap. A vacuum collar which contained the feed-throughs was mated with an 18-inch diameter glass belljar.

MASS SPECTROMETER

A Quad 150 residual gas analyzer made by Electronic Associates Inc. (EAI) was used to monitor the background gas composition present during the outgassing experiment. This analyzer has an extended mass range of 1 to about 150 atomic mass units. Data obtained with the analyzer is used to qualitatively identify the residual vapors present before and while the samples are heated. This instrument was also used to determine relative outgassing rates during the experiment as a function of time to determine the time necessary for adequate collection while preventing prolongation of the experiment. This instrument also provided a comparison of outgassing rates for two RTV samples which were cured under different schedules. Another good point, the qualitative residual gas analyzer data is available for comparison with previous or subsequent experiments.

OUTGASSING FIXTURES

A very simple fixture (Figure 2) was designed to hold the window and to support and heat the RTV specimen. For the experiment there were RTV specimens placed symmetrically about the spacecraft window. Each resistance heater shown radiatively heated a six-inch square copper plate on which the RTV specimens were mounted. Thermocouples were placed in the copper

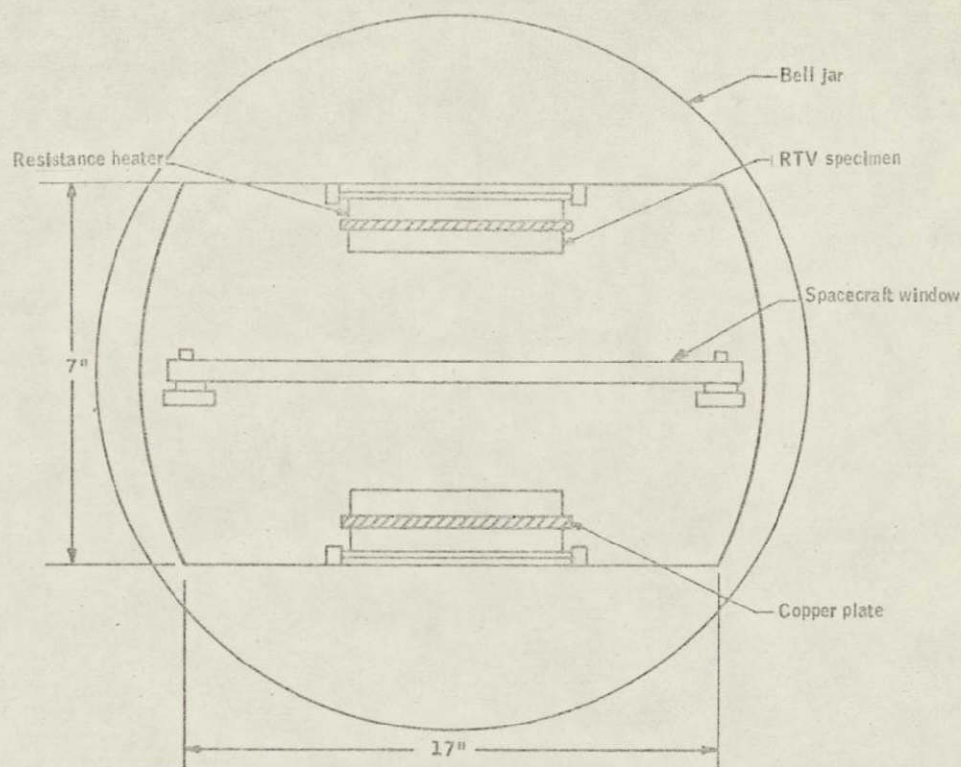


Figure 2. Schematic Diagram of RTV Outgassing Fixtures

plates to monitor the temperatures at which the RTV was being maintained. The fixture can be seen in a photograph of the apparatus in Figure 3.

RTV SPECIMENS

Twelve pounds of RTV R60 (silicone rubber) was purchased from the General Electric Company. This RTV was all from the same lot. Six by six by one-eighth-inch thick slabs of the RTV were prepared using two General Electric-recommended curing processes; a room temperature cure, and a high-temperature cure. The high-temperature cure used consisted of the following steps:

- 1) The RTV was weighed in a container to obtain an approximate amount used to make a slab.
- 2) This container was then placed in a vacuum chamber and pumped to about 10^{-3} torr pressure.

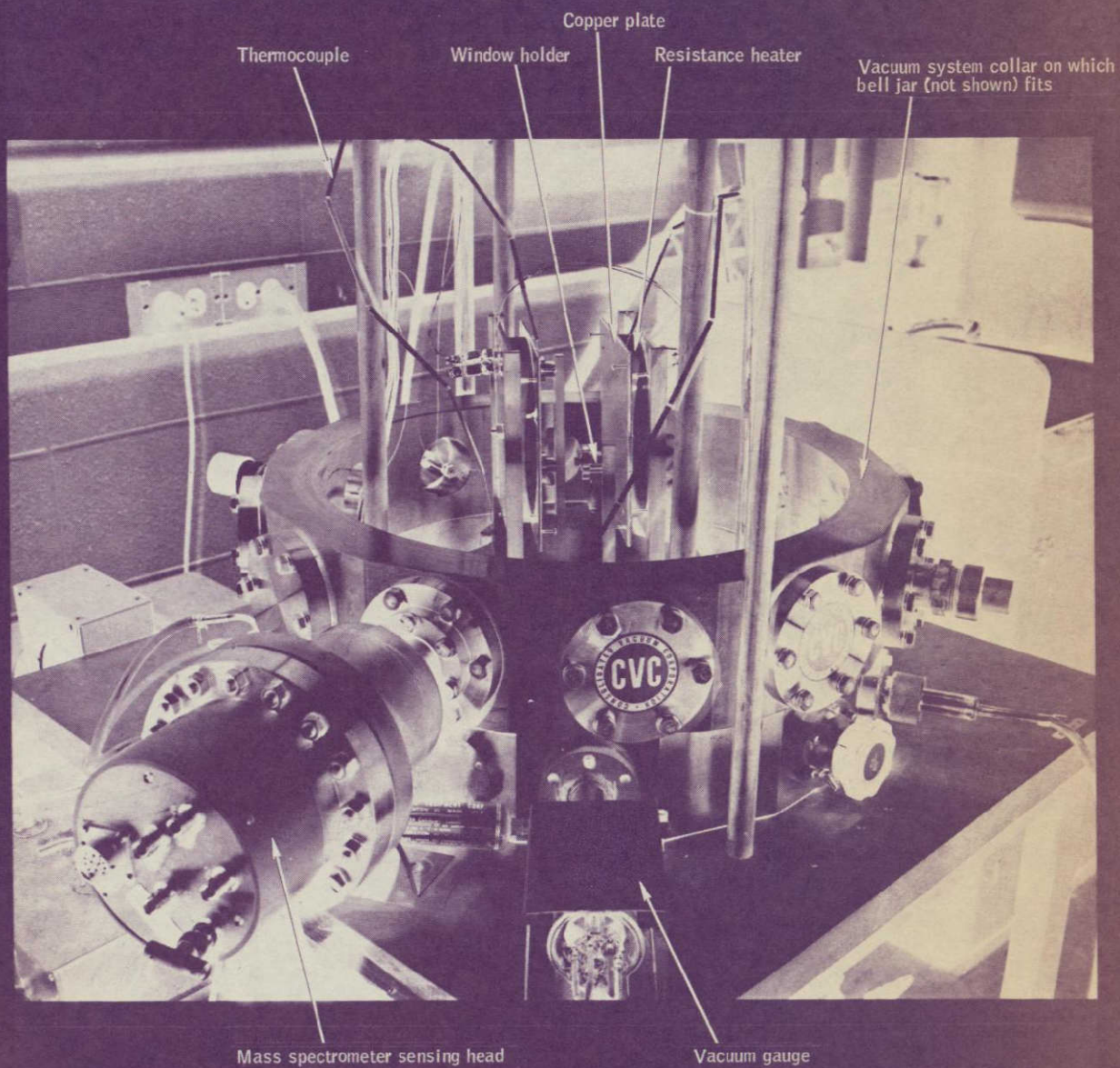


Figure 3. Photograph of Vacuum System

- 3) After the RTV had completed its boiling (outgassing), the container was removed from the vacuum system and the RTV was then carefully poured into the mold in which the RTV was cured.
- 4) The mold containing the RTV was again placed in the vacuum station and pumped to approximately 10^{-3} torr pressure.
- 5) Upon completion of the outgassing of the RTV, the mold containing the RTV was placed in a furnace and maintained at 400°F for 48 hours.
- 6) At the end of this time period the RTV slab was removed from the mold and found to be thoroughly cured, at least on the outer surfaces.

The RTV-560 material tested and that which has been actually used on flight vehicles did not have the same history. Since the outgassing characteristics depend on the manufacture process, cure, and any post-cure treatments, the outgassing probably differed somewhat from the RTV-560 used on Apollo vehicles or tested by others. However, sufficient RTV-560 material was procured on a same batch/same lot basis to prepare all samples needed so that a valid comparison was made as to the effect of cure on subsequent scattering.

MATERIAL COLLECTORS

Two different materials were used to collect outgassing products in the vacuum chamber, in addition to the windows. Glass microscope slides and sodium chloride flats were used as collectors. The sodium chloride flats were standard chemically pure crystals obtainable from Harshaw Chemical Co. The flats, nominally 1/8-inch thick by 3/4-inch square, were received packaged in sealed polyethylene bags. These packages were only opened just prior to insertion in the vacuum system to avoid contamination by the atmosphere.

During the experiment, the collector sample temperature was held at about 70°F because the window temperature during the subsequent scattering measurements was approximately 70°F, and also comparable collection of RTV 560 gassing products has been done at this temperature (see ref. 2). The sodium chloride collectors were used for infrared scans following the gassing experiments; these scans provide fingerprints of the collected material and permit qualitative comparison of effects of the two cures. The glass slide collectors were given to NASA/Ames Research Center for their use. The sodium chloride collectors were scanned from 2.5 to 15 microns

with a Beckman IR-12 Infrared Spectrometer. The scans were run during approximately the same time period as the scattering measurements in the windows in order to compensate for any room temperature outgassing from the windows.

APOLLO GLASS SPECIMEN HOLDER

A special holder had to be fabricated so that the Apollo window sample could be held in the same plane as the Vycor windows studied. This fixture is shown in Figure 4. Due to the small size of the Apollo glass sample, large angles between the direction of the incident beam and the normal surface of the window could not be obtained as in previous studies. These angles are designated ψ as shown in Figure 5.

WINDOW SAMPLES

The window samples used in this investigation were supplied by NASA. They were space vehicle windows which were repolished and recoated by OCLI. The glass was Corning Vycor, and it was high-efficiency, antireflection (HEA) coated. The windows were assigned a numerical designation as follows:

<u>Number</u>	<u>Coating</u>
244	HEA
246	HEA

This numerical identification is used throughout this report.

In addition, a small glass specimen that had been flown on an Apollo mission was measured to determine light scatter magnitude.

EXPERIMENTAL TECHNIQUE

This section contains a detailed description of the cleaning procedures used, together with a description of the Apollo glass specimen.

CLEANING PROCEDURE

The cleaning procedure which was developed at Honeywell was used on the first phase of this contract and was described in ref. 1. The general procedure used, repeated here for ready reference, is:

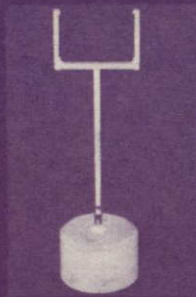


Figure 4. Photograph of Apollo Window Holder

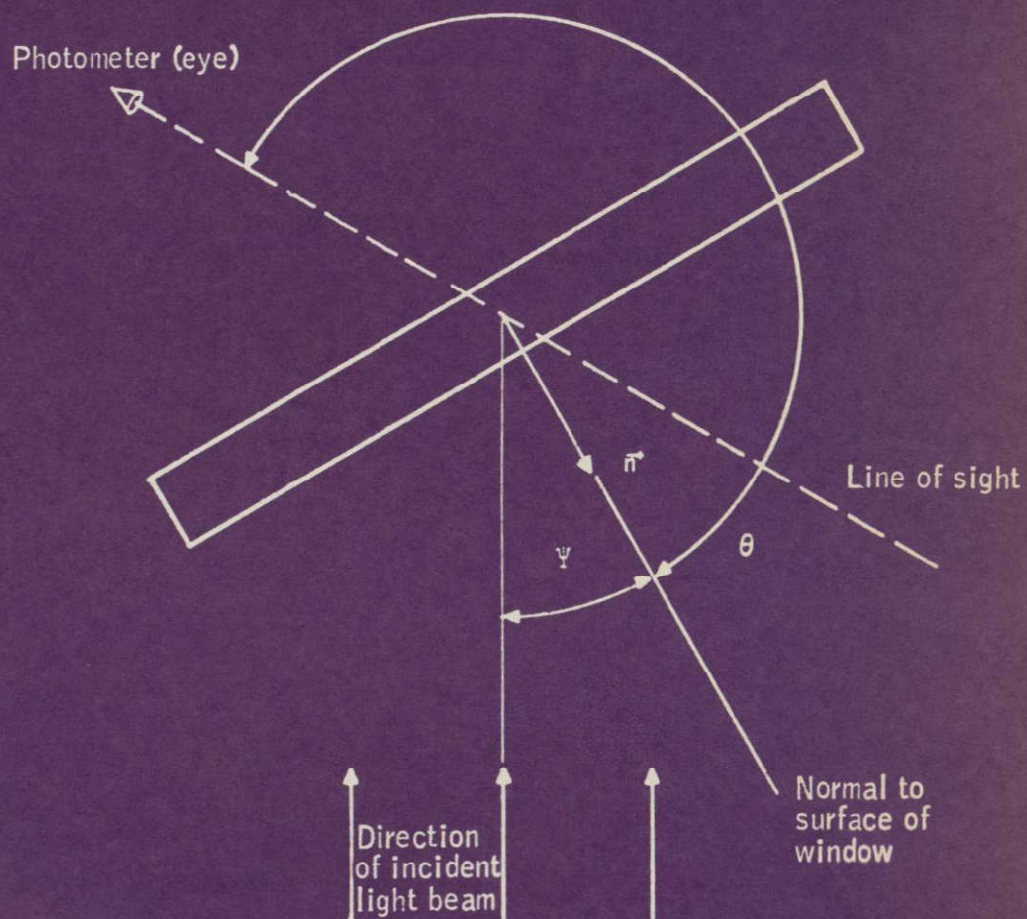


Figure 5. Definition of Angles Used

- 1) Soak the element for several hours in hot "MICRO" detergent solution
- 2) Rinse and rub with wet cotton swab, using deionized filtered water. Repeat this several times.
- 3) In a final step, the optical surface is covered with deionized water which is blown off with a jet of dry nitrogen. The removal of the water should be completed. Also, care should be taken not to permit water droplets from the edge to flow across the optical surface after it is dry.
- 4) Inspect the cleaned surface by directing a bright collimated beam of light on the surface and viewing the surface against a black background in a darkened room.
- 5) If step (4) shows the optical element to be clean, proceed to measure scattering levels.

The on-pad cleaning procedure apparently used by NASA was also used in this study to clean the Vycor windows. The procedure has been described in a North American Aviation Inc. document with a code identification number 03935. The specification as described in that document was written to cover windows processed to the extent of having sealant dam bonded in place so that the window could no longer be cleaned by immersion or flooding with a cleaning solvent (as specified in LA 0110-020)

The on-pad cleaning procedure is:

- 1) Air blow - All glass surfaces are blown with a gentle stream of clean, dry air from a hand-operated rubber aspirator or syringe, or with a bottle of compressed dry argon or nitrogen gas to remove loosely adhering particles.
- 2) Distilled water wash - Following the air blow, the window shall be washed with distilled water to remove deposited salts and the remaining dust particles.
- 3) Methyl ethyl ketone wash - Following the water wash, the window shall be washed with chemically pure methyl ethyl ketone to remove any organic stains such as transferred adhesive from the protective paper on the window, fingerprints, or other body oils.
- 4) Isopropyl alcohol wash - Following the methyl ethyl ketone wash, the window shall be washed with chemically pure isopropyl alcohol as the final washing step to remove any residues from the previous washings

- 5) Inspection - The cleanliness of the window can be determined by reflected light. A fluorescent tube about one foot long should be used. Enclose the tube in a metal container (shim stock wrapped around the tube will be suitable). The enclosure should have a 1/16 x 4 inch-long slit milled in it so that a uniform beam of light can be reflected from the surface of the glass.

In the case of coated windows, the uniformity of the color of the reflected light will indicate the degree of cleanliness.

The general washing procedure monitored above in the window cleaning operation involves the following steps:

- 1) Saturate a Johnson and Johnson "Preptic" absorbent cotton ball or the equivalent with solvent.
- 2) Wash a small section of the window at a time. Apply sufficient pressure on the cotton ball to release a desired amount of solvent so that running does not become excessive.
- 3) Immediately wipe the washed portion of the window with a clean, dry, lint-free, soft cotton cloth to absorb all of the solvent before it evaporates.
- 4) Repeat the procedure until the entire window has been washed with one solvent before proceeding to the next solvent.
- 5) When the cleaning operation has been completed, examine the window for uniformity of cleanliness. If dirty areas remain, they may be spot washed using the same procedure as before.

The on-pad cleaning procedure was able to randomly get the window exceptionally clean. The use of the word randomly is in the following context. Step five of the on-pad cleaning procedure is concerned with inspection. Due to the technique described above, one cannot absolutely determine the cleanliness of the window. However, if the window is placed in the intense light generated in the system described under the section titled Experimental Apparatus, using the on-pad clean procedures, it is possible to obtain an exceptionally clean window, therefore, the word randomly characterizes the inspection technique rather than actual cleaning procedure.

In the on-pad cleaning procedure there is a subsection concerned with the general washing procedure. Step 3 of that procedure is worthy of comment at this point. A baby diaper that has been washed many times is an extremely good approximation of the clean, dry, lint-free, soft cotton cloth specified in the procedure. Gently wiping the surface with this baby diaper removes any remaining lint and results in a window having only extremely small amounts of light scatter.

In ref. 1, note was made of the use of the Honeywell cleaning procedure on various Vycor windows. During the course of that work it was noted that the surface of window 246 (HEA coated window) appeared relatively milky. This appearance was still evident at the beginning of this investigation. However, the application of the on-pad clean procedure eliminated this opaque film. Subsequent recleaning using the Honeywell cleaning procedure resulted in the partial reestablishment of that film. It would appear that the MICRO detergent chemically reacts in some manner with the HEA coating that has been placed on the surface of the window. It is also apparent that in some way the chemicals used (i.e., methyl-ethyl-ketone and isopropyl alcohol) also apparently react with the film which is a result of the reaction previously mentioned. Due to the scope of this work, no efforts were made to identify the chemical reactions discussed above.

It should be mentioned that if either of the two cleaning procedures was used, with the inspection technique which is described as step 4 of the Honeywell procedure, the windows would appear equally clean to the naked eye. This statement excludes window 246 which had a milky film.

APOLLO GLASS SPECIMENS

The dimensions of the Apollo glass specimens are given in Figure 6. The material used in the Apollo window specimen was a Corning Glass Works product in accordance with Grumman Aircraft Corp. Specification LSM 14-4404. The inboard surface of the glass was coated with high-efficiency, anti-reflectance coating Grumman Aircraft Corp. Specification LSM 14-4402. The outboard surface of the glass was coated with a multilayer blue-red coating according to Grumman Aircraft Corp. Specification LSM 14-4403. Shipped with the Apollo glass specimen was paper work which documented the following. The outboard section contained RTV remnants. There was a note to the effect that a fingerprint was removed from the inboard surface near the center of the glass specimen. The materials used for the cleaning were noted to be ethyl alcohol and isopropyl alcohol. This cleaning was performed on 19 March 1969.

During the period of time that this window was in the possession of Honeywell, it was handled with the utmost care. To best of our knowledge no additional contamination was added to the surface nor was any of the contamination originally present intentionally removed.

PREDICTION OF VISUAL THRESHOLDS FOR STAR MAGNITUDES

PREMISES FOR STELLAR THRESHOLD MODEL

People with normal vision making observations from earth under normally clear atmospheric conditions are able to detect stars up to about the 6th magnitude. This range may be extended to the 7th magnitude when viewing

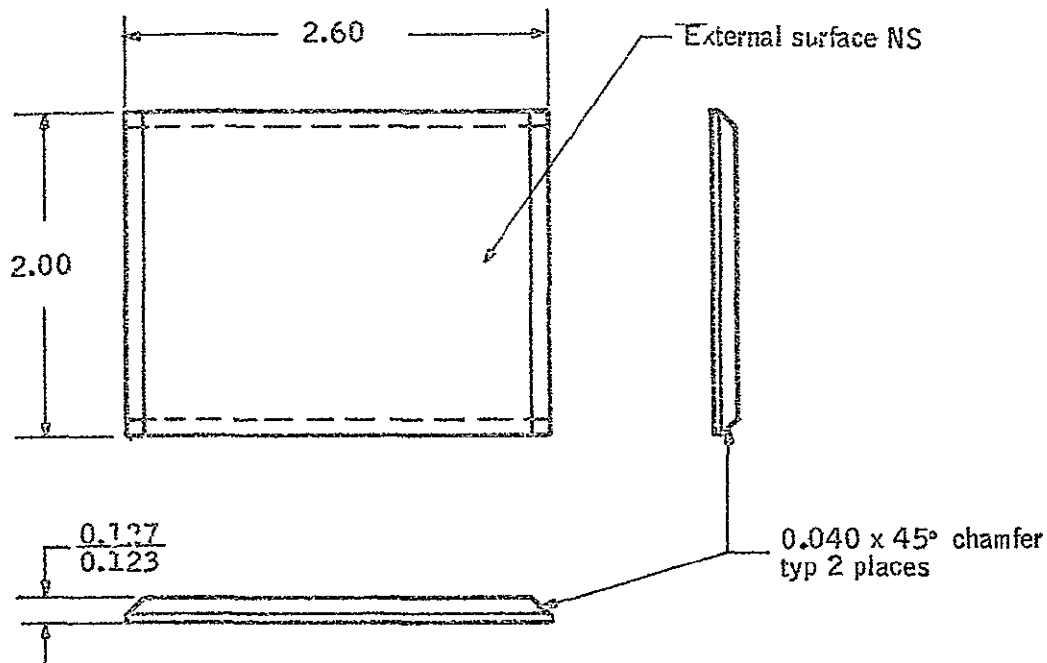


Figure 6 Apollo Glass Specimen

where haze and extraneous light attenuation factors are significantly reduced. Although many factors are related to optimal viewing conditions, four general factors can be defined that play a large role in the detection of a specific star: (1) the viewer's adaptation level, (2) the illuminance level of the star in the plane of the viewer's eye, (3) background luminance level and (4) the viewer's knowledge of star location. For our purpose, two assumptions have been made regarding these four factors: (1) the adaptation level of the viewer corresponds to the existing luminance level, and (2) the viewer is knowledgeable concerning the location of the star. The acceptance of these two assumptions greatly simplifies the star threshold prediction task and, in addition, makes it possible to draw on some available probability-of-detection data to supplement the detection threshold values.

Stellar magnitude, as established, is based on sea level illuminance levels. Consequently, to predict star magnitude threshold values from spacecraft, it is necessary to correct stellar magnitude values for light losses due to atmospheric absorption and scatter. Baker (ref. 3) has equated this factor to a 30 percent increase in illumination at the edge of the atmosphere. This value converted to star magnitude extends the magnitude range by a factor of 0.22.

Viewing with the prescribed monocular telescope is herein idealized. We consider the telescope to be a perfect optical instrument. Thus, optical aberrations which may reduce image quality and illumination to some degree are ignored. Only the transmittance and light amplification factors which correspond to the characteristics of a typical telescope are considered.

Backwell's Tiffany study (ref. 4) and Hardy's treatment (ref. 5) of Blackwell's data are used as a basis for a visual star detection prediction model. The specific reasons for such a choice are presented in ref. 1

Figure 7 was developed in ref. 1 to serve as our stellar prediction threshold model. It is repeated here for ready reference. The abscissa corresponds to the background luminance level which is superimposed upon the star luminance. On the righthand ordinate or margin an illumination scale has been included which permits the reader to relate a threshold value to a corresponding illumination value (E_t). The illumination scale is a logarithmic scale with values expressed in positive form in accordance with mathematical convention. Thus, a characteristic of (-8 00) would have an equivalent form of (4 00 - 12 00)

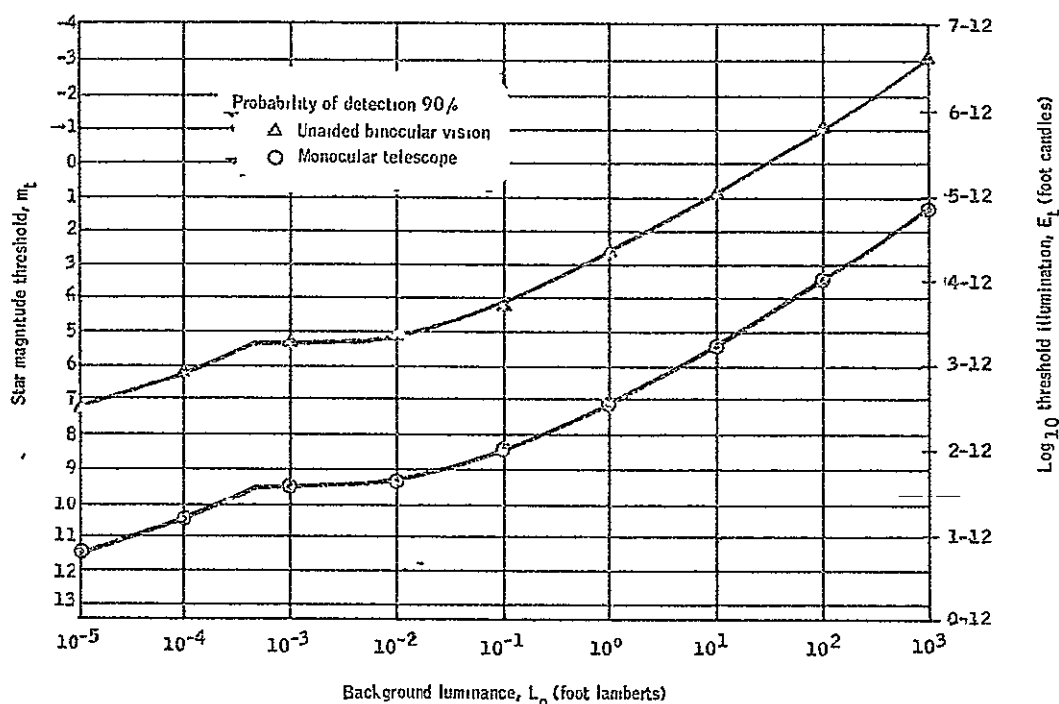


Figure 7. Star Magnitude Detection Threshold versus Background Luminance (in space)

The star threshold model is simply a two-curve plot with two scales that permit relating thresholds either in terms of stellar magnitude or illumination in units of foot candles. All values have been corrected to read star magnitude thresholds for the 90 percent probability of detection level and for exoatmospheric viewing conditions.

DISCUSSION OF STAR THRESHOLD MODEL FOR SEXTANT TELESCOPE

A stellar magnitude threshold curve has been generated that corresponds to a sextant telescope with a 32-mm objective lens, 4-mm exit pupil, a magnification factor (M) of 8X and a light transmittance factor (τ) of 0.65. The telescope threshold values are based on the premise that illumination from the background is decreased by the transmittance factor 0.65 and that illumination from a star is increased by the numerical factor 41.6. The factor 41.6 is arrived at by calculating the product of $M^2 \tau$ or by the more accepted method of multiplying the transmittance factor time the square of the ratio of the objective lens to the exit pupil.

It is assumed that the pupil of the eye is always as large or larger than or of the same size as the exit pupil of the monocular telescope.

To correct for the expected change in star magnitude threshold values when viewing through a telescope of these characteristics, we first corrected for the threshold change resulting in a background luminance level reduction and then considered the stellar illumination increase. Star magnitude was not been altered for the window transmittance factor because the nominal transmittance was near 1.0 and thus its effect is second order.

The former correction may be made by a number of methods. One method would be to refer to the star magnitude curve for the unaided eye. Using each decade interval (10^{-5} , 10^{-4}) on the abscissa as reference points and, from points on the abscissa corresponding to 0.65 x these reference points, construct vertical lines to the above unaided eye detection curve. At these junctions draw horizontal lines back to the vertical grid line corresponding to each of their respective reference values. These junctions would then serve as loci to construct a curve which would correct star magnitude threshold for the background luminance reduction occurring with a prescribed telescope.

Although this procedure is straightforward, a measure of accuracy can be gained by constructing a plot of contrast threshold versus background luminance based on Hardy's star magnitude thresholds for a 0.01-minute stimulus size. This information is presented as Figure 8.

Contrast thresholds are determined from an enlarged plot of Figure 8. These contrast threshold values are then used to determine the illumination threshold (E_t) in foot candles. These illumination threshold values thus correspond to stellar magnitude thresholds while viewing with our prescribed telescope with consideration given only to the background luminance change that would result due to the transmittance factor.

The second step necessary is to consider the increase in stellar illumination realized while viewing with the telescope. As stated, a 41.6 x increase in stellar illumination has been assumed when viewing with the sextant telescope. This set of values then serves as the numerical base for the stellar magnitude threshold curve as a function of background luminance for the aided eye.

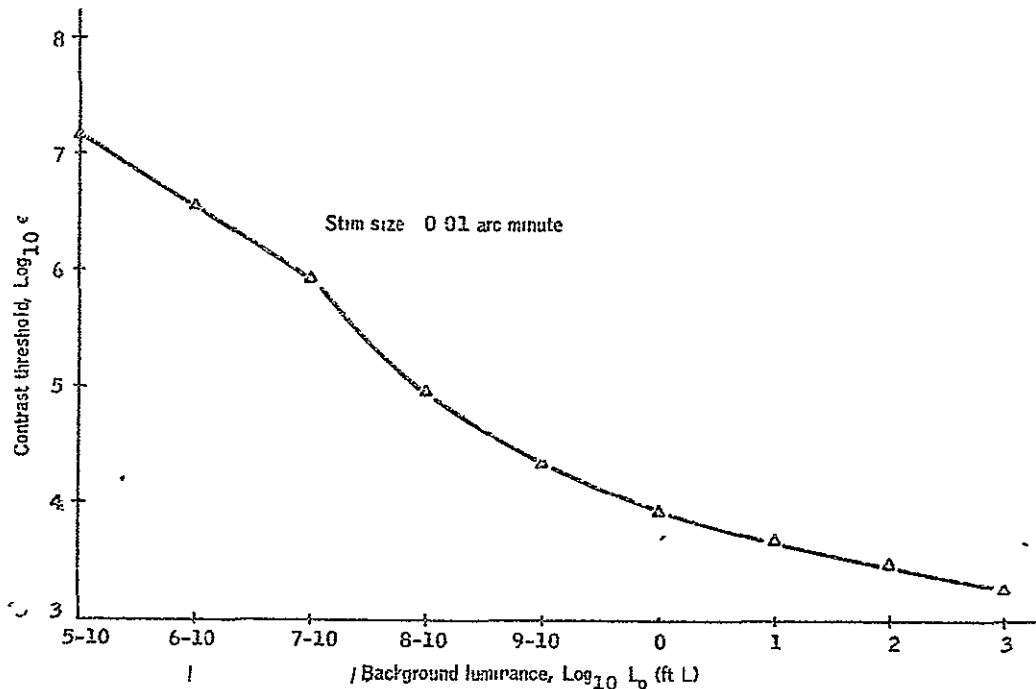


Figure 8. Contrast Thresholds as a Function of Background Luminance for Stimulus Size of 0.01 Arc Minute

In practice, the above model has some evident shortcomings. Regarding the reduction in background luminance level when viewing with or without the telescope, it is not likely that the viewing field will be devoid of other stars. Stars in close proximity to the viewing star will obviously contribute somewhat to light adaptation, increasing the visual threshold. In addition, instant dark adaptation has been assumed when in reality this is a rather slow process, therefore, the assumption of complete adaption is only partially correct for this case.

STAR THRESHOLD CALCULATIONS

This section summarizes the calculation techniques used in making the star threshold predictions. Three different calculation procedures were used, one for each of the following conditions: the window distant from the planet, the window near the planet, and back reflections inside the spacecraft. Each of these has been described in detail in ref. 1.

The condition where the window is distant from a planet is the easiest and will be discussed first. The illumination incident (foot candles) on the window can be assumed collimated and incident from a single direction. Therefore, the two-dimensional experimental scatter data is directly applicable. The incident illumination is multiplied by the percent of scattering to give the scattered contribution to the background luminance. This background value is used to obtain the star magnitude threshold. A numerical example of this particular calculation is presented in Appendix B.

The technique describing the window near the planet situation follows. The two-dimensional experimental scattering data could not be applied directly to this three-dimensional physical condition, so a somewhat realistic but highly simplified calculation scheme was devised. The illumination incident on the spacecraft window was calculated for conical segments symmetric about the window normal.

Two experimental two-dimensional angles fall in the conical segment. All the energy was assumed to be contained in the first quadrant. For the conditions where the illumination was contained in more than one conical section, the total scatter luminance was computed by summing the individual contributions.

Back reflection inside the spacecraft was considered in two separate ways. First, the transmitted light beam was assumed to reflect from an 85 percent diffuse reflection space suit one foot from the window. Because the entire 6-inch diameter beam was assumed to be reflected from the suit, the suit was approximated by a semi-infinite diffuse plane. Reflections off the window (see Appendix C for experimental data) as well as scattering were included in the computation.

The interior of the spacecraft was also modeled by a 9-foot diameter sphere that diffusely reflected 85 percent of the illumination. Again, the specular reflection measured in the laboratory (Appendix C) was included in the computational scheme. To simplify the numerical effort, a computer program was written to accomplish the computations. Results for each of the above models are presented in the next section, along with the data which assumed no internal reflections.

DISCUSSION OF RESULTS

INTRODUCTION

Scatter measurements were performed on two separate windows as well as on a sample specimen that had been flown on an Apollo mission. Both of the windows were HEA-coated [an Optical Coatings Laboratory Inc. (OCLI) proprietary antireflection coating]. Using the scatter distributions for each respective window, threshold conditions were computed under which an astronaut could detect a star through such background luminance as was afforded by the scattered light (or reflected light from the spacecraft interior).

All of the experimental data obtained during the course of the experiment is presented in Appendix C. The objective of this effort was to obtain from that data the maximum, minimum, and the arithmetic average values of star magnitude that could be detected.

An anomalous condition was discovered regarding the cleaning techniques used. The Honeywell technique used in ref. 1 was originally to be replaced in this study by the on-pad technique used by NASA. When the on-pad technique was utilized, the scatter levels were slightly lower than those

measured in ref. 1. In order that a proper reference (in time) be readily available, the windows were contaminated and recleaned using the Honeywell technique. Subsequent remeasurement of the scattering characteristics of the windows resulted in slightly more scatter than obtained after the on-pad cleaning, but still less scatter than that originally obtained using the Honeywell procedure as described in ref. 1.

To hold down the size of this report not all of the available data has been put on graphs. It is felt that sufficient understanding of the trends of the available data can be obtained from data encompassing selected maximum and minimum scatter values.

SCATTER MEASUREMENTS

Figures 9 through 12 illustrate the scattering distributions at the particular window incident orientation (Ψ angles) where the maximum and the minimum scattering occurs for windows 244 and 246 after contamination. Window 244 was contaminated in the vacuum system by the offgassing products of the room-temperature-cured RTV. The data presented for window 246, on the other hand, was obtained after the window was contaminated from the products of the high-temperature-cured RTV. The discontinuous character of the data indicates a few data inputs during the course of the experiment that are not scattering data.

The discontinuities evident in Figures 9 through 12 are due to physical constraints inherent in the measurement apparatus and the physics of the problem. The data for those discontinuities are presented in Appendix C. In particular, referring to Figure 9, WR denotes the specular reflection from the window. As the window-sun angle increases (i.e., $\Psi > 0^\circ$) the specular reflection from the window is incident on the photometer at larger θ values. Although a valid measurement can be (and was) made at this position, the data, from a scattering standpoint, is anomalous. Also when the photometer is rotated to $\theta = 90$ degrees or 270 degrees, WE, the line of sight is parallel with the front and back surfaces of the window. In effect, the measurement is of the background only. The notation TB refers to the transmitted beam. The intense 6-inch diameter beam is, to a large extent, transmitted by the window(s). Again, measurements could have been made but they would have indicated the transmittance of the window and not the scattering in a particular direction. When the photometer is rotated such that the blackbody is flooded by the transmitted beam, the photometer views a background (the illuminated blackbody) that is of higher intensity than the scattering. Consequently, measurement cannot be made at this position. In like manner, the blackbody cannot be placed directly in the path of the light beam which is specularly reflected from the window. This instance is denoted BR.

Of particular interest is a direct comparison of Figures 9 and 10. These data were obtained after the windows were subjected to outgassing from RTV in a vacuum environment. These curves include the locations where the lowest scattering value occurs for windows 244 and 246. The two scattering

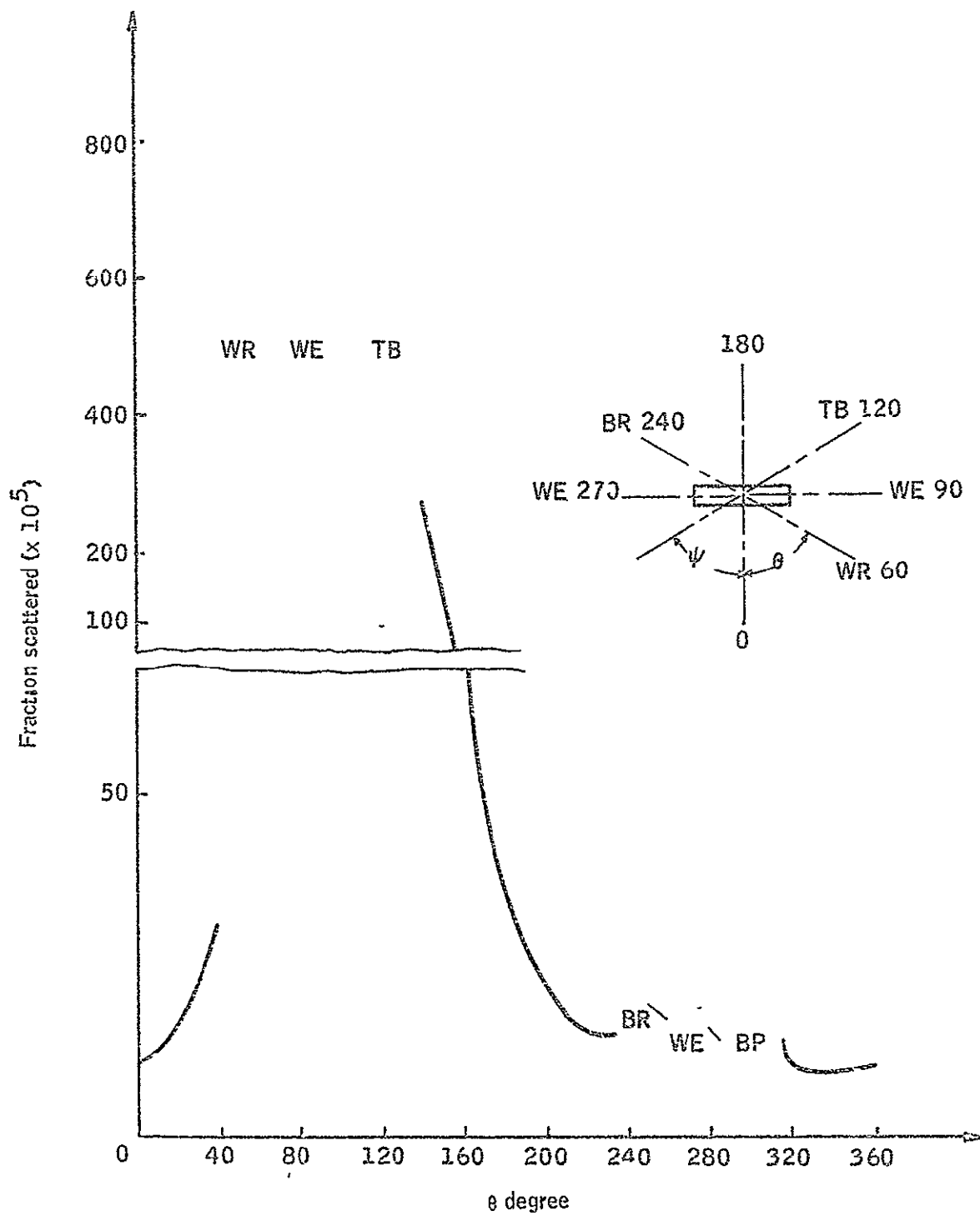


Figure 9 Scatter Distribution for Window 246 ($\psi = 60^\circ$)
Contaminated with High-Temperature-Cured RTV

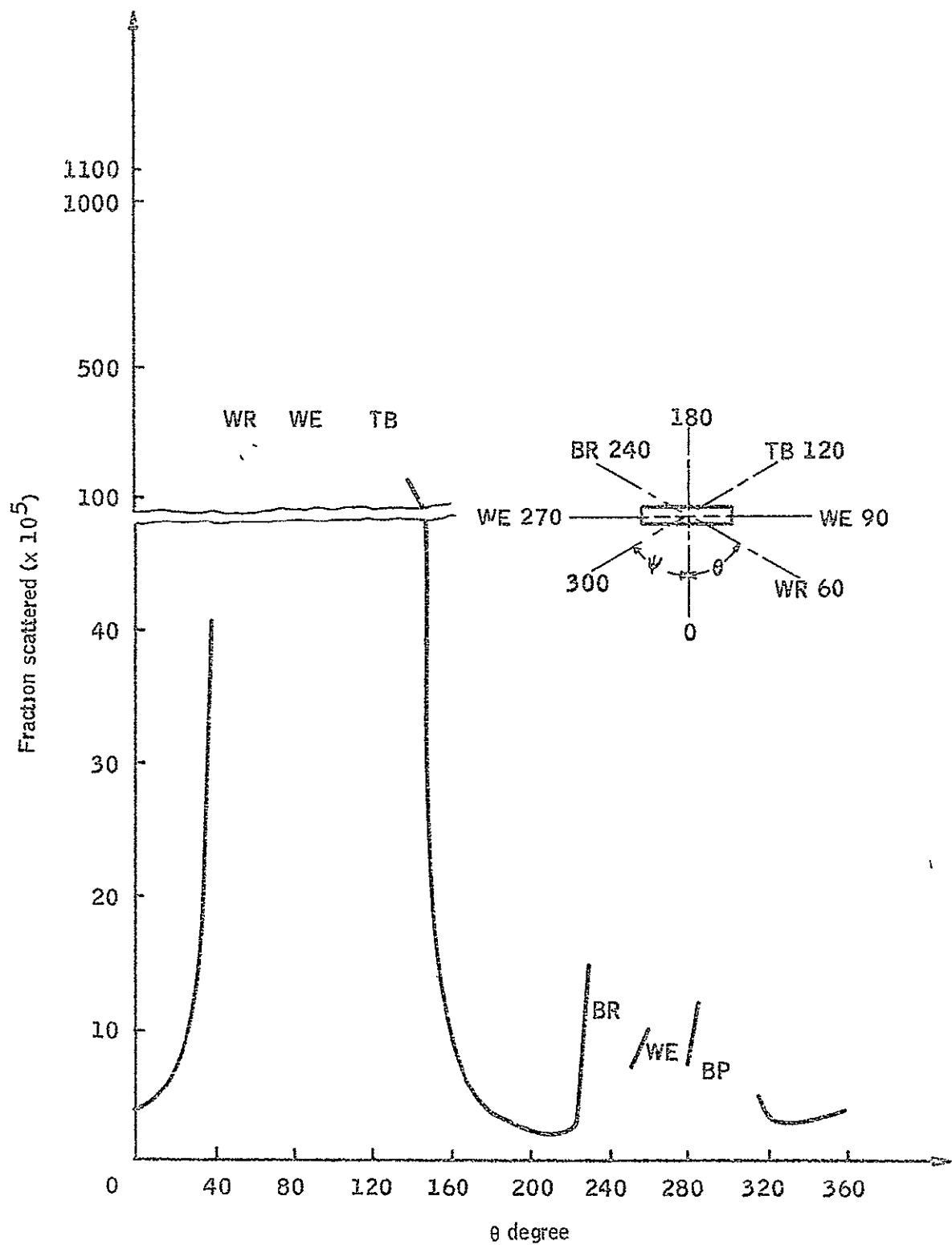


Figure 10 Scatter Distribution of Window 244 ($\psi = 60^\circ$)
Contaminated with Room-Temperature-Cured RTV

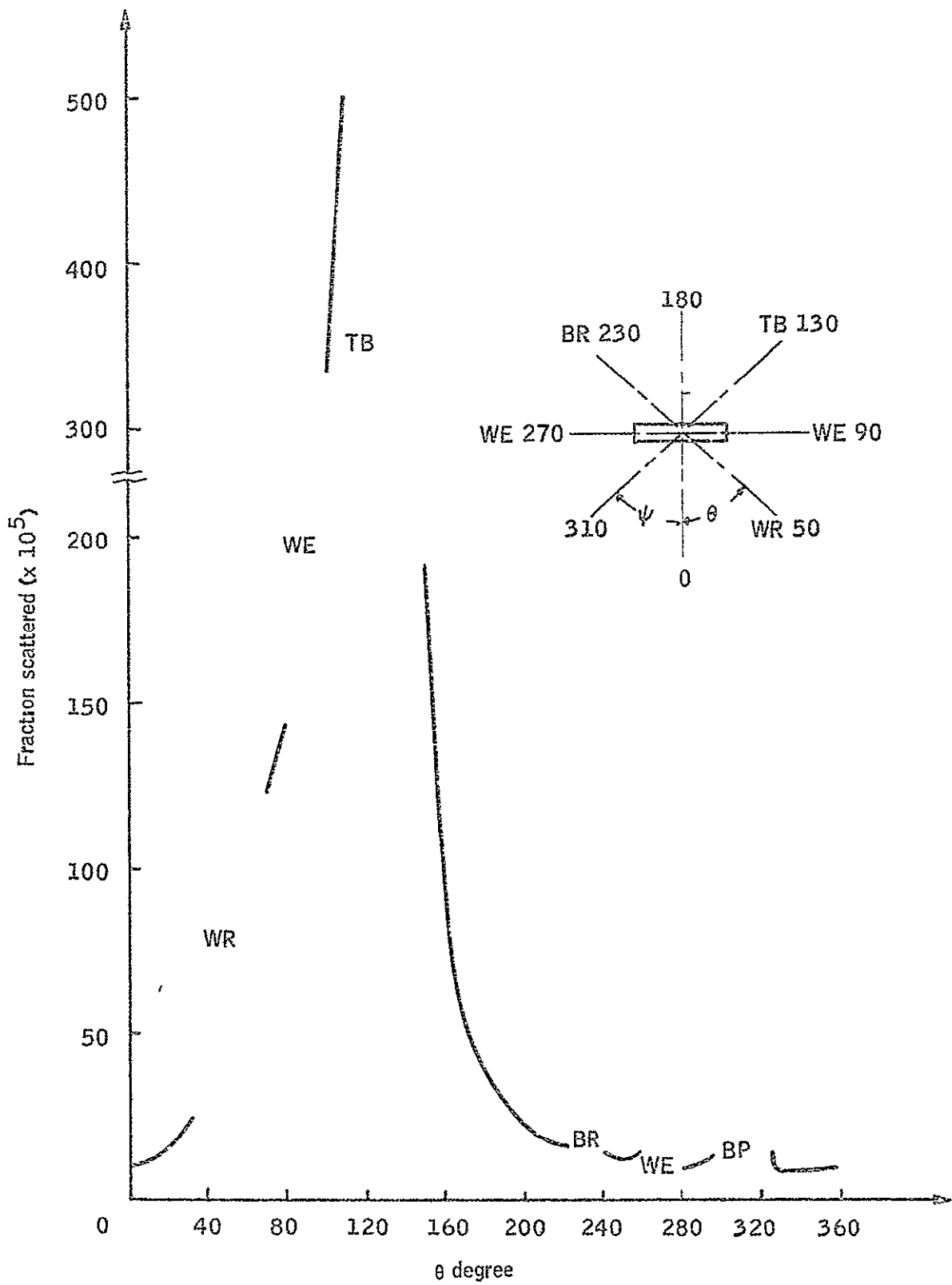


Figure 11. Scatter Distribution for Window 246 ($\psi = 50^\circ$)
Contaminated with High-Temperature-Cured RTV

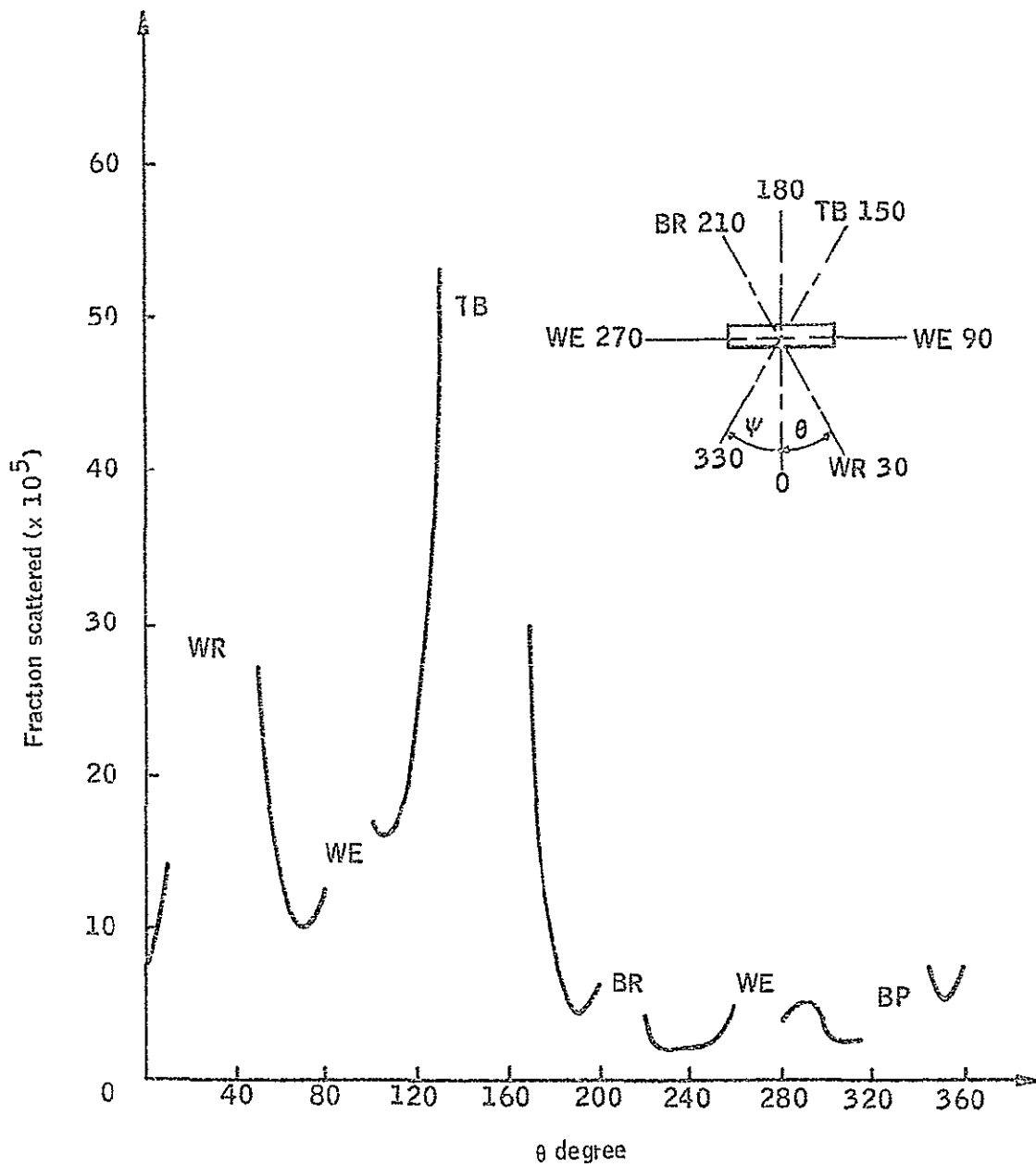


Figure 12. Scatter Distribution for Window 244 ($\psi = 30^\circ$)
Contaminated with Room-Temperature-Cured RTV

distributions are quite similar. This likeness is remarkable in light of the differences in the contamination history of the two windows. By referring to Appendix C other similarities are evident in the bulk of the scattering data.

Quantitative data has also been obtained for the windows after cleaning with the Honeywell procedure as well as the NASA on-pad procedure. This data is presented in Appendix C.

Specifically, the scatter levels obtained from the windows cleaned by the on-pad procedure were somewhat less than obtained in the first phase of this contract (ref. 1). There was a contaminant film that caused the scatter levels of window 246 (in ref. 1) to be about an order of magnitude greater than for all other windows considered. The on-pad cleaning procedure used in the investigation removed some of (or reacted with) that film. In so doing, the light scatter levels were diminished somewhat. There is no quantitative measure of the mechanism affecting this phenomena. However, it is assumed that for that particular HEA-coated window (note: 244 is also an OCLI HEA-coated window), some form of chemical interaction with the coating apparently had occurred.

In order that a data base be established in the same time frame, the windows (244 and 246) were re-cleaned using the Honeywell procedure. Subsequent scatter measurements proved to be quite interesting. The scatter levels were generally lower than those obtained in ref. 1, but they were higher than those obtained after cleaning with the on-pad cleaning procedure. The quantitative results were confirmed by qualitative visual observations of each window.

One possible explanation of the results described above is that the MICRO detergent used in the Honeywell procedure to clean the windows reacts chemically with the antireflection coating. The chemicals used in the on-pad cleaning procedure also apparently react with the products of the previous reaction, eliminating them from a light-scatter standpoint.

The scattering distribution was also measured from a test blank flown on an Apollo mission and acquired inflight on an Apollo mission and acquired inflight by EVA. These data are presented in Appendix C. The general scatter levels from the Apollo specimen were higher than those obtained from the clean or the contaminated windows. It is, however, obvious that this sample had undergone more severe contamination during its history than did the windows. The information has qualitative bearing for any future efforts of this nature due to the handling of the sample.

OUTGASSING STUDIES

During the course of the outgassing studies, several observations have been recorded. They are included here for completeness.

Initially, the vacuum system was operated without either RTV or a window present. The heaters were energized and the copper backing plates brought up to and maintained at 200°F. After the initial system outgassing was terminated, a vacuum of 3.2×10^{-7} torr was maintained for five days. No appreciable outgassing was evident upon completion of the heating vacuum period. The window and the high-temperature-cured RTV were then inserted into the system and a vacuum was reestablished. Once the vacuum was obtained, the heaters were energized and the RTV was brought up to and maintained at 200°F. This resulted in immediate and extreme outgassing (visibly evident). The inner surface of the glass bell jar was covered with droplets of a transparent fluid. Each component within the system likewise appeared "wet". The fluid was obviously a product of the RTV outgassing.

The vacuum gauge also provided information concerning the outgassing. The pressure rose considerably upon heating the RTV. Upon reaching 200°F, it took about two days of pumping to obtain a low enough vacuum so that the mass spectrometer could be used (3×10^{-6} torr). The best vacuum obtained after one week of pumping was 1×10^{-7} torr, where a vacuum of 3.2×10^{-7} was easily reached before the RTV was inserted and heated. This outgassing was so severe that the sensing head (photomultiplier tube) of the mass spectrometer was severely contaminated. The mass spectrometer would not operate initially because of the large amounts of liquid contamination present. To remedy the problem, a heater tape was placed around the sensing head and the head was baked at about 175°F. This heating of the sensing head increased the system pressure by two orders of magnitude for about 24 hours. After heating, the mass spectrometer was again energized and operated normally.

Subsequent insertion of the second window (244) with room-temperature-cured RTV samples resulted in less apparent outgassing in the system. The window upon completion of the tests, also had less visible contamination, the measurements verified this observation. One can chemically interpret the cause of this result. To ascertain that a high-temperature-cured specimen from that particular lot of RTV would cure completely through the sample, an experiment was conducted. A 2-inch cube of RTV was cast and cured with the high-temperature procedure. Three days after curing was complete, the cube was cut in two and examined. The cure was complete throughout the sample. Thus a theory that only the outer surface cured was proven wrong.

Another qualitative test was run near the end of the investigation to ensure that the observed results were without error. The vacuum system was prepared and high-temperature-cured RTV-560 was inserted with a clean window. The system was pumped down and heating begun in the same fashion as for window 246. The initial condensation of outgassing products occurred at about the same time after heating and the quantity was approximately the same. After the RTV reached 200°F, the contamination within the belljar and on the window and fixtures visually had the same appearance. After the system had been heated for three days (a shorter period than before) the window was removed from the vacuum station. It appeared to be contaminated to a degree comparable with window 246. No mass spectrometer data was

taken during this test. Scatter measurements were not performed on the window after contamination. Qualitatively, however, the state of contamination was comparable to window 246

The mass spectrometer scans of the residual gas composition in the vacuum system after each of the RTV samples was heated are presented in Appendix D. Those scans indicate that large quantities of hydrogen are present. Other elements such as nitrogen and oxygen are also evident, but to a lesser degree.

The identification of outgassing products from RTV 560 as determined by Pustinger and Hodgson (ref. 6) is presented in Table 1. Each of the compounds identified in that study contained large concentrations of hydrogen. This bears out the mass spectrometer data taken herein. A gas chromatogram of the outgassing products of RTV 560 has also been obtained in ref. 6. This data is presented in Figure 13 for reference.

TABLE 1 - GAS-OFF PRODUCTS FROM SILICONE, RTV 560
[ref. 6]

Component	Weight of Component (mg/10 gms Candidate Material)			
	14 Days (68°C)	30 Days (25°C)	60 Days (25°C)	90 Days (25°C)
Methanol	0.04	N D	0.004	N D.
Acetone	0.003	0.006	0.007	0.003
Ethanol	0.09	0.1	0.4	0.3
Toluene	0.001	0.01	N D.	N.D.
Xylene	0.002	0.005	N D	N.D.
Carbon monoxide	0.003	0.001	0.004	0.005

N D = Not detected

Other specific data has been documented by McPherson (ref. 7). The properties of RTV 560 obtained in that study are given in Table 2. Typical weight loss data for RTV 560 are given in Figures 14 and 15. Of particular significance to this study is the mass spectrometer data as obtained by McPherson (ref. 7) and presented in Figures 16 and 17.

The glass microscope slides which were placed in the vacuum system were sent to the contract monitor at NASA/Ames Research Center for his use and disposal. The sodium chloride flats which were placed in the system were placed in the Beckman spectrophotometer for IR scanning. The results of these scans are presented in Appendix D. These data confirm the qualitative and quantitative results evidenced in the RTV outgassing studies of the room and high-temperature-cured samples.

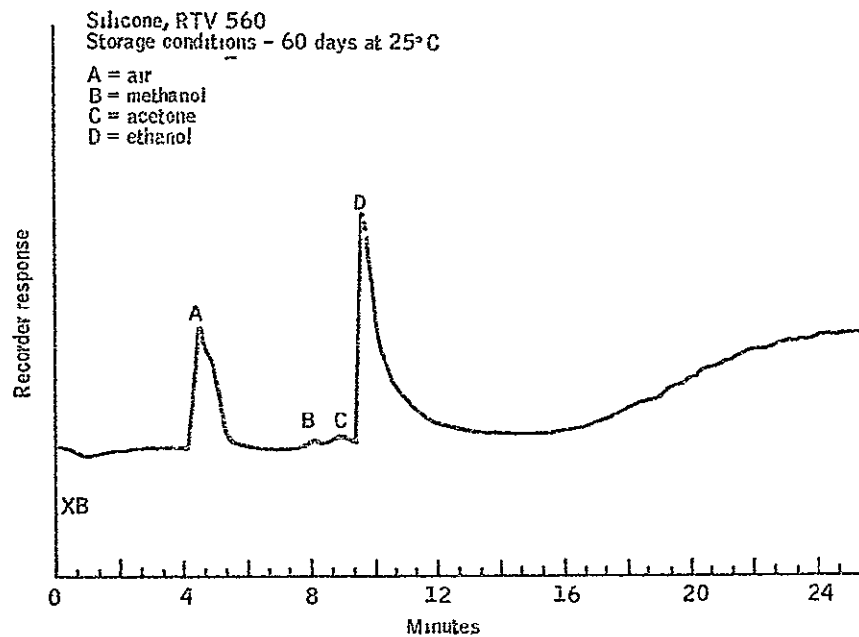


Figure 13 Gas Chromatogram of Gas-Off Products
from Silicon, RTV 560 (60 days 25°C)

TABLE 2 - TYPICAL CURED PROPERTIES OF RTV 560 [ref 7]

Hardness, shore A	60
Tensile strength, psi	800
Elongation, %	160
Tear resistance, LB/in	45
Bashore resilience, %	70
Brittle point	Below - 150°F
Weight loss at steady state, g/cm ² /sec	8.9×10^{-9}

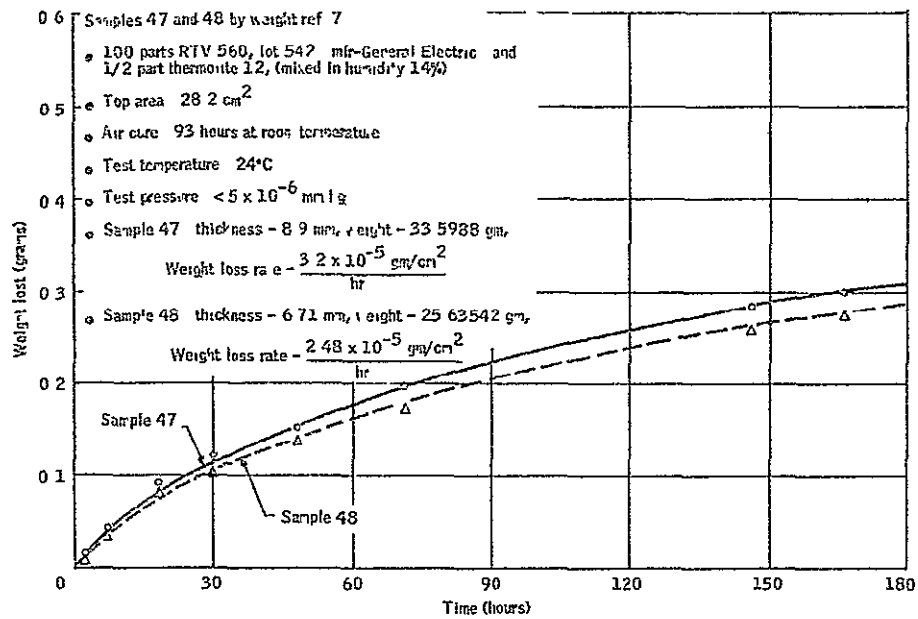


Figure 14 Weight Loss Data for RTV 560

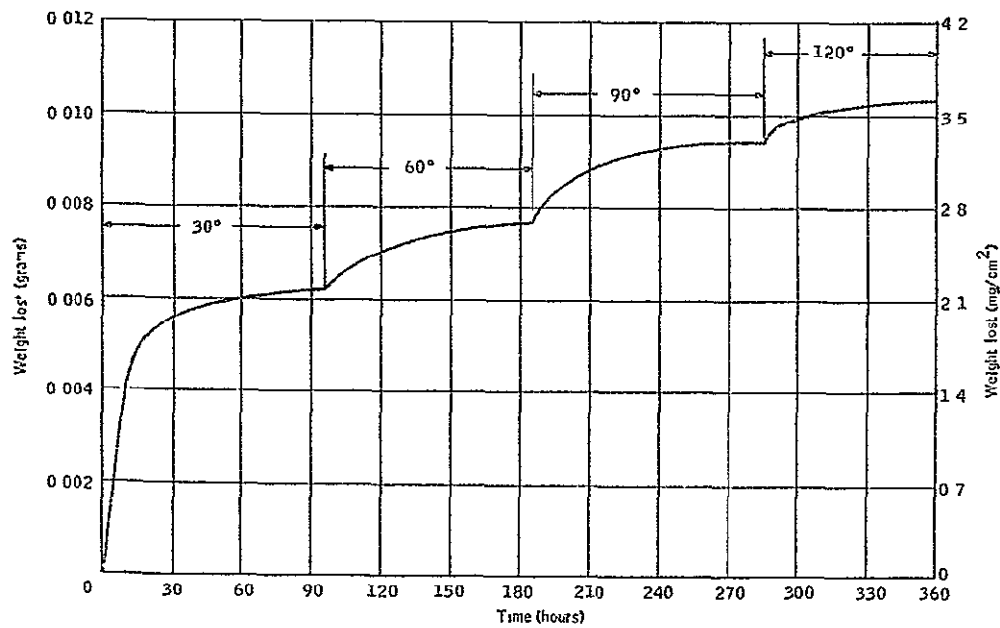


Figure 15 Weight Loss Data with Successively Increasing Temperatures of RTV 560, ref. 7

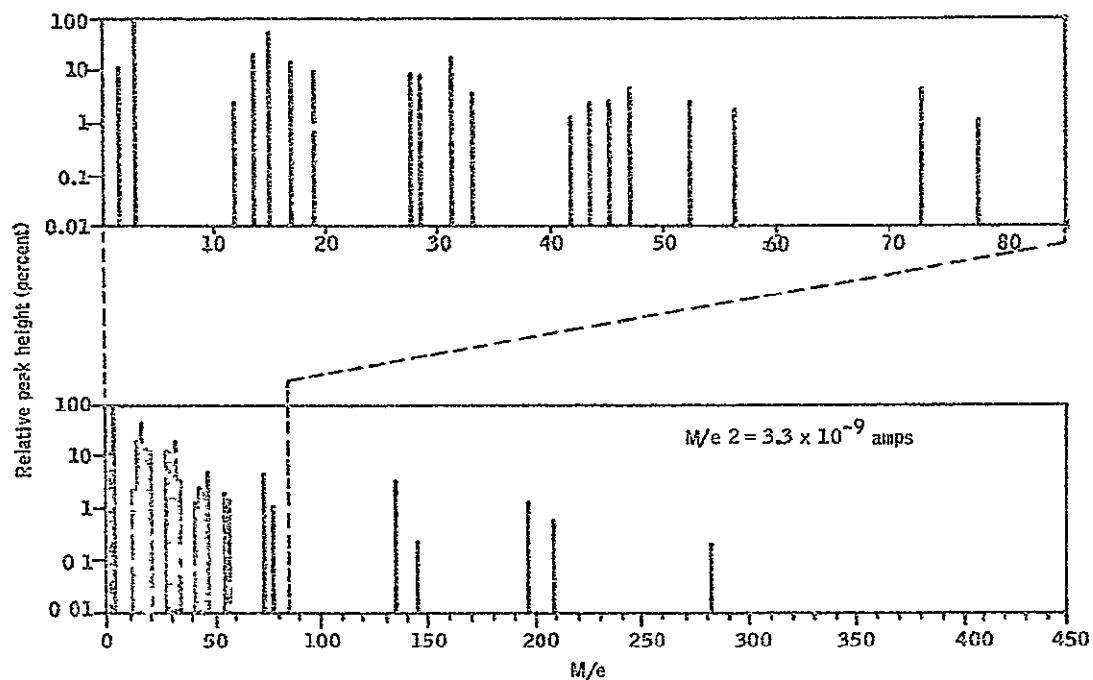


Figure 16 Significant Mass Fragments of RTV 560
After 90 Hours at 30°C, ref 7

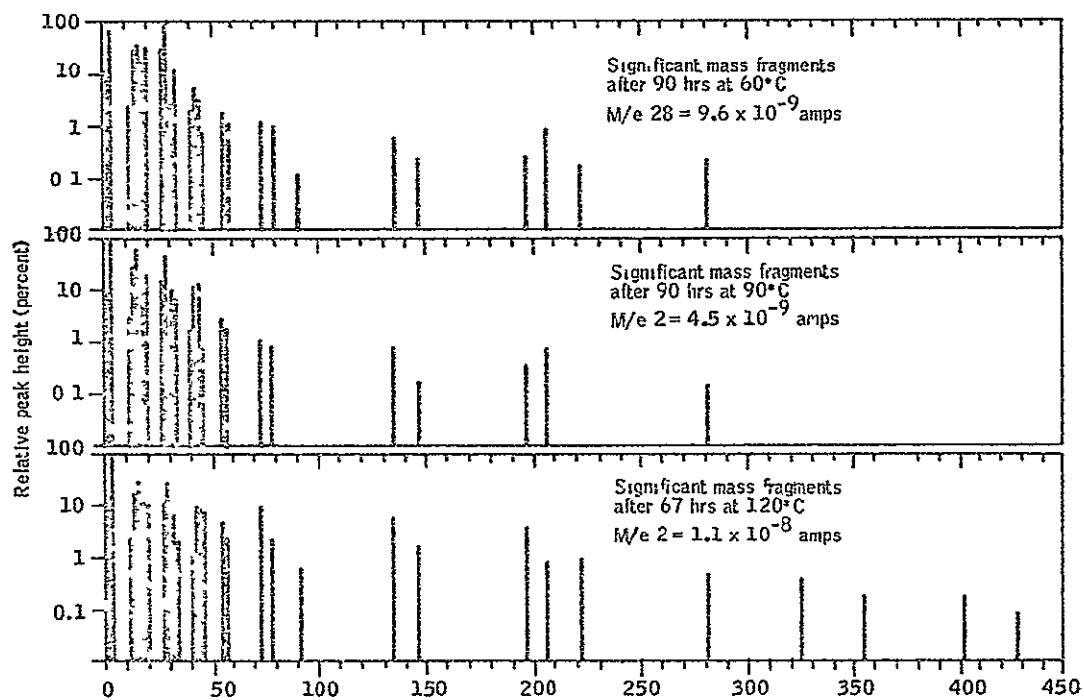


Figure 17 Significant Mass Fragments of RTV 560
at 60, 90 and 120°C, ref 7

PHOTOGRAPHS OF WINDOWS CONTAMINATED BY RTV IN A VACUUM ENVIRONMENT

To ensure that a permanent visible record of the state of contamination would be available, photographs were taken of the contaminated windows. Specifically, Figure 18 shows window 244 after contamination by the outgassing from room-temperature-cured RTV in a vacuum environment. The spots are scatter centers which developed during the condensation of the outgassing products. The bright circular area is the lens image as seen in Figure 1

Figure 19, on the other hand is the analogous photograph of window 246 after contamination by the outgassing from high-temperature-cured RTV in a vacuum environment. The entire window is covered with the condensed products of offgassing. The light source so evident in Figure 18 cannot be seen due to the transparent nature of the condensed film. The relative order of magnitude of the outgassing effects on vision through spacecraft windows is obvious from the two figures discussed above.

Of particular interest is a comparison of the light scatter from the windows under various states of contamination. This comparison can be made by referring to Figure 26 of ref. 1 where the two windows (244 and 246) are shown in a clean condition.

A very complete discussion of the field of organosilicon chemistry is presented in ref. 8. This discussion is a quantitative basis for the substantiation of the results seen in this study, that is, the high-temperature-cured RTV 560 outgassing much more than the room-temperature-cured RTV 560.

Briefly the results discussed in ref. 8 can be summarized as follows. An interchange and equilibration can be affected thermally. Monvolatile polymer was found to rearrange and yield distillable dimethylcyclsiloxanes upon heating to 400°C. These siloxanes are obvious in the data taken during IR scans of the microscope slides as presented in Appendix D. The particular reactions and their causes are described in detail in ref. 8. The reference also documents our results from a theoretical and a specific experimental standpoint.

DETECTION THRESHOLDS

The data from the two windows and the two-window combination was used to make star magnitude detection threshold predictions based on the vision theory outlined earlier in this report for a specific source of luminance. The windows studied were HEA coated designated as 244 and 246. Star magnitude detection threshold predictions are presented for each window in an uncontaminated ('clean') condition, for window 244 after contamination in a vacuum environment by offgassing products of room cured RTV, and for window 246 after contamination in a vacuum environment by offgassing products of high-temperature cured RTV.

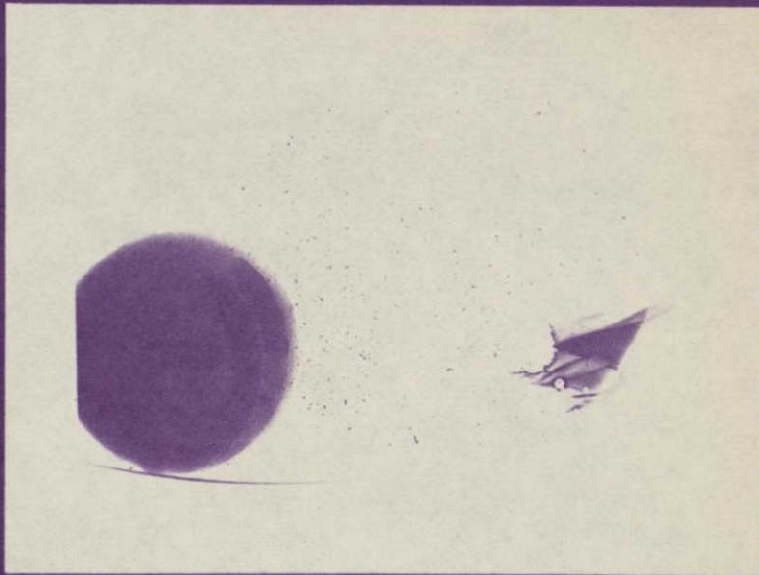


Figure 18. Window Contaminated by Room Temperature Cured RTV

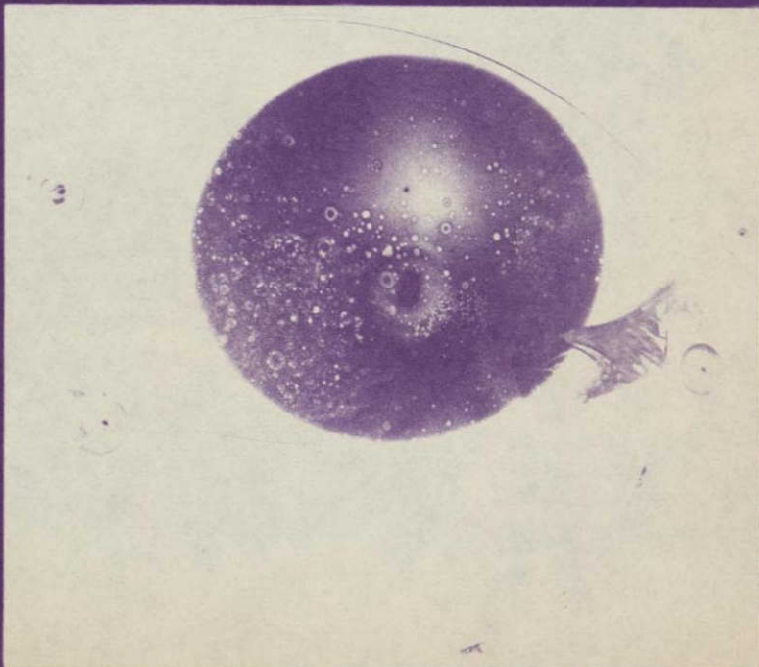


Figure 19. Window Contaminated by High Temperature Cured RTV

The first star magnitude threshold predictions are presented in Tables 3 and 4. These star threshold values are presented for each contaminated window studied illuminated by an external source of light.

The tables contain star threshold values for the maximum, minimum, and average scattering values measured for the windows specified. Specific values of Ψ and θ are given for the maximum and minimum. The star threshold computations are based on two modes of observations, i.e., the naked eye and the telescope. Maximum means the largest valid scattering value measured. Obviously measurements made of the transmitted beam, the specular reflection, or if the blackbody in the transmitted beam would be greatest in magnitude. However, such measurements are not considered valid scattering measurements. For example, when $\Psi = 0$ deg, the transmitted beam extends from θ of 165 to 195 degrees. Therefore, the valid data points adjoining this segment are θ of 160 degrees and 200 degrees (see Appendix C). Other anomalous data points are also self evident in the raw data sheets presented in Appendix C. The minimum data point refers to the lowest valid scattering value measured, the average refers to an arithmetic average of the maximum and the minimum scattering for the window considered.

Table 3 indicates that, using a sextant telescope, an astronaut in a spacecraft that is distant from the earth or moon will be able to see stars brighter than a magnitude of 4.5 through a contaminated window. With the naked eye, an astronaut would have extreme difficulty detecting the usual navigational stars under background conditions produced by the light scatter from contaminated windows studied under this program.

The star magnitude prediction thresholds for 'clean' windows are presented in Tables 5 and 6. These values are presented for illumination by light sources of interest. These predictions are presented for comparison with the predictions given in Tables 3 and 4 for contaminated windows. Comments previously given that describe the structure of the tables are also applicable for Tables 5 and 6.

POLYMERIZATION OF OUTGASSING

Polymerization of condensed outgassing products on the collector drastically changes the properties of the condensate. Subsequent gassing of the collector is diminished and optical characteristics are altered. The most common polymerization agent is the ultraviolet component of solar energy. It appears plausible that recurring window problems during Apollo flights are due to the combination of outgassing and UV-induced polymerization. Therefore, additional experiments duplicating the effect of cure on scattering but involving UV irradiation of the window during the outgassing are recommended in future studies of this nature.

TABLE 3. - STAR MAGNITUDE PREDICTIONS, SINGLE WINDOWS

	Mode of Observation	Sun at 1 AU		Earth at 2×10^5 Km		Earth at 10^5 Km	
		Window		Window		Window	
		244 (a)	246 (b)	244	246	244	246
Maximum		$\Psi = 80^\circ$ $\theta = 120^\circ$	$\Psi = 60^\circ$ $\theta = 100^\circ$	$\Psi = 80^\circ$ $\theta = 120^\circ$	$\Psi = 60^\circ$ $\theta = 100^\circ$	$\Psi = 80^\circ$ $\theta = 120^\circ$	$\Psi = 60^\circ$ $\theta = 100^\circ$
	Telescope Eye	4 30 -0 20	3.2 -1.05	3.80 -0 80	4 50 0.00	3 50 1 00	3 40 -1 20
Minimum		$\Psi = 30^\circ$ $\theta = 230^\circ$	$\Psi = 50^\circ$ $\theta = 250^\circ$	$\Psi = 30^\circ$ $\theta = 230^\circ$	$\Psi = 50^\circ$ $\theta = 250^\circ$	$\Psi = 30^\circ$ $\theta = 230^\circ$	$\Psi = 50^\circ$ $\theta = 250^\circ$
	Telescope Eye	6.70 2.20	4.20 -0 25	8 80 4 60	7 20 3.10	8 70 4 40	6 60 2 30
Average	Telescope Eye	4.20 -0 30	2.70 -0 17	5 30 0 80	5.00 0 50	5 20 0 70	5.00 0.60
	Mode of Observation	Moon at 3.8×10^5 Km		Earth at 200 Km		Moon at 130 Km	
		Window		Window		Window	
		244 (a)	246 (b)	244	246	244	246
Maximum		$\Psi = 80^\circ$ $\theta = 120^\circ$	$\Psi = 60^\circ$ $\theta = 100^\circ$	$\Psi = 80^\circ$ $\theta = 120^\circ$	$\Psi = 60^\circ$ $\theta = 100^\circ$	$\Psi = 80^\circ$ $\theta = 120^\circ$	$\Psi = 60^\circ$ $\theta = 100^\circ$
	Telescope Eye	4 50 0 00	5 40 1 00	1.90 -2 55	0.00 -4 95	3 50 -1.20	1.70 -2 75
Minimum		$\Psi = 30^\circ$ $\theta = 120^\circ$	$\Psi = 50^\circ$ $\theta = 250^\circ$	$\Psi = 30^\circ$ $\theta = 230^\circ$	$\Psi = 50^\circ$ $\theta = 250^\circ$	$\Psi = 30^\circ$ $\theta = 230^\circ$	$\Psi = 50^\circ$ $\theta = 250^\circ$
	Telescope Eye	9 20 5 00	7 75 3 45	5 70 1.35	2.75 -1 40	6 70 2 30	5.00 0 50
Average	Telescope Eye	6.40 1 80	5 90 1 50	2 00 -3.25	0 25 -4 25	4.75 0 35	1 85 -0 75

^aWindow 244 - Contaminated by room-temperature-cured RTV^bWindow 246 - Contaminated by high-temperature-cured RTV

TABLE 4. - STAR MAGNITUDE PREDICTIONS, MULTIPLE
WINDOWS, 244 AND 246

Mode of Observation		Sun at 1 AU	Earth at 2×10^5 Km	Earth at 10^5 Km
Maximum		$\Psi = 60^\circ$ $\theta = 100^\circ$	$\Psi = 60^\circ$ $\theta = 100^\circ$	$\Psi = 60^\circ$ $\theta = 100^\circ$
	Telescope Eye	1.30 -3.00	3.00 -1.40	2.10 -2.20
Minimum		$\Psi = 0^\circ$ $\theta = 100^\circ$	$\Psi = 0^\circ$ $\theta = 100^\circ$	$\Psi = 0^\circ$ $\theta = 100^\circ$
	Telescope Eye	5.80 1.25	6.80 2.50	7.70 3.20
Average				
	Telescope Eye	1.80 -2.60	3.15 -1.35	2.40 -2.00
Mode of Observation		Moon at 3.8×10^5	Earth at 200 Km	Moon at 130 Km
Maximum		$\Psi = 60^\circ$ $\theta = 100^\circ$	$\Psi = 60^\circ$ $\theta = 100^\circ$	$\Psi = 60^\circ$ $\theta = 100^\circ$
	Telescope Eye	4.00 -0.50	0.00 -4.50	1.00 -3.50
Minimum		$\Psi = 0^\circ$ $\theta = 100^\circ$	$\Psi = 0^\circ$ $\theta = 100^\circ$	$\Psi = 0^\circ$ $\theta = 100^\circ$
	Telescope Eye	7.90 3.60	2.50 -2.30	5.25 0.75
Average				
	Telescope Eye	4.1 -0.3	0.25 -4.30	1.50 -3.05

Window 244 - Contaminated by room-temperature-cured RTV

Window 246 - Contaminated by high-temperature-cured RTV

TABLE 5. - STAR MAGNITUDE PREDICTIONS, SINGLE WINDOWS

	Mode of Observation	Sun at 1 AU		Earth at 2×10^5 Km		Earth at 10^5 Km	
		Window		Window		Window	
		244 (a)	246 (b)	244	246	244	246
Maximum		$\Psi = 60^\circ$ $\theta = 100^\circ$	$\Psi = 50^\circ$ $\theta = 100^\circ$	$\Psi = 60^\circ$ $\theta = 100^\circ$	$\Psi = 50^\circ$ $\theta = 100^\circ$	$\Psi = 60^\circ$ $\theta = 100^\circ$	$\Psi = 50^\circ$ $\theta = 100^\circ$
	Telescope Eye	5.50 1.00	3.70 -0.75	4.90 0.15	5.10 0.60	4.00 -0.50	4.10 0.30
Minimum		$\Psi = 80^\circ$ $\theta = 220^\circ$	$\Psi = 80^\circ$ $\theta = 210^\circ$	$\Psi = 80^\circ$ $\theta = 220^\circ$	$\Psi = 80^\circ$ $\theta = 210^\circ$	$\Psi = 80^\circ$ $\theta = 220^\circ$	$\Psi = 80^\circ$ $\theta = 210^\circ$
	Telescope Eye	9.50 5.25	6.50 2.25	9.60 5.65	8.00 3.75	9.60 5.40	7.50 3.20
Average	Telescope Eye	6.00 1.50	4.25 -0.25	7.35 3.00	5.80 1.25	6.40 2.00	5.70 1.20
	Mode of Observation	Moon at 3.8×10^5 Km		Earth at 200 Km		Moon at 130 Km	
		Window		Window		Window	
		244	246	244	246	244	246
Maximum		$\Psi = 60^\circ$ $\theta = 100^\circ$	$\Psi = 50^\circ$ $\theta = 100^\circ$	$\Psi = 60^\circ$ $\theta = 100^\circ$	$\Psi = 50^\circ$ $\theta = 100^\circ$	$\Psi = 60^\circ$ $\theta = 100^\circ$	$\Psi = 50^\circ$ $\theta = 100^\circ$
	Telescope Eye	5.80 1.30	5.95 1.40	2.40 -2.10	1.00 -3.75	4.10 -0.30	2.25 -2.20
Minimum		$\Psi = 80^\circ$ $\theta = 220^\circ$	$\Psi = 80^\circ$ $\theta = 210^\circ$	$\Psi = 80^\circ$ $\theta = 220^\circ$	$\Psi = 80^\circ$ $\theta = 210^\circ$	$\Psi = 80^\circ$ $\theta = 220^\circ$	$\Psi = 80^\circ$ $\theta = 210^\circ$
	Telescope Eye	9.90 5.55	8.35 4.15	6.70 2.30	3.75 -1.30	7.30 3.15	6.50 2.10
Average	Telescope Eye	7.75 3.45	6.30 2.00	2.50 -2.05	1.25 -3.25	4.60 0.20	2.50 -2.30

^aWindow 244 - Honeywell cleaning procedure^bWindow 246 - Honeywell cleaning procedure

1

TABLE 6 - STAR MAGNITUDE PREDICTIONS, MULTIPLE
WINDOWS, 244 AND 246

Mode of Observation		Sun at 1 AU	Earth at 2×10^5 Km	Earth at 10^5 Km
Maximum		$\Psi = 60^\circ$ $\theta = 100^\circ$	$\Psi = 60^\circ$ $\theta = 100^\circ$	$\Psi = 60^\circ$ $\theta = 100^\circ$
	Telescope Eye	3.30 -1.15	5.10 0.50	3.75 -0.75
Minimum		$\Psi = 60^\circ$ $\theta = 220^\circ$	$\Psi = 60^\circ$ $\theta = 220^\circ$	$\Psi = 60^\circ$ $\theta = 220^\circ$
	Telescope Eye	6.75 2.35	8.00 3.75	7.75 3.40
Average	Telescope Eye	3.80 -0.45	5.80 1.30	5.40 1.00
Mode of Observation		Moon at 3.8×10^5	Earth at 200 Km	Moon at 130 Km
Maximum		$\Psi = 60^\circ$ $\theta = 100^\circ$	$\Psi = 60^\circ$ $\theta = 100^\circ$	$\Psi = 60^\circ$ $\theta = 100^\circ$
	Telescope Eye	5.60 1.10	0.50 -4.60	1.70 -2.75
Minimum		$\Psi = 60^\circ$ $\theta = 220^\circ$	$\Psi = 60^\circ$ $\theta = 220^\circ$	$\Psi = 60^\circ$ $\theta = 220^\circ$
	Telescope Eye	8.10 3.90	3.25 -0.80	5.90 1.50
Average	Telescope Eye	6.10 1.60	0.75 -3.75	1.90 -2.10

Window 244 - Honeywell cleaning procedure

Window 246 - Honeywell cleaning procedure

CONCLUSIONS

A vacuum station was fixtured so that spacecraft windows could be contaminated under conditions similar to the spacecraft environment. The light scatter from these windows in various directions was determined using an apparatus designed and fabricated under Phase 1 of this contract (ref. 1) Star threshold predictions were made using light scatter data together with predictions of illumination incident on spacecraft in various orbit positions

The results of this investigation produced several significant conclusions:

- The NASA - Apollo on-pad cleaning technique removes contamination which the Honeywell technique does not.
- High-temperature-cured RTV-560 outgasses more upon heating in a vacuum than does room-temperature-cured RTV-560.
- A glass specimen flown on an Apollo mission and recovered by EVA displayed a scatter distribution characteristic of highly contaminated windows
- After outgassing RTV-560 (either room-or high-temperature-cured) in a vacuum environment surrounding the windows, the star thresholds are greatly reduced

RECOMMENDATIONS

Based on the investigation findings, Honeywell recommends that for any further studies, consideration be given to:

- Obtaining a time history of the light scatter from the window during outgassing
- Further identifying the cure schedules concerning the effects on RTV outgassing properties
- A specific determination of the effects evident on window 246 after washing with the various procedures
- Performing ultraviolet degradation studies of the polymerization

APPENDIX A LITERATURE REVIEW

REVIEW

Considerable concern has been recently expressed within the scientific community as to the probability of degradation of Apollo vehicle-based solar and stellar optical experiments and the lack of suitable navigation by astronauts as a result of various contaminants emanating from the spacecraft and condensing on the windows. Preliminary estimates suggest the possibility of "debris comet" up to several kilometers in diameter surrounding some vehicles. Depending upon the size, density, and composition of the components of such a cloud which condense on the windows of the spacecraft, the astronauts' vision through the windows could be seriously degraded.

Since widespread concern over the contamination problem has only recently been aroused, little information is available on the subject. This review of the literature is brief and only includes those references containing information which directly bear on this study.

An initial effort which preceded this investigation has been published as reference 1. In that work, an apparatus was constructed to determine the angular distribution of forward and backward scattering of collimated light with approximately the solar spectra incident on clean spacecraft windows with various coatings. Knowing the incident luminous flux, the absolute scatter distribution was described in dimensionless form.

Measurements were made on one MgF_2 coated, two HEA coated and one uncoated Corning 7913 glass windows. The angle of incidence of the collimated beam of light was varied as was the viewing angle for all windows. Each window was cleaned prior to the measurement with the best laboratory cleaning procedures known. This cleaning was performed to minimize scatter by contamination.

A rather extensive study of outgassing characteristics of polymers was performed by Muraca and Whittick (ref. 2). The basic objective of their program was to assist the Jet Propulsion Laboratory (JPL) in the selection of polymeric materials to be used in connection with spacecraft design. Special attention was given to the determination of the effects of a simulated spacecraft environment on selected commercial products. The theory of the release and condensation of substances from polymers exposed to the thermal vacuum environment is discussed in detail. The equipment and procedures used for identifying and measuring the release of volatile condensible material are described.

Pustinger and Hodgson (ref. 6) tested 98 candidate materials for space cabin construction to establish possible volatile outgassing and oxidation products. Test conditions were designed to simulate the normal space cabin environment.

After pretreatment at 0.1 torr and at 25°C, candidate materials were stored in bench-scale simulators for 14 days at 68°C, and for 30, 60 and 90 days at 25°C, in a 5 psia oxygen atmosphere with 20 to 40 percent relative humidity. Individual components of the volatile contaminants were identified and the quantities evolved were estimated by gas chromatographic and mass spectrometric analyses. In addition to the outgassing experiments, a cryogenic system for serial trapping of atmospheric contaminants was constructed for use at Wright-Patterson Air Force Base, Ohio. Gas chromatographic and mass spectrometric analyses were performed on four samples of atmospheres from bioenvironmental systems.

McPherson (ref. 7) identified nonmetallic materials exposed to space vacuum for the Apollo system. Outgassing properties for most of these materials were obtained from the literature or by experiment. Materials discharging and leaking from spacecraft systems and cabins were identified quantitatively and qualitatively. An evaluation was made of the probability of contaminants in the debris cloud condensing on critical optical elements. Deleterious effects on the results of all experiments could result from such condensation, since the cloud contains materials which condense at Apollo system operating temperatures. Specific and general recommendations are made in the report for reducing the contaminants' threats and for deriving more conclusive results.

Bolstad et al (ref. 8) have determined the gassing characteristics of 150 candidate materials for use in Honeywell-developed devices on Apollo vehicles. The extensive investigation included identification of the major gassing products by gas chromatography.

DISCUSSION OF OUTGASSING*

Background

The advent of space research has generated considerable effort to characterize many nonfunctional properties of materials. These properties include flammability, ignition temperatures, odor, and gassing. The gassing properties are of prime importance to manned systems because of toxic effects but can also be of significance for unmanned systems because of the effect of contamination on windows and other optical elements.

In order to estimate the effects on light scattering from spacecraft windows, it is necessary to evaluate what materials may be involved, their quantities, and characteristics. Thus, it is important that structural and ablative materials, surface coatings, sealants, etc. on the spacecraft can be identified

*"Gassing" generally refers to the evolution of various species from a material. "Outgassing" is used when the material is in a vacuum environment and "offgassing" is used for a nonvacuum environment.

which, through mechanisms such as outgassing, may contribute potential debris and contamination to the space contiguous to the window. Having identified the source materials, outgassing characteristics of these materials must be established in order to determine the quantity, kind, and form of the contaminants potentially available to form a debris cloud. Materials emitted from the spacecraft systems, such as the waste management system, reaction control system, etc., must also be identified, together with rates of emission. This experimental study was concerned only with the contamination introduced by RTV 560, a General Electric silicon rubber.

Characterization of Gassing

The determination of gassing properties has improved with more rigorous quantitative and objective methods as longer-term space flights were considered. For the short-term flights of the Mercury program, materials were flight-qualified (in regard to gassing) exclusively by subjective odor tests. For the longer flights in the Gemini, Apollo and MOL programs, additional tests have been used for qualification of the individual gassing species. Programs have been established to determine toxicity thresholds for gassing products and possible synergistic effects, these programs are not directly related to window contamination, except that they have resulted in identification of the major gassing products.

Reference 9 reports the gassing characteristics of 150 candidate materials for use in devices on Apollo. The study included identification of the major gassing products by gas chromatography. The major gassing products of the silicone rubbers, RTV-90 and RTV-503, were found to be acetone, ethyl alcohol, toluene, methyl-isobutyl-ketone and benzene. Recently, Crook, (ref 10) also completed a study of 50 candidate materials for use in Honeywell devices on MOL; RTV-632, RTV-881 and RTV-882 were included, but individual gassing products were not identified.

RTV-560 gassing products, in terms of mass spectrometric fragmentation patterns, have been identified in a study of contamination aspects of the Apollo telescope mount (ref 7). The spectra are given as a function of time and temperature over an m/e (mass to charge ratio) range of 1-450. The majority of the fragments seen had an m/e ratio of less than 250.

Mechanism of Gassing

Polymers, with few exceptions, are stable at temperatures below 125°C; RTV-560 in particular, is stable. The gassing arises from nonpolymeric components present in the polymers. These components include unreacted materials used in manufacture of the monomeric material, low polymeric species due to insufficient cures, catalysts used in the manufacturing process or curing process, residual solvents, and various additives incorporated into the polymer.

These materials outgas from an exposed surface of the polymer after diffusion through the polymer. Data on RTV-560 shows the gassing rate, as determined by sample weight loss, decreases markedly after a day or so (ref. 6 and 7). Since the gassing corresponds to evaporation of the gassing species from the exposed polymer surface, the gassing rate increases with increasing temperature. Also, the diffusion of the gassing species through the polymer is enhanced by higher temperatures. Eventually the gassing rate decreases to zero as the polymer becomes depleted of the gassing species. Because of this, a vacuum-bake treatment can be used to "clean-up" polymers after curing; the "clean" polymer has markedly lower offgassing characteristics.

Condensible Gassing Products

The gassing products probably contaminate windows during a space flight as they collect or condense on them. The condensation of a particular gassing species is primarily a function of the temperature of the collector. If the collected species does not change species through reaction or polymerization, it will in turn be outgassed by the collector. The amount of condensed material will then depend on the gassing rate of the source material, the collection efficiency and the outgassing rate of the collector. These three factors typically cause the amount of condensed material to peak after 24 to 36 hours. Subsequently, the amount decreases as the source material depletes and the collector outgasses. Work on RTV-560 shows about 70 percent of the total gassing products evolved in 24 hours are collected by a room temperature collector (ref. 7). The use of suitable collectors (e.g., sodium chloride flats) permits fingerprinting the collected materials by infrared absorption spectra.

If the collected gassing species react, subsequent outgassing characteristics of the collector would be changed. For example, ultraviolet-induced polymerization would produce polymers with inherently low outgassing characteristics and such polymerized materials would be retained indefinitely by the collector. Figure 3-13 of reference 7 illustrates the effect of UV on a viewing window of a vacuum chamber; the window area exposed to UV appears hazy while the adjacent protected area remains clear. As a direct result of the data gathering tasks performed in reference 7, known materials were identified on the Apollo command service module, the multiple docking adapter, the lunar module ascent stage, the ATM rack, the resupply module, the airlock module, the spacecraft launch adapter, and the S-IVB orbital workshop. In particular, they found that RTV silicones manufactured by the General Electric Company are used as sealants around the windows, entry hatch, reaction control system engines, vents, and inspection doors. According to unofficial information received from North American Aviation, the exposed surface area is on the order of approximately 9,000 cm² for RTV 511, 5,000 cm² for RTV 560 and 450 cm² for RTV 577. It is obvious from the foregoing as well as the data obtained by McPherson (ref. 7) why the material chosen herein for the outgassing studies was RTV 560.

It has been demonstrated in references 6 and 7 that the main sources of high-molecular-weight contaminants on spacecraft originate from outgassing, evaporation, and sublimation from the nonmetals. This investigation is directly concerned with the effects of contamination of RTV 560 on vision through spacecraft windows.

Identification of Products

Under certain simple conditions, the loss of material in vacuum by evaporation and/or sublimation is given by Knudsen-Langmuir as:

$$W = 5.83 \times 10^{-2} P \left(\frac{M}{T} \right)^{1/2} \quad (A1)$$

where:

- P = (constant $\exp \left(-\frac{B}{T} \right)$), or the vapor pressure of the material in torr
- W = weight loss in grams per cm^2 per second
- M = molecular weight (not mass of molecule)
- B = constant for each material
- T = temperature

For most metals and pure simple organic compounds, the vapor pressure and molecular weights are relatively well known or can be estimated with fair accuracy. For inorganic compounds, the problem is normally more complex because the loss of material can occur by several mechanisms; i. e., molecules of the compound can evaporate and/or decompose into elements or simpler compounds which in turn may evaporate. Furthermore, when the space environment is considered, other mechanisms can be induced or accelerated by various types of radiation. Some organic materials of low molecular weight can evaporate in vacuum without decomposition, and if their thermodynamic properties are known, the Knudsen-Langmuir equation gives good estimates of losses in vacuum.

However, most organic materials used in spacecraft are long-chain, polymeric compounds that can be depolymerized or unraveled in the thermal environment of the spacecraft into more volatile fragments of unknown structure and molecular weight and also suffer photolysis when exposed to radiation.

The thermal unraveling of these large molecules is a complex process and takes place throughout the body of the material. Then there is a complicated diffusion and solubility problem coupled with the evaporative loss for each material. For polymeric materials, the calculations for weight loss in vacuum involve many data which are usually unknown, or if the values are known, the calculations may be too complicated to be useful. It is almost necessary to measure the weight loss in vacuum for complex compounds.

Weight loss rates in vacuum for materials can be misleading if other characteristics are not taken into account. An excellent example of this is the irradiated polyolefin materials. Their weight loss rates are among the lowest, but experience has shown that their outgassed products can severely contaminate nearby objects. This fact is well documented by McPherson (ref. 7).

Based on the work of Muraca and Whittick (ref. 2) it is estimated that at least 50 percent of the total weight loss is condensable on a 25°C surface in a vacuum. All RTV-type silicones tested have failed to qualify for use on spacecraft in critical areas and were not recommended for use in the proximity of critical optical and electrical components.

The amount of surface coverage by molecules condensing on the surface can be described approximately as follows:

If n molecules strike a unit surface per unit time and remain for an average time (τ), then there are N molecules per unit area of surface, i. e.,

$$N = n\tau \text{ molecules cm}^{-2} \quad (\text{A2})$$

The number of molecules striking a $\text{cm}^2 \text{ sec}^{-1}$ is

$$n = 3.52 \times 10^{22} P (\text{MT})^{-1/2} \quad (\text{A3})$$

The average sitting time (τ) of a molecule on a surface is given by Frenkel (ref. 11) .

$$\tau = \tau_0 \exp (Q/RT) \quad (\text{A4})$$

where

Q = heat of absorption

and τ_0 is related to the lattice vibrations of the solid surface and has a value of about 10^{-12} to 10^{-14} sec.

Equation (A4) describes the thermally driven absorption-desorption of molecules on surfaces, but, in the presence of photons, the situation is somewhat different. Photons can cause desorption of molecules, i. e., photons ($\lambda < 2400\text{\AA}$) desorb CO from nickel surfaces and water from cadmium and zinc, the latter under partial dissociation (ref. 12). Lange and Riemersma (ref. 13) studied photon desorption of CO from a monolayer on nickel and found a maximum yield of about 2×10^{-8} per photon at $\lambda = 3350 \text{\AA}$ or 3.7 ev.

Photon interaction with molecules on surfaces can also make them stay longer. Photons excite molecules, and the reactions of these excited molecules may occur from an entirely different array of potential energy surfaces than those encountered in the thermally excited systems.

With the present limited quantitative knowledge of sublimated materials about Apollo-type spacecraft, it is difficult to make a quantitative judgment about the contamination threat for spacecraft windows. Most of the surface materials and large areas of the spacecraft have not been identified. Additional work in several areas is discussed in the recommendations.

APPENDIX B

SAMPLE THRESHOLD CALCULATION

Our star magnitude threshold determinations were made by referring to our raw data in the laboratory-determined scattering value and relating this value to the scattering level that would exist in space for the specified external-source condition and eye-window-source configuration and orientation.

We have chosen a sample threshold calculation to illustrate the step procedure followed.

Window:	No. 244 (HEA coating) room temperature cured RTV-Silicon Contaminated Surface
External light source:	Earth at 2×10^5 km ($E_S = 12,723$ ft. candles)
Beam-window angle:	$\Psi = 80^\circ$
Photometer (eye) - window angle:	$\theta = 120^\circ$
BaSO ₄ disc luminance:	$\bar{L}_d = 187$ foot lamberts
Disc reflectance factor:	$\rho_d = 0.957$
Scattering luminance:	$L_w = 470 \times 10^{-3}$ foot lamberts
Experimental ambient luminance:	$L_B = 8.5 \times 10^{-4}$ foot lamberts

- (1) Incident illumination on window surface in laboratory:

$$E_o \cos \Psi \text{ (lab)} = \left(\frac{\bar{L}_d}{\rho_d} \right) \cos \Psi = \left(\frac{187}{0.957} \right) 0.1737 = 33.93 \text{ foot candles}$$

- (2) Incident illumination from earth at 2×10^5 km

$$F_{12} E_S \cos \Psi = 446 \text{ foot candles}$$

In this work, F_{12} is defined as the configuration factor from surface 2 to surface 1. Briefly, the configuration factor, F_{1-2} , is the ratio of the flux originating from body 1 incident on body 2 to the total flux originating at body 1. Mathematically, if the emission of a surface is assumed to be diffuse, that is according to Lambert's Cosine Law, the fraction of emitted energy from a small area dA_1 on body 1 intercepted by a differential area dA_2 on body 2 is given by

$$F_{dA_1 - dA_2} = \frac{\cos \phi_1 \cos \phi_2 dA_2 dA_1}{\pi D^2}$$

where the geometrical notation is indicated in Figure B1. For the case where area A_1 is very small compared to area A_2 , the configuration factor becomes

$$F_{dA_1 - A_2} = \int_{A_2} \frac{\cos \phi_1 \cos \phi_2 dA_2}{\pi D^2} \quad (B1)$$

This equation serves as the basis for the calculations presented in ref. 1.

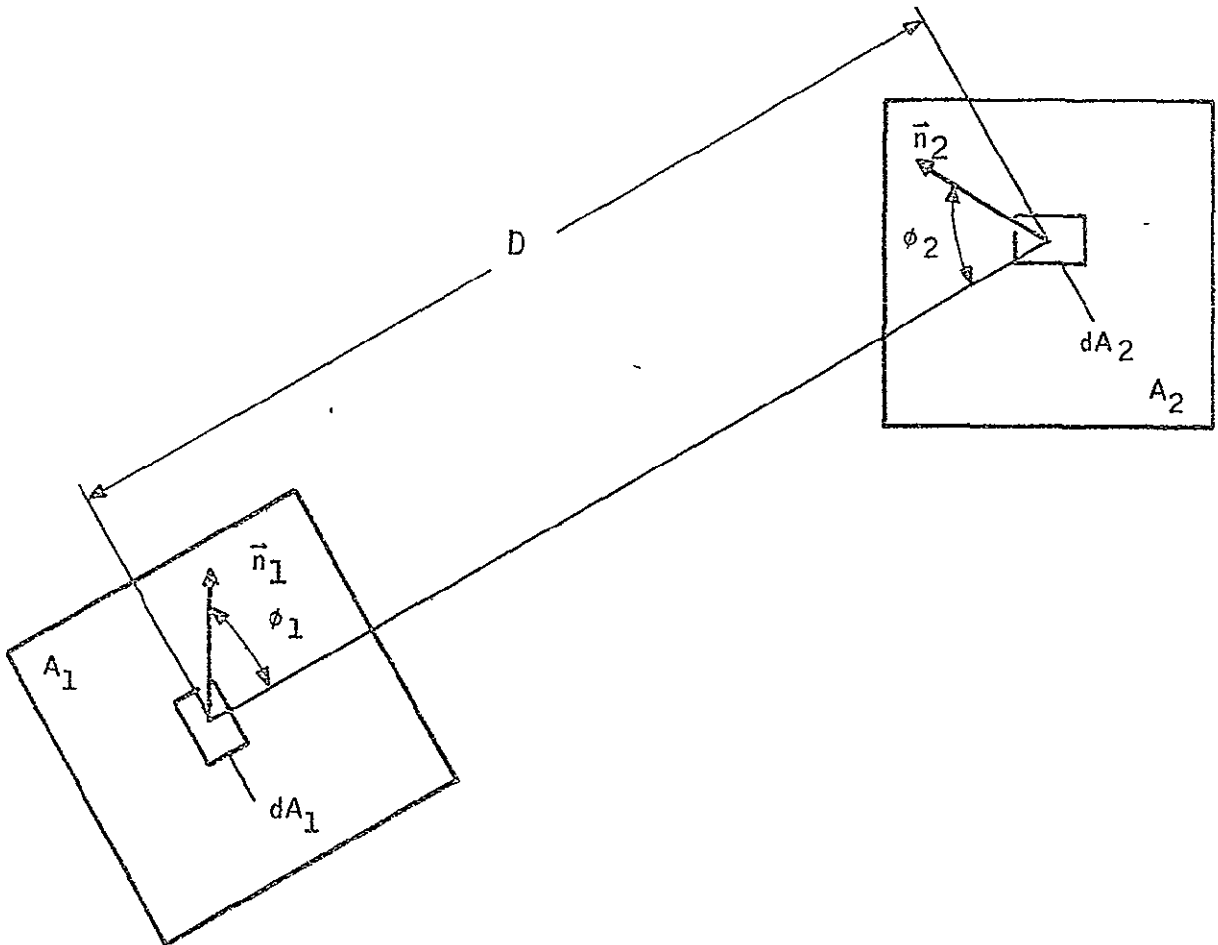


Figure B1 Coordinate System

The details of the computations and results are given in ref 1.

- (3) Scattering at measured window surface in laboratory:

$$\frac{L_W - L_B}{E_o \cos \Psi \text{ (lab)}} = \frac{0.470 - 0.00085}{33.93} = 1.38 \times 10^{-2}$$

- (4) Window luminance level equated to scattering in space.

$$\left[\frac{L_W - L_B}{E_o \cos \Psi \text{ (lab)}} \right] = \left[F_{12} E_S \cos \Psi \text{ (space)} \right]$$

$$= (138 \times 10^{-2}) 446 = 6.18 \text{ foot lamberts}$$

- (5) Referring to the stellar threshold model (Figure 7) we can determine that an astronaut viewing against a background of 6.18 foot lamberts would be able to detect a star of magnitude 1.3 with unaided binocular vision and a star of magnitude 5.8 with the prescribed monocular telescope.

APPENDIX C

MEASURED DATA

This appendix includes all data obtained during the course of the experiment. As such, both raw and reduced data are presented. Portions of the data require explanation.

There are several gaps in the data due to physical considerations. The 6-inch diameter light beam prohibits one from performing scatter measurements ± 15 degrees from $\Psi = 0$ and $\Psi = 180$ degrees. This range is denoted by the letter TB on the data sheets. As the photometer is rotated 360 degrees about the window, at two positions (i. e., say $\Psi = 0$, then $\theta = 90$ and 270 degrees) the photometer will view parallel to the window surfaces. This data again is invalid for scatter purposes and it is denoted WE (window edge) on the data sheets. At non-zero values of Ψ (the window inclined with respect to the incident light), the window reflection has a large specular component that reflects at some angle θ . For example, if $\Psi = 10$ degrees, then, at $\theta = 10$ degrees, the beam is reflected and instead of measuring a relatively small scattered component of light, a large reflected value is recorded. This specular reflection off the window is evident not only when the photometer points directly at the specular reflection but also at the conjugate position. That is when the off-axis cone blackbody is flooded by the specular reflection and the photometer looks through the window and records an invalid luminance reflected from the inefficient blackbody. The situation where the photometer views directly the specular reflection is denoted WR (window reflection), and, where the photometer views the blackbody, it is denoted BR (blackbody reflection) on the data sheets on the following pages.

In the data presented on the following pages a digital computer has been used to reduce and record the necessary information. The use of such a machine precluded the notation heretofore described. Instead of L_d the computer types out LD, for instance, other notational change are,

<u>Appendix C</u>	<u>Text</u>
PSI	Ψ
THETA	θ
LW	L_w
LD	L_d

The raw and reduced data is presented in the manner in which it was recorded. For clarity the data is given in the following order.

<u>Window</u>	<u>3D Angle</u>	<u>Comments</u>
244	0°	NASA cleaning procedure
244	0°	Honeywell cleaning procedure
244	0°	After contamination by room-temperature-cured RTV-560
244	0°	After Honeywell cleaning and placing in vacuum system to calibrate for system contamination without RTV outgassing
246	0°	NASA cleaning procedure
246	0°	Honeywell cleaning procedure
246	0°	After contamination by high-temperature-cured RTV-560
244 & 246	0°	NASA cleaning procedure
244 & 246	0°	244 contaminated by room-temperature-cured RTV, 246 contaminated by high-temperature-cured RTV.
Apollo glass specimen	0°	Large angles are invalid data due to reflection from fixture. This sample was contaminated in space on an Apollo mission.

NASA Cleaning Procedure

26/11/1969 WINDOW NO 244

START LD 196.000 END LD 209.000

MEAN LD 202.50 E COS(PSI) 211.60

PSI 0 DEGREE

THETA	LW*E-3	LB*E-4	(LW-LB)/(E*COS(PSI))*E-5
20	3.9000	1.9000	1.753
30	3.0000	2.6000	1.295
40	2.6000	1.6000	1.153
50	2.3200	1.2000	1.040
60	2.1200	1.0000	0.955
70	2.2200	0.8000	1.011
80	2.8000	0.8000	1.285
100	2.5000	0.7000	1.148
110	3.0000	0.8000	1.380
120	3.5000	0.9000	1.612
130	4.1000	1.1000	1.886
140	5.3000	1.5000	2.434
150	7.9000	2.1000	3.634
160	15.4000	10.2000	6.796
200	23.0000	11.4000	10.331
210	9.4000	2.6000	4.319
220	5.9000	1.6000	2.713
230	5.0000	1.2000	2.306
240	3.9000	1.0000	1.796
250	3.6000	0.9000	1.659
260	4.1000	0.8000	1.900
280	2.9000	0.9000	1.328
290	2.2700	1.0000	1.026
300	1.9800	1.1000	0.884
310	1.9300	0.9000	0.870
320	2.0600	1.5000	0.903
330	2.3700	2.3000	1.011
340	3.1000	4.2000	1.267

 26/11/1969 WINDOW NO 244
 START LD 209.20 END LD 211.00
 MEAN LD 210.00 E COS(Psi) 216.10

PSI 10 DEGREE

THETA	LW*E-3	LB*E-4	(LW-LB)/(E*COS(Psi))*E-5
10	148.000	1.900	68486.094
20	11.800	2.600	5.340
30	4.100	1.700	1.819
40	3.300	1.200	1.472
50	2.900	1.000	1.296
60	2.800	0.800	1.259
70	2.800	0.750	1.261
80	4.000	0.700	1.819
100	5.300	0.800	2.416
110	4.900	0.950	2.223
120	6.300	1.100	2.864
130	8.300	1.400	3.776
140	10.300	2.200	4.664
150	18.700	10.200	8.181
190	27.700	11.200	12.300
200	8.700	3.100	3.882
210	5.700	1.800	2.554
220	4.100	1.400	1.832
230	3.500	1.000	1.573
240	3.100	0.900	1.393
250	2.900	0.800	1.305
260	3.200	0.800	1.444
280	2.800	1.100	1.245
290	2.280	1.100	1.004
300	2.120	0.900	0.939
310	2.110	1.500	0.907
320	2.270	2.300	0.944
330	2.770	4.200	1.087

26/11/1969 WINDOW NO 244

START LD 211.00 END LD 213.00
MEAN LD 212.00 E COS(Psi) 208.17

PSI 20 DEGREE

THETA	LW*E-3	LB*E-4	(LW-LB)/(E*COS(Psi))*E-5
0	3.500	1.900	1.590
10	7.100	2.600	3.286
20	221999.959	1.700	106645.562
30	22.900	1.200	10.943
40	4.400	1.000	2.066
50	3.700	0.800	1.739
60	3.500	0.750	1.645
70	3.700	0.700	1.744
80	5.600	0.700	2.657
100	8.100	1.000	3.843
110	8.700	1.200	4.122
120	10.700	1.500	5.068
130	13.300	2.200	6.283
140	22.600	10.200	10.367
180	17.400	11.200	7.821
190	9.100	3.200	4.218
200	9.600	1.800	4.525
210	3.900	1.500	1.801
220	3.100	1.000	1.441
230	2.900	0.900	1.350
240	2.500	0.800	1.163
250	2.290	0.800	1.062
260	3.300	1.000	1.537
280	3.500	1.200	1.624
290	2.150	0.900	0.990
300	2.040	1.500	0.908
310	2.100	2.400	0.894
320	2.400	4.100	0.956

1/12/1969 WINDOW NO 244
 START LD 195.00 END LD 204.00
 MEAN LD 199.50 E COS(PSI) 180.54

PSI 30 DEGREE

THETA	LW*E-3	LB*E-4	(LW-LB)/(E*COS(PSI))*E-5
0	2.550	2.600	1.268
10	2.800	1.600	1.462
20	22.900	1.200	12.618
30	42.000	1.000	232641.687
40	11.200	0.800	6.159
50	5.300	0.750	2.894
60	4.300	0.600	2.349
70	4.900	0.700	2.675
80	8.100	0.800	4.442
100	12.800	1.100	7.029
110	13.900	1.500	7.616
120	17.600	2.200	9.627
130	30.000	10.200	16.052
170	17.600	11.200	9.128
180	8.400	3.100	4.481
190	4.700	1.900	2.498
200	3.400	1.500	1.800
210	10.200	1.000	5.594
220	2.400	0.800	1.285
230	2.100	0.800	1.119
240	2.100	0.800	1.119
250	2.100	1.000	1.108
260	2.100	1.100	1.102
280	2.800	1.000	1.496
290	3.100	1.500	1.634
300	2.700	2.400	1.363
310	2.700	4.000	1.274
350	2.900	1.800	1.507

1/12/1969 WINDOW NO 244

START LD 284.88 END LD 284.88
MEAN LD 284.88 E COS(PSI) 163.29

PSI 40 DEGREE

THETA	LW*E-3	LB*E-4	(LW-LB)/(E*COS(PSI))*E-5
0	1.850	1.600	1.035
10	1.950	1.200	1.121
20	2.500	1.000	1.470
30	34.000	0.800	20.772
40	130000.000	0.800	79610.594
50	70.000	0.600	42.831
60	8.800	0.700	5.346
70	8.700	0.800	5.279
80	11.500	1.000	6.981
100	23.500	1.500	14.299
110	26.500	2.200	16.094
120	4.500	10.200	2.131
160	22.000	11.200	12.787
170	9.000	3.100	5.322
180	5.200	1.800	3.074
190	3.100	1.600	1.800
200	2.300	1.000	1.347
210	2.400	0.800	1.421
220	23.500	0.800	14.342
230	2.100	0.800	1.237
240	1.750	1.000	1.010
250	1.700	1.000	0.980
260	1.850	1.000	1.072
280	3.000	1.500	1.745
290	3.600	2.500	2.052
300	3.000	4.100	1.586
340	2.500	1.800	1.421
350	2.200	2.600	1.188

28/11/1969 WINDOW NO 244
 START LD 186.000 END LD 196.000
 MEAN LD 191.000 E COS(PST) 128.29

PST 50 DEGREE

THETA	LW*E-3	LB*E-4	(LW-LB)/(E*COS(PST))*E-5
0	1.570	1.200	1.130
10	1.590	1.000	1.161
20	1.830	0.850	1.360
30	3.100	0.800	2.354
40	77.000	0.700	59.966
50	186.000	0.700	14498.475
60	280.000	0.800	218.195
70	25.000	0.900	19.417
80	30.000	1.300	23.283
100	47.000	2.200	36.465
110	68.000	9.400	52.273
150	23.100	11.200	17.133
160	10.100	3.100	7.631
170	6.000	1.800	4.537
180	3.600	1.500	2.689
190	2.180	1.000	1.621
200	1.680	0.800	1.247
210	1.420	0.800	1.045
220	2.290	0.800	1.723
230	62.000	1.100	48.243
240	2.700	1.200	2.011
250	1.760	1.400	1.263
260	2.040	1.100	1.504
280	3.700	4.000	2.572
290	3.300	4.700	2.206
330	1.920	1.800	1.356
340	1.630	2.600	1.068
350	1.570	1.600	1.099

1/12/1969 WINDOW NO 244

START LD 203.000 END LD 219.000
MEAN LD 211.000 E COS(PSI) 110.24

PSI 60 DEGREE

THETA	LW*E-3	LB*E-4	(LW-LB)/(E*COS(PSI))*E-5
0	1.3000	1.0000	1.089
10	1.3500	0.9500	1.138
20	1.5500	0.8000	1.333
30	2.3000	0.8000	2.014
40	5.4000	0.8000	4.826
50	42.0000	0.9000	38.017
60	950000.0000	2.0000	8617534.0000
70	460.0000	3.9000	416.916
80	76.0000	8.2000	68.196
100	145.0000	12.8000	130.370
140	32.0000	11.1000	28.021
150	12.5000	3.2000	11.049
160	6.5000	1.8000	5.733
170	4.0000	1.6000	3.483
180	2.6000	1.1000	2.259
190	1.9000	0.9000	1.642
200	1.5500	0.9000	1.324
210	1.4000	0.9000	1.188
220	1.4500	1.1000	1.216
230	4.6000	1.5000	4.037
240	190.0000	1.8000	172.187
250	5.0000	2.0000	4.354
260	4.4000	3.8000	3.647
280	4.8000	8.2000	3.610
320	1.9500	1.8000	1.606
330	1.6500	2.6000	1.261
340	1.5500	1.7000	1.252
350	1.4500	1.2000	1.206

1/12/1969 WINDOW NO 244
 START LD 219.000 END LD 201.000
 MEAN LD 210.000 E COS(PHI) 75.05

PSI 70 DEGREE

THETA	LW*E-3	LB*E-4	(LW-LB)/(E*COS(PHI))*E-5
0	0.890	0.950	1.059
10	0.950	0.800	1.159
20	1.180	0.800	1.466
30	1.840	0.800	2.345
40	3.200	0.950	4.137
50	7.800	1.300	10.220
60	57.000	5.000	75.282
70	310.000	14.500	413.498
80	460.000	42.000	6123.530
130	42.000	10.900	54.509
140	15.000	3.100	19.573
150	7.300	1.800	9.487
160	4.300	1.600	5.516
170	2.700	1.100	3.451
180	1.930	0.900	2.452
190	1.480	0.800	1.865
200	1.230	0.900	1.519
210	1.090	1.100	1.306
220	1.120	1.300	1.319
230	1.410	1.800	1.639
240	2.070	2.000	2.492
250	36.000	4.000	479.138
260	9.100	10.000	10.793
310	1.700	2.200	1.972
320	1.170	2.900	1.173
330	0.910	1.700	0.986
340	0.840	1.200	0.959
350	0.810	1.000	0.946

 -28/11/1969-----WINDOW NO-244-----

START LD 223.000 END LD 208.000
 MEAN LD 215.500 E COS(PSI) 39.10

PSI 80 DEGREE

THETA	LW*E-3	LB*E-4	(LW-LB)/(E*COS(PSI))*E-5
0	0.790	0.800	1.816
10	0.850	0.800	1.969
20	1.000	0.800	2.353
30	1.700	0.950	4.105
40	3.400	1.000	8.439
50	8.600	1.600	21.584
60	100.000	6.100	254.177
70	165.000	26.000	415.318
80	800.000	139.000	204589856.000
120	44.000	8.500	110.351
130	12.000	3.200	29.870
140	4.900	1.900	12.045
150	2.700	1.600	6.496
160	1.700	1.100	4.066
170	1.250	1.000	2.941
180	0.950	0.800	2.225
190	0.680	0.800	1.534
200	0.600	1.000	1.279
210	0.600	1.200	1.228
220	0.620	1.300	1.253
230	0.850	1.500	1.790
240	1.350	2.900	2.711
250	2.500	17.000	2.046
260	810.000	19.500	2066.486
300	3.000	2.600	7.007
310	1.150	3.200	2.123
320	0.850	1.900	1.688
330	0.870	1.300	1.892
340	0.730	1.000	1.611
350	0.740	0.950	1.650

Honeywell Cleaning Procedure

2/12/1969 WINDOW NO 244			
START LD	200.00	END LD	203.00
MEAN LD	201.50	E COS(Psi)	210.55
(
PSI 0 DEGREE			
THETA	LW*E-3	LB*E-4	(LW-LB)/(E*COS(Psi))*E-5
15	14.500	1.900	6.796
20	6.700	1.900	3.892
30	4.300	2.600	1.919
40	3.400	1.600	1.539
50	3.000	1.200	1.368
60	3.100	1.000	1.425
70	3.500	0.800	1.624
80	4.100	0.800	1.909
100	5.600	0.700	2.626
110	5.800	0.800	2.717
120	6.700	0.900	3.139
130	8.300	1.100	3.890
140	11.100	1.500	5.201
150	18.900	2.100	8.877
160	40.000	10.200	18.513
200	38.000	11.400	17.506
210	19.200	2.600	8.995
220	11.400	1.600	5.338
230	8.400	1.200	3.932
240	7.100	1.000	3.325
250	6.300	0.900	2.949
260	7.200	0.800	3.382
280	4.200	0.900	1.952
290	3.500	1.000	1.615
300	2.900	1.100	1.325
310	2.900	0.900	1.335
320	3.200	1.500	1.449
330	3.900	2.300	1.743
340	6.000	4.200	2.650
345	8.200	8.400	3.496

---2/12/1969--- WINDOW NO 244 ---

START LD 203.000 END LD 203.000
MEAN LD 203.000 E COS(PSI) 208.90

PSI 10 DEGREE

THETA	LW*E-3	LB*E-4	(LW-LB)/(E*COS(PSI))*E-5
5	212.000	1.900	101.394
10	251999.969	1.900	120632.594
20	14.200	2.600	6.673
30	6.500	1.700	3.030
40	4.800	1.200	2.240
50	4.100	1.000	1.915
60	4.100	0.800	1.924
70	4.700	0.750	2.214
80	5.800	0.700	2.743
100	8.700	0.800	4.126
110	9.500	0.950	4.502
120	11.300	1.100	5.357
130	15.100	1.400	7.161
140	22.300	2.200	10.570
150	46.000	10.200	21.532
190	48.000	11.200	22.442
200	17.800	3.100	8.372
210	9.800	1.800	4.605
220	7.300	1.400	3.427
230	5.700	1.000	2.681
240	5.000	0.900	2.350
250	4.600	0.800	2.164
260	4.800	0.800	2.259
280	3.500	1.100	1.623
290	3.100	1.100	1.431
300	2.700	0.900	1.249
310	2.700	1.500	1.221
320	3.000	2.300	1.326
330	3.700	4.200	1.570
335	4.500	8.500	1.747

2/12/1969 WINDOW NO 244
 START LD 203.000 END LD 196.000
 EAN LD 199.500 E COS(PSI) 195.89

PSI 20 DEGREE

THETA	LW*E-3	LB*E-4	(LW-LB)/(E*COS(PSI))*E-5
0	5.500	1.900	2.711
10	20.000	2.600	10.077
20	340000.000	1.700	173564.875
30	18.300	1.200	9.281
40	6.800	1.000	3.420
50	5.400	0.800	2.716
60	5.300	0.750	2.667
70	6.300	0.700	3.180
80	7.900	0.700	3.997
100	12.700	1.000	6.432
110	14.300	1.200	7.239
120	19.500	1.500	9.878
130	25.600	2.200	12.956
140	49.000	10.200	24.493
180	34.000	11.200	16.785
190	15.800	3.200	7.902
200	14.400	1.800	7.259
210	5.900	1.500	2.935
220	4.400	1.000	2.195
230	3.800	0.900	1.894
240	3.400	0.800	1.695
250	3.200	0.800	1.593
260	3.600	1.000	1.787
280	2.870	1.200	1.404
290	2.710	0.900	1.337
300	2.420	1.500	1.159
310	2.520	2.400	1.164
320	2.900	4.100	1.271
325	3.500	8.400	1.358
355	12.800	1.900	6.437

3/12/1969 WINDOW NO 244

START LD 195.000 END LD 204.000
MEAN LD 199.500 E COS(PHI) 180.54

PSI 30 DEGREE

THETA	LW*E-3	LB*E-4	(LW-LB)/(E*COS(PHI))*E-5
0	3.500	2.600	1.795
10	4.900	1.600	2.626
20	17.100	1.200	9.405
30	77.000	1.000	426.509
40	29.000	0.800	16.019
50	9.200	0.750	5.054
60	8.900	0.600	4.897
70	10.200	0.700	5.611
80	13.400	0.800	7.378
100	22.600	1.100	12.457
110	26.500	1.500	14.596
120	40.000	2.200	22.034
130	58.000	10.200	31.562
170	38.000	11.200	20.428
180	16.800	3.100	9.134
190	8.500	1.900	4.603
200	5.300	1.500	2.853
210	15.200	1.000	8.364
220	3.200	0.800	1.728
230	2.700	0.800	1.451
240	2.600	0.800	1.396
250	2.500	1.000	1.329
260	3.100	1.100	1.656
280	2.900	1.000	1.551
290	2.800	1.500	1.468
300	2.700	2.400	1.363
310	3.000	4.000	1.440
315	3.400	8.200	1.429
345	9.600	1.800	5.218
350	3.300	1.800	1.728

3/12/1969 WINDOW NO 244
 START LD 203.00 END LD 193.00
 MEAN LD 198.00 E COS(PSI) 158.49

PSI 40 DEGREE

THETA	LW*E-3	LB*E-4	(LW-LB)/(E*COS(PSI))*E-5
0	2.450	1.600	1.445
10	3.200	1.200	1.943
20	5.200	1.000	3.218
30	45.000	0.800	28.342
40	160.000	0.800	160.951
50	95.000	0.600	59.902
60	15.500	0.700	9.736
70	17.500	0.800	10.991
80	22.000	1.000	13.818
100	40.000	1.500	25.143
110	50.000	2.200	31.409
120	90.000	10.200	56.142
160	36.000	11.200	22.007
170	15.500	3.100	9.584
180	8.000	1.800	4.934
190	4.800	1.600	2.928
200	3.200	1.000	1.956
210	3.000	0.800	1.842
220	27.000	0.800	16.985
230	2.450	0.800	1.495
240	1.000	1.000	1.136
250	1.900	1.000	1.136
260	2.300	1.000	1.388
280	2.550	1.500	1.514
290	2.500	2.500	1.420
300	2.500	4.100	1.319
305	3.000	8.000	1.388
335	8.500	1.800	5.249
340	2.500	1.800	1.464
350	2.250	2.600	1.256

- 3/12/1969 - WINDOW NO 244 -
 START LD 193.000 END LD 185.000
 MEAN LD 189.000 E COS(PSI) 126.95

PSI 50 DEGREE

THETA	LW*E-3	LB*E-4	(LW-LB)/(E*COS(PSI))*E-5
0	1.860	1.200	1.371
10	2.290	1.000	1.725
20	3.300	0.850	2.533
30	5.900	0.800	4.585
40	99.000	0.700	77.931
50	400000.000	0.700	3150957.000
60	490.000	0.800	385.929
70	38.000	0.900	29.863
80	44.000	1.300	34.558
100	84.000	2.200	65.997
110	114.000	9.400	89.062
150	39.000	11.200	29.840
160	17.300	3.100	13.384
170	8.900	1.800	6.869
180	5.100	1.500	3.899
190	3.300	1.000	2.521
200	2.240	0.800	1.702
210	1.800	0.800	1.355
220	2.780	0.800	2.127
230	66.000	1.100	51.904
240	2.800	1.200	2.111
250	1.620	1.400	1.166
260	1.930	1.100	1.434
280	2.410	4.000	1.583
290	2.710	4.700	1.765
295	2.780	8.500	1.520
325	9.500	1.800	7.342
330	2.090	1.800	1.505
340	1.810	2.600	1.221
350	1.770	1.600	1.268

3/12/1969 WINDOW NO 244
 START LD 185.000 END LD 185.000
 MEAN LD 185.000 E COS(PSI) 96.66

PSI 60 DEGREE

THETA	LW*E-3	LB*E-4	(LW-LB)/(E*COS(PSI))*E-5
0	1.550	1.000	1.550
10	1.840	0.950	1.805
20	2.610	0.800	2.618
30	4.500	0.800	4.573
40	9.700	0.800	9.953
50	50.000	0.900	51.637
60	108.000	2.000	117.362
70	90.000	3.900	93.732
80	114.000	8.200	117.095
100	195.000	12.800	200.422
140	45.000	11.100	45.408
150	18.500	3.200	18.809
160	8.600	1.800	8.711
170	5.100	1.600	5.111
180	3.300	1.100	3.300
190	2.280	0.900	2.266
200	1.660	0.900	1.624
210	1.430	0.900	1.386
220	1.470	1.100	1.407
230	3.900	1.500	3.880
240	178.000	1.800	183.972
250	4.800	2.000	4.759
260	2.800	3.800	2.504
280	3.700	8.200	2.980
285	3.900	10.600	2.938
315	4.100	1.800	4.056
320	1.860	1.800	1.738
330	1.530	2.600	1.314
340	1.430	1.700	1.304
350	1.470	1.200	1.397

-- 3/12/1969 WINDOW NO 244

START LD 193.60 END LD 194.60
MEAN LD 193.50 E COS(Psi) 69.15

PSI 70 DEGREE

THETA	LW*E-3	LB*E-4	(LW-LB)/(E*COS(Psi))*E-5
0	1.280	0.950	1.714
10	1.550	0.800	2.126
20	2.150	0.800	2.993
30	3.800	0.800	5.379
40	8.000	0.950	11.431
50	21.000	1.300	30.179
60	95.000	5.000	136.650
70	280.000	14.500	404.890
80	1350.000	42.000	1946.075
130	60.000	10.900	85.186
140	22.000	3.100	31.365
150	9.500	1.800	13.477
160	5.600	1.600	7.866
170	3.300	1.100	4.613
180	2.300	0.900	3.196
190	1.600	0.800	2.198
200	1.250	0.900	1.677
210	1.150	1.100	1.504
220	1.150	1.300	1.475
230	1.550	1.800	1.981
240	2.400	2.000	3.181
250	440.000	4.000	635.677
260	7.000	10.000	8.676
270	18.500	15.500	24.510
300	8.000	2.200	11.250
310	1.750	2.200	2.212
320	1.350	2.900	1.533
330	1.200	1.700	1.489
340	1.150	1.200	1.489
350	1.180	1.000	1.562

3/12/1969 WINDOW NO 244

START LD 194.00 END LD 195.00
EAN LD 194.50 E COS(PSI) 35.29

PSI 80 DEGREE

THETA	LW*E-3	LB*E-4	(LW-LB)/(E*COS(PSI))*E-5
0	0.800	0.800	2.040
10	1.050	0.800	2.748
20	1.450	0.800	3.882
30	2.600	0.950	7.098
40	5.400	1.000	15.018
50	13.000	1.600	36.382
60	44.000	6.100	122.945
70	193.000	26.000	539.497
80	720.000	139.000	2040.113
120	78.000	8.500	218.604
130	21.000	3.200	58.597
140	9.000	1.900	24.963
150	4.400	1.600	12.014
160	2.500	1.100	6.772
170	1.580	1.000	4.194
180	1.150	0.800	3.032
190	0.870	0.800	2.238
200	0.740	1.000	1.813
210	0.680	1.200	1.587
220	0.730	1.300	1.700
230	0.950	1.500	2.267
240	1.400	2.900	3.145
250	2.300	17.000	1.700
260	780.000	19.500	2204.598
295	7.400	2.600	20.231
300	2.200	2.600	5.497
310	0.950	3.200	1.785
320	0.770	1.900	1.643
330	0.700	1.300	1.615
340	0.700	1.000	1.700
350	0.710	0.950	1.743

After Vacuum Outgas

27/12/1969 WINDOW NO 244

START LD 198.88 END LD 198.88
EAN LD 198.88 E COS(PSI) 198.54

PSI ° DEGREE

THETA	LW×E_3	LB×E_4	(LW-LB)/(E×COS(PSI))×E_5
15	68.888	1.988	38.125
20	28.888	1.988	14.887
30	14.888	2.688	6.921
40	9.188	1.688	4.523
50	7.888	1.288	3.868
60	7.188	1.888	3.526
70	7.188	0.888	3.536
80	7.688	0.888	3.788
100	10.888	0.788	5.082
110	8.288	0.888	4.890
120	7.488	0.988	3.682
130	8.188	1.188	4.824
140	10.188	1.588	5.812
150	16.188	2.188	8.884
160	42.888	10.288	28.641
200	46.888	11.488	22.595
210	16.588	2.688	8.188
220	10.288	1.688	5.857
230	7.888	1.288	3.868
240	7.388	1.888	3.627
250	8.188	0.988	4.835
260	12.888	0.888	6.884
280	9.288	0.988	4.589
290	9.788	1.088	4.835
300	7.888	1.188	3.873
310	7.888	0.988	3.883
320	9.788	1.588	4.818
330	15.888	2.388	7.439
340	38.888	4.288	14.899
345	46.888	8.488	22.746

27/12/1969 WINDOW NO 244

START LD	197.66	END LD	191.00
EAN LD	198.50	E COS(PSI)	196.04

PSI 10 DEGREE

THETA	LW×E_3	LB×E_4	(LW-LB)/(E×COS(PSI))×E_5
5	4000.000	1.900	2040.351
10	295000.000	1.900	1504830.000
20	190.000	2.600	96.789
30	29.000	1.700	14.707
40	13.800	1.200	6.978
50	10.300	1.000	5.203
60	9.000	0.800	4.550
70	8.600	0.750	4.349
80	9.500	0.700	4.810
100	12.600	0.800	6.387
110	9.700	0.950	4.900
120	10.300	1.100	5.198
130	12.500	1.400	6.305
140	21.000	2.200	10.600
150	51.000	10.200	25.495
190	173.000	11.200	87.678
200	16.700	3.100	8.361
210	8.700	1.800	4.346
220	6.300	1.400	3.142
230	5.400	1.000	2.704
240	5.200	0.900	2.607
250	6.400	0.800	3.224
260	10.000	0.800	5.060
280	8.000	1.100	4.025
290	9.800	1.100	4.943
300	6.400	0.900	3.219
310	6.200	1.500	3.086
320	7.300	2.300	3.606
330	9.700	4.200	4.734
335	11.500	8.500	5.433

27/12/1969 WINDOW NO 244
 START LD 191.000 END LD 195.000
 EAN LD 193.000 E COS(PSI) 189.51

PSI 20 DEGREE

THETA	LW*E_3	LB*E_4	(LW-LB)/(E*COS(PSI))*E_5
0	28.000	1.900	14.675
10	70.000	2.600	369.237
20	270.000	1.700	1424729.500
30	250.000	1.200	131.856
40	32.000	1.000	16.833
50	17.200	0.800	9.034
60	12.500	0.750	6.556
70	11.000	0.700	5.768
80	13.300	0.700	6.981
100	18.000	1.000	9.445
110	15.000	1.200	7.852
120	17.800	1.500	9.314
130	27.000	2.200	14.131
140	64.000	10.200	33.233
180	45.000	11.200	23.154
190	21.000	3.200	10.912
200	128.000	1.800	67.448
210	9.600	1.500	4.987
220	4.500	1.000	2.322
230	4.000	0.900	2.063
240	4.300	0.800	2.227
250	5.500	0.800	2.860
260	9.300	1.000	4.855
280	7.400	1.200	3.841
290	9.000	0.900	4.702
300	5.700	1.500	2.929
310	5.400	2.400	2.723
320	6.500	4.100	3.214
325	7.400	8.400	3.462
355	30.000	1.900	15.730

27/12/1969

WINDOW NO 244

START LD	195.00	END LD	193.00
EAN LD	194.00	E COS(PSI)	175.56

PSI 30 DEGREE

THETA	LW×E_3	LB×E_4	(LW-LB)/(E×COS(PSI))×E_5
0	12.800	2.600	7.143
10	25.000	1.600	14.149
20	68.000	1.200	387.268
30	220.000	1.000	1253147.750
40	430.000	0.800	244.888
50	47.000	0.750	26.729
60	24.000	0.600	13.637
70	17.500	0.700	9.928
80	22.000	0.800	12.486
100	30.000	1.100	17.026
110	29.000	1.500	16.433
120	43.000	2.200	24.368
130	94.000	10.200	52.963
170	54.000	11.200	30.121
180	15.500	3.100	8.652
190	7.800	1.900	4.335
200	12.000	1.500	6.750
210	115.000	1.000	65.448
220	7.700	0.800	4.340
230	3.400	0.800	1.891
240	3.600	0.800	2.005
250	4.500	1.000	2.506
260	9.200	1.100	5.178
280	6.700	1.000	3.759
290	8.900	1.500	4.984
300	5.000	2.400	2.711
310	5.000	4.000	2.620
315	5.500	8.200	2.666
345	12.500	1.800	7.018
350	9.200	1.800	5.138

27/12/1969 WINDOW NO 244

START LD	193.00	END LD	190.00
EAN LD	191.50	E COS(PSI)	153.29

PSI 40 DEGREE

THETA	LW×E_3	LB×E_4	(LW-LB)/(E×COS(PSI))×E_5
0	7.800	1.600	4.984
10	11.500	1.200	7.424
20	25.700	1.000	16.700
30	66.000	0.800	430.507
40	1950.000	0.800	1272107.500
50	520.000	0.600	339.189
60	67.000	0.700	43.663
70	33.000	0.800	21.476
80	38.000	1.000	24.725
100	58.000	1.500	37.739
110	74.000	2.200	48.131
120	160.000	10.200	103.713
160	68.000	11.200	43.630
170	16.000	3.100	10.236
180	8.100	1.800	5.167
190	4.900	1.600	3.092
200	3.800	1.000	2.414
210	11.500	0.800	7.450
220	105.000	0.800	68.446
230	6.000	0.800	3.862
240	3.100	1.000	1.957
250	4.100	1.000	2.609
260	9.000	1.000	5.806
280	6.000	1.500	3.816
290	11.000	2.500	7.013
300	4.800	4.100	2.864
305	5.100	8.000	2.805
335	13.200	1.800	8.494
340	5.500	1.800	3.471
350	6.000	2.600	3.745

27/12/1969 WINDOW NO 244

START LD 195.000 END LD 191.000
EAN LD 193.000 E COS(PSI) 129.63

PSI 50 DEGREE

THETA	LW×E-3	LB×E-4	(LW-LB)/(E×COS(PSI))×E-5
0	5.500	1.200	4.150
10	7.500	1.000	5.708
20	11.800	0.850	9.037
30	30.000	0.800	23.081
40	67.000	0.700	516.793
50	330.000	0.700	2545663.000
60	140.000	0.800	1079.917
70	150.000	0.900	115.643
80	110.000	1.300	84.755
100	195.000	2.200	150.256
110	410.000	9.400	315.554
150	88.000	11.200	67.020
160	20.000	3.100	15.189
170	8.000	1.800	6.032
180	5.200	1.500	3.896
190	3.700	1.000	2.777
200	2.900	0.800	2.175
210	2.600	0.800	1.944
220	13.500	0.800	10.352
230	12.500	1.100	9.558
240	5.300	1.200	3.996
250	4.000	1.400	2.978
260	9.000	1.100	6.858
280	6.500	4.000	4.706
290	9.300	4.700	6.812
295	8.100	8.500	5.593
325	7.000	1.800	5.261
330	4.200	1.800	3.101
340	4.000	2.600	2.885
350	4.500	1.600	3.348

27/12/1969

WINDOW NO 244

START LD 191.000 END LD 187.00

EAN LD 189.000 E COS(PSI) 98.75

PSI 60 DEGREE

THETA	LW×E_3	LB×E_4	(LW-LB)/(E×COS(PSI))×E_5
0	3.800	1.000	3.747
10	4.800	0.950	4.765
20	6.800	0.800	6.805
30	12.300	0.800	12.375
40	40.000	0.800	40.427
50	110.000	0.900	1113.877
60	860.000	2.000	8709206.000
70	330.000	3.900	3341.510
80	590.000	8.200	596.662
100	1050.000	12.800	1062.037
140	128.000	11.100	128.501
150	27.500	3.200	27.525
160	10.000	1.800	9.945
170	5.400	1.600	5.307
180	3.800	1.100	3.737
190	2.800	0.900	2.744
200	2.300	0.900	2.238
210	2.230	0.900	2.167
220	2.450	1.100	2.370
230	14.500	1.500	14.532
240	225.000	1.800	227.675
250	6.700	2.000	6.583
260	10.000	3.800	9.742
280	7.800	8.200	7.069
285	12.500	10.600	11.585
315	4.800	1.800	4.679
320	3.500	1.800	3.362
330	2.900	2.600	2.674
340	3.000	1.700	2.866
350	3.200	1.200	3.119

27/12/1969 WINDOW NO 244
 START LD 187.000 END LD 187.000
 IEAN LD 187.000 E COS(PSI) 66.83

PSI 70 DEGREE

THETA LW*E-3 LB*E-4 (LW-LB)/(E*COS(PSI))*E-5

0	2.650	0.950	3.823
10	3.300	0.800	4.818
20	4.500	0.800	6.614
30	7.300	0.800	10.803
40	15.900	0.950	23.649
50	82.000	1.300	122.502
60	1160.000	5.000	1734.959
70	25300.000	14.500	37856368.000
80	14400.000	42.000	21540.422
130	242.000	10.900	360.473
140	45.000	3.100	66.870
150	11.800	1.800	17.387
160	6.000	1.600	8.738
170	3.700	1.100	5.372
180	2.630	0.900	3.801
190	2.180	0.800	3.142
200	1.950	0.900	2.783
210	1.840	1.100	2.589
220	2.080	1.300	2.918
230	2.600	1.800	3.621
240	9.000	2.000	13.167
250	380.000	4.000	567.995
260	15.100	10.000	21.098
275	810.000	15.500	1209.683
305	7.100	2.200	10.295
310	3.400	2.200	4.758
320	2.400	2.900	3.157
330	2.120	1.700	2.918
340	2.070	1.200	2.918
350	2.300	1.000	3.292

27/12/1969 WINDOW NO 244

START LD 187.00 END LD 187.00

EAN LD 187.00 E COS(PST) 33.93

PSI 80 DEGREE

THETA	LW*E_3	LB*E_4	(LW-LB)/(E*COS(PST))*E_5
0	1.760	0.800	4.951
10	2.400	0.800	6.837
20	3.000	0.800	8.606
30	4.400	0.950	12.687
40	8.700	1.000	25.345
50	31.000	1.600	90.890
60	235.000	6.100	690.779
70	1400.000	26.000	1178.871
80	6700.000	139.000	197457888.000
120	17.000	8.500	132.648
130	66.000	3.200	193.568
140	16.800	1.900	48.952
150	6.900	1.600	19.864
160	3.800	1.100	10.875
170	2.550	1.000	7.220
180	2.050	0.800	5.806
190	1.780	0.800	5.010
200	1.640	1.000	4.539
210	1.500	1.200	4.067
220	1.620	1.300	4.391
230	2.150	1.500	5.804
240	2.970	2.900	7.898
250	5.600	17.000	11.404
260	70.000	19.500	2057.247
295	13.300	2.600	38.431
300	4.600	2.600	12.791
310	2.030	3.200	5.040
320	1.480	1.900	3.802
330	1.360	1.300	3.625
340	1.430	1.000	3.920
350	1.570	0.950	4.347

15/12/1969 WINDOW NO 244

START LD 193.000 END LD 194.000
EAN LD 193.500 E COS(PSI) 202.19

PSI 0 DEGREE

THETA LW*E-3 LB*E-4 (LW-LB)/(E*COS(PSI))*E-5

15	1.830	1.900	0.811
20	4.800	1.900	2.280
30	3.600	2.600	1.652
40	3.100	1.600	1.454
50	0.290	1.200	0.084
60	0.290	1.000	0.093
70	3.300	0.800	1.593
80	5.300	0.800	2.582
100	5.900	0.700	2.883
110	6.000	0.800	2.928
120	6.300	0.900	3.071
130	7.000	1.100	3.408
140	8.800	1.500	4.278
150	1.220	2.100	0.500
160	2.660	10.200	0.811
200	31.000	11.400	14.768
210	1.520	2.600	0.623
220	10.300	1.600	5.015
230	7.800	1.200	3.798
240	7.700	1.000	3.759
250	6.400	0.900	3.121
260	6.800	0.800	3.324
280	6.300	0.900	3.071
290	4.400	1.000	2.127
300	0.290	1.100	0.089
310	0.280	0.900	0.093
320	0.290	1.500	0.069
330	3.600	2.300	1.667
340	4.800	4.200	2.166
345	6.800	8.400	2.948

15/12/1969

WINDOW NO 244

START LD 193.00 END LD 194.00

EAN LD 193.50 E COS(Psi) 199.12

Psi 10 DEGREE

THETA	LW*E-3	LB*E-4	(LW-LB)/(E*COS(Psi))*E-5
5	660.000	1.900	331.359
10	890.000	1.900	44696.000
20	15.100	2.600	7.453
30	8.100	1.700	3.982
40	4.600	1.200	2.250
50	3.700	1.000	1.808
60	3.400	0.800	1.667
70	4.100	0.750	2.021
80	6.800	0.700	3.380
100	8.400	0.800	4.178
110	8.900	0.950	4.422
120	9.600	1.100	4.765
130	1.100	1.400	0.482
140	1.500	2.200	0.643
150	2.850	10.200	0.919
190	37.000	11.200	18.019
200	1.350	3.100	0.522
210	8.800	1.800	4.329
220	6.400	1.400	3.144
230	5.300	1.000	2.611
240	4.800	0.900	2.365
250	4.600	0.800	2.270
260	5.200	0.800	2.571
280	5.400	1.100	2.657
290	3.900	1.100	1.903
300	3.700	0.900	1.813
310	2.600	1.500	1.230
320	2.800	2.300	1.291
330	3.600	4.200	1.597
335	4.300	8.500	1.733

15/12/1969 WINDOW NO 244
 START LD 194.00 END LD 192.00
 (EAN LD 193.00 E COS(PSI) 189.51

PSI 20 DEGREE

THETA	LW*E-3	LB*E-4	(LW-LB)/(E*COS(PSI))*E-5
0	4.300	1.900	2.169
10	2.500	2.600	1.182
20	10400.000	1.700	5487.758
30	8.700	1.200	4.527
40	4.700	1.000	2.427
50	4.100	0.800	2.121
60	4.300	0.750	2.229
70	4.900	0.700	2.549
80	8.600	0.700	4.501
100	1.120	1.000	0.538
110	1.220	1.200	0.580
120	1.400	1.500	0.660
130	1.850	2.200	0.860
140	35.000	10.200	17.930
180	28.000	11.200	14.184
190	1.300	3.200	0.517
200	1.150	1.800	0.512
210	5.700	1.500	2.929
220	4.400	1.000	2.269
230	3.600	0.900	1.852
240	3.500	0.800	1.805
250	3.500	0.800	1.805
260	4.000	1.000	2.058
280	4.700	1.200	2.417
290	3.500	0.900	1.799
300	2.500	1.500	1.240
310	2.800	2.400	1.351
320	3.100	4.100	1.419
325	3.700	8.400	1.509
355	1.790	1.900	0.844

15/12/1969 WINDOW NO 244
 START LD 203.00 END LD 201.00
 EAN LD 202.00 E COS(PSI) 182.80

PSI 30 DEGREE

THETA	LW*E-3	LB*E-4	(LW-LB)/(E*COS(PSI))*E-5
0	3.100	2.600	1.554
10	4.000	1.600	2.101
20	40.000	1.200	21.816
30	180000.000	1.000	98469.625
40	10.500	0.800	5.700
50	6.100	0.750	3.296
60	7.000	0.600	3.797
70	7.500	0.700	4.065
80	12.000	0.800	6.521
100	18.000	1.100	9.787
110	21.800	1.500	11.297
120	25.500	2.200	14.377
130	45.000	11.200	24.606
170	25.000	11.200	15.252
180	13.000	3.100	6.942
190	7.700	1.900	4.105
200	5.200	1.500	3.145
210	11.000	1.800	5.303
220	3.200	0.800	1.707
230	2.900	0.800	1.543
240	2.700	0.800	1.433
250	2.300	1.000	1.532
260	1.800	1.100	2.566
280	4.000	1.700	2.352
290	3.300	1.500	1.723
300	2.600	2.400	1.291
310	2.050	4.000	1.240
315	2.400	0.200	1.411
345	17.000	1.000	1.251
350	3.200	1.000	1.650

15/12/1969 WINDOW NO 244
 START LD 201.00 END LD 191.00
 (EAN LD 196.00 E COS(PSI) 156.89

PSI 40 DEGREE

THETA	LW*E-3	LB*E-4	(LW-LB)/(E*COS(PSI))*E-5
0	2.200	1.600	1.300
10	2.600	1.200	1.581
20	4.400	1.000	2.741
30	80.000	0.800	50.940
40	5200.000	0.800	33140.250
50	16.500	0.600	10.479
60	9.500	0.700	6.011
70	12.500	0.800	7.916
80	17.800	1.000	11.282
100	28.800	1.500	18.261
110	36.000	2.200	22.806
120	62.000	10.200	38.868
160	30.000	11.200	18.408
170	13.000	3.100	8.088
180	7.500	1.800	4.666
190	4.900	1.600	3.021
200	3.600	1.000	2.231
210	3.900	0.800	2.435
220	20.000	0.800	12.697
230	2.400	0.800	1.479
240	2.100	1.000	1.275
250	2.300	1.000	1.402
260	4.300	1.000	2.677
280	4.000	1.500	2.454
290	3.000	2.500	1.753
300	2.800	4.100	1.523
305	3.100	8.000	1.466
335	18.500	1.800	11.677
340	2.400	1.800	1.415
350	2.080	2.600	1.160

15/12/1969 WINDOW NO 244
 START LD 191.000 END LD 188.000
 EAN LD 189.500 E COS(PSI) 127.28

PSI 50 DEGREE

THETA	LW*E-3	LB*E-4	(LW-LB)/(E*COS(PSI))*E-5
0	1.810	1.200	1.328
10	2.120	1.000	1.587
20	2.960	0.850	2.259
30	6.100	0.800	4.730
40	154.000	0.700	120.937
50	179000.000	0.700	140633.000
60	58.000	0.800	45.505
70	23.400	0.900	18.314
80	30.000	1.300	23.468
100	53.000	2.200	41.467
110	81.000	9.400	62.900
150	37.000	11.200	28.190
160	14.800	3.100	11.384
170	8.200	1.800	6.301
180	5.100	1.500	3.889
190	3.500	1.000	2.671
200	2.700	0.800	2.058
210	2.090	0.800	1.579
220	4.300	0.800	3.315
230	49.000	1.100	38.411
240	2.240	1.200	1.666
250	1.920	1.400	1.398
260	2.700	1.100	2.035
280	3.900	4.000	2.750
290	3.200	4.700	2.145
295	3.200	8.500	1.846
325	18.100	1.800	14.079
330	2.220	1.800	1.603
340	1.750	2.600	1.171
350	1.690	1.600	1.202

15/12/1959 WINDOW NO 244
 START LD 188.00 END LD 185.00
 EAN LD 186.50 E COS(PSI) 97.44

PSI 60 DEGREE

THETA	LW*E-3	LB*E-4	(LW-LB)/(E*COS(PSI))*E-5
0	1.440	1.000	1.375
10	1.790	0.950	1.740
20	2.180	0.800	2.155
30	3.200	0.800	3.202
40	7.200	0.800	7.307
50	350.000	0.900	359.103
60	370000.000	2.000	3797211.000
70	127.000	3.900	129.936
80	61.000	8.200	61.761
100	122.000	12.800	123.892
140	41.000	11.100	40.938
150	16.400	3.200	16.502
160	8.500	1.800	8.539
170	5.000	1.600	4.967
180	3.300	1.100	3.274
190	2.230	0.900	2.196
200	1.680	0.900	1.632
210	1.460	0.900	1.406
220	1.560	1.100	1.488
230	8.400	1.500	8.467
240	122.000	1.800	125.021
250	2.310	2.000	2.165
260	2.840	3.800	2.525
280	4.300	8.200	3.571
285	4.400	10.600	3.428
315	7.900	1.800	7.923
320	1.920	1.800	1.786
330	1.560	2.600	1.334
340	1.400	1.700	1.262
350	1.450	1.200	1.365

15/12/1969

WINDOW NO 244

START LD 185.00

END LD

185.00

EAN LD 185.00

E CCS(PSI)

66.12

PSI 70 DEGREE

THETA	LW*E-3	LB*E-4	(LW-LB)/(E*COS(PSI))*E-5
0	1.220	0.950	1.702
10	1.360	0.800	1.936
20	1.870	0.800	2.707
30	2.750	0.800	4.038
40	5.000	0.950	7.419
50	14.100	1.300	21.129
60	87.000	5.000	1315.097
70	1210.000	14.500	18300.952
80	310.000	42.000	462.515
130	54.000	10.900	80.025
140	18.200	3.100	27.058
150	8.700	1.800	12.886
160	4.900	1.600	7.169
170	3.100	1.100	4.522
180	2.100	0.900	3.040
190	1.540	0.800	2.208
200	1.240	0.900	1.739
210	1.090	1.100	1.482
220	1.130	1.300	1.512
230	1.560	1.800	2.087
240	9.800	2.000	14.520
250	330.000	4.000	498.512
260	5.700	10.000	7.109
275	147.000	15.500	219.990
305	7.500	2.200	11.011
310	1.770	2.200	2.344
320	1.360	2.900	1.618
330	1.140	1.700	1.467
340	1.070	1.200	1.437
350	1.100	1.000	1.512

15/12/1969 WINDOW NO 244

START LD 185.000 END LE 193.000
 EAN LD 189.000 E COS(PSI) 34.29

PSI 80 DEGREE

THETA	LW*E-3	LB*E-4	(LW-LB)/(E*COS(PSI))*E-5
0	0.870	0.800	2.304
10	1.070	0.800	2.887
20	1.460	0.800	4.024
30	2.070	0.950	5.759
40	3.400	1.000	9.623
50	8.100	1.600	23.153
60	31.000	6.100	88.616
70	370.000	26.000	1071.319
80	4200.000	139.000	122469744.000
120	65.000	8.500	187.058
130	16.400	3.200	46.888
140	7.500	1.900	21.316
150	4.400	1.600	12.364
160	2.410	1.100	6.707
170	1.630	1.000	4.461
180	1.140	0.800	3.091
190	0.880	0.800	2.333
200	0.760	1.000	1.925
210	0.730	1.200	1.779
220	0.780	1.300	1.895
230	0.970	1.500	2.391
240	1.670	2.900	4.024
250	8.800	17.000	20.703
260	500.000	19.500	1452.288
295	4.700	2.600	12.947
300	4.800	2.600	13.238
310	1.060	3.200	2.158
320	0.880	1.900	2.012
330	0.780	1.300	1.895
340	0.770	1.000	1.954
350	0.780	0.950	1.997

NASA Cleaning Procedure

23/12/1969 WINDOW NO 246

START LD 185.00 END LD 200.00
EAN LD 192.50 E COS(PSI) 201.15

PSI 0 DEGREE

THETA	LW×E_3	LB×E_4	(LW-LB)/(E×COS(PSI))×E_5
15	34.000	1.900	16.808
20	24.000	1.900	11.837
30	17.600	2.600	8.620
40	14.800	1.600	7.278
50	13.500	1.200	6.652
60	14.500	1.000	7.159
70	16.700	0.800	8.263
80	26.300	0.800	13.035
100	47.000	0.700	23.331
110	54.000	0.800	26.806
120	62.000	0.900	30.778
130	72.000	1.100	35.740
140	87.000	1.500	43.177
150	112.000	2.100	55.576
160	176.000	10.200	86.990
200	190.000	11.400	93.890
210	119.000	2.600	59.031
220	89.000	1.600	44.166
230	73.000	1.200	36.232
240	64.000	1.000	31.767
250	57.000	0.900	28.292
260	54.000	0.800	26.806
280	22.500	0.900	11.141
290	21.600	1.000	10.689
300	18.500	1.100	9.142
310	17.000	0.900	8.407
320	16.600	1.500	8.178
330	19.500	2.300	9.580
340	25.300	4.200	12.369
345	30.000	8.400	14.497

24/12/1969

WINDOW NO 246

START LD 190.000 END LD 190.000
EAN LD 190.000 E COS(PSI) 195.52

PSI 10 DEGREE

THETA	LW*E-3	LB*E-4	(LW-LB)/(E*COS(PSI))*E-5
5	400.000	1.900	204.485
10	600.000	1.900	306872.500
20	65.000	2.600	33.112
30	27.000	1.700	13.722
40	21.000	1.200	10.679
50	18.500	1.000	9.411
60	18.500	0.800	9.421
70	22.500	0.750	11.469
80	31.000	0.700	15.819
100	66.000	0.800	33.715
110	70.000	0.950	40.356
120	92.000	1.100	46.998
130	110.000	1.400	56.188
140	140.000	2.200	71.491
150	215.000	10.200	109.441
190	208.000	11.200	105.810
200	120.000	3.100	61.216
210	86.000	1.800	43.893
220	69.000	1.400	35.219
230	56.000	1.000	28.590
240	49.000	0.900	25.015
250	42.000	0.800	21.440
260	38.000	0.800	19.394
280	19.200	1.100	9.764
290	15.200	1.100	7.718
300	13.500	0.900	6.859
310	13.000	1.500	6.572
320	14.000	2.300	7.043
330	16.200	4.200	8.071
335	18.000	8.500	8.771

24/12/1969 WINDOW NO 246
 START LD 190.000 END LD 187.00
 MEAN LD 188.50 --- E COS(PSI) 185.09

PSI 20 DEGREE

THETA	LW×E-3	LB×E-4	(LW-LB)/(E×COS(PSI))×E-5
0	22.000	1.900	11.783
10	58.000	2.600	31.195
20	68.000	1.700	367386.750
30	68.000	1.200	36.674
40	26.000	1.000	13.993
50	21.000	0.800	11.303
60	20.500	0.750	11.035
70	24.500	0.700	13.109
80	36.000	0.700	19.412
100	77.000	1.000	41.547
110	94.000	1.200	50.721
120	110.000	1.500	59.349
130	138.000	2.200	74.439
140	203.000	10.200	109.125
180	170.000	11.200	91.242
190	100.000	3.200	53.855
200	85.000	1.800	45.826
210	55.000	1.500	29.634
220	44.000	1.000	23.718
230	37.000	0.900	19.942
240	32.000	0.800	17.246
250	28.000	0.800	15.084
260	24.500	1.000	13.183
280	14.000	1.200	7.499
290	11.500	0.900	6.165
300	10.500	1.500	5.592
310	10.300	2.400	5.435
320	10.800	4.100	5.613
325	11.800	8.400	5.921
355	23.000	1.900	12.324

24/12/1969 WINDOW NO 246
 START LD 187.000 END LD 191.000
 EAN LD 189.000 E COS(PSI) 171.03

PSI 30 DEGREE

THETA	LW*E-3	LB*E-4	(LW-LB)/(E*COS(PSI))*E-5
0	15.000	2.600	8.618
10	20.000	1.600	11.600
20	72.000	1.200	42.027
30	125.000	1.000	73.085
40	96.000	0.800	56.083
50	28.000	0.750	16.327
60	26.000	0.600	15.167
70	30.000	0.700	17.500
80	44.000	0.800	25.679
100	95.000	1.100	55.480
110	120.000	1.500	70.074
120	150.000	2.200	87.574
130	220.000	10.200	128.034
170	160.000	11.200	92.894
180	95.000	3.100	55.364
190	67.000	1.900	39.063
200	50.000	1.500	29.146
210	60.000	1.000	35.022
220	31.000	0.800	18.078
230	26.000	0.800	15.155
240	23.000	0.800	13.401
250	20.500	1.000	11.928
260	18.000	1.100	10.460
280	11.800	1.000	6.841
290	9.700	1.500	5.584
300	9.500	2.400	5.414
310	9.200	4.000	5.145
315	9.600	8.200	5.134
345	16.000	1.800	9.250
350	12.500	1.800	7.203

24/12/1969 WINDOW NO 246

START LD 191.600 END LD 190.00

MEAN LD 190.500 E COS(PHI) 152.49

PSI 40 DEGREE

THETA LW*E_3 LB*E_4 (LW-LB)/(E*cos(PHI))*E_5

0	11.200	1.600	7.240
10	14.400	1.200	9.365
20	20.200	1.000	13.181
30	105.000	0.800	68.805
40	245.000	0.800	1606679.000
50	245.000	0.600	160.629
60	46.000	0.700	30.120
70	47.000	0.800	30.770
80	62.000	1.000	40.593
100	137.000	1.500	89.744
110	180.000	2.200	117.897
120	267.000	10.200	174.426
160	174.000	11.200	113.372
170	95.000	3.100	62.096
180	68.000	1.800	44.476
190	48.000	1.600	31.373
200	36.000	1.000	23.543
210	29.000	0.800	18.965
220	64.000	0.800	41.918
230	19.800	0.800	12.932
240	16.800	1.000	10.952
250	15.000	1.000	9.771
260	13.500	1.000	8.788
280	9.400	1.500	6.066
290	8.800	2.500	5.607
300	8.500	4.100	5.305
305	8.800	8.000	5.246
335	14.100	1.800	9.129
340	9.500	1.800	6.112
350	9.900	2.600	6.322

27/12/1969 WINDOW NO 246 /
 START LD 198.88 END LD 187.88
 MEAN LD 188.58 E-COS(PSI) 126.61

PSI 50 DEGREE

THETA	LW×E-3	LB×E-4	(LW-LB)/(E×COS(PSI))×E-5
0	9.888	1.288	7.814
10	18.588	1.888	8.214
20	14.588	0.858	11.385
30	23.588	0.888	18.498
40	238.888	0.788	181.685
50	528888.888	0.788	4187118.888
60	388.888	0.888	236.885
70	95.888	0.988	74.963
80	118.888	1.388	86.779
100	235.888	2.288	185.436
110	368.888	9.488	283.596
150	175.888	11.288	137.335
160	95.888	3.188	74.789
170	63.888	1.888	49.617
180	45.888	1.588	35.424
190	34.888	1.888	26.775
200	26.888	0.888	28.472
210	28.588	0.888	16.128
220	19.588	0.888	15.338
230	183.888	1.188	81.266
240	14.888	1.288	18.963
250	11.888	1.488	9.289
260	11.588	1.188	8.996
280	9.888	4.888	6.793
290	9.888	4.788	6.737
295	9.888	8.588	6.437
325	17.588	1.888	13.688
330	7.388	1.888	5.624
340	7.388	2.688	5.568
350	7.888	1.688	6.834

27/12/1969 WINDOW NO 246
 START LD 187.00 END LD 191.00
 EAN LD 189.00 E COS(Psi) 98.75

PSI 60 DEGREE

THETA	LW*E-3	LB*E-4	(LW-LB)/(E*COS(Psi))*E-5
0	7.200	1.000	7.190
10	8.600	0.950	8.613
20	10.500	0.800	10.552
30	15.500	0.800	15.616
40	30.000	0.800	30.300
50	480.000	0.900	486.000
60	1430.000	2.000	1448.000
70	850.000	3.900	860.399
80	300.000	8.200	302.979
100	590.000	12.800	596.196
140	205.000	11.100	206.479
150	100.000	3.200	100.946
160	66.000	1.800	66.656
170	46.000	1.600	46.422
180	33.000	1.100	33.308
190	25.500	0.900	25.733
200	19.500	0.900	19.656
210	15.500	0.900	15.606
220	13.000	1.100	13.054
230	17.500	1.500	17.570
240	235.000	1.800	237.802
250	11.000	2.000	10.937
260	10.000	3.800	9.742
280	9.200	8.200	8.486
285	9.300	10.600	8.345
315	9.000	1.800	8.932
320	6.000	1.800	5.894
330	5.600	2.600	5.408
340	5.700	1.700	5.600
350	6.300	1.200	6.258

27/12/1969 WINDOW NO 246

START LD	191.00	END LD	193.00
EAN LD	192.00	E COS(PSI)	68.62

PSI 70 DEGREE

THETA	LW×E_3	LB×E_4	(LW-LB)/(E×COS(PSI))×E_5
0	5.900	0.950	8.460
10	7.100	0.800	10.230
20	9.000	0.800	12.999
30	12.000	0.800	17.371
40	20.300	0.950	29.445
50	40.000	1.300	71.220
60	360.000	5.000	523.911
70	3100.000	14.500	45177328.000
80	3500.000	42.000	5094.545
130	191.000	10.900	276.762
140	78.000	3.100	113.220
150	48.000	1.800	69.690
160	32.000	1.600	46.401
170	23.600	1.100	34.233
180	17.200	0.900	24.935
190	13.100	0.800	18.974
200	10.200	0.900	14.734
210	8.400	1.100	12.081
220	7.200	1.300	10.303
230	6.800	1.800	9.648
240	11.000	2.000	15.739
250	450.000	4.000	655.217
260	10.000	10.000	13.116
275	720.000	15.500	1047.021
305	9.200	2.200	13.087
310	5.300	2.200	7.403
320	4.600	2.900	6.281
330	4.400	1.700	6.165
340	4.700	1.200	6.675
350	5.200	1.000	7.432

27/12/1969 WINDOW NO 246
 START LD 193.00 END LD 193.00
 MEAN LD 193.00 E COS(PSI) 35.02

PSI 80 DEGREE

THETA	LWxE_3	LBxE_4	(LW-LB)/(ExCOS(PSI))*E_5
0	4.200	0.800	11.765
10	5.200	0.800	14.620
20	6.700	0.800	18.903
30	9.000	0.950	25.428
40	13.700	1.000	38.835
50	28.400	1.600	80.640
60	110.000	6.100	312.365
70	550.000	26.000	1563.108
80	76000.000	139.000	217018944.000
120	207.000	8.500	588.664
130	55.000	3.200	156.139
140	30.000	1.900	85.123
150	19.000	1.600	53.798
160	13.600	1.100	38.521
170	10.000	1.000	28.270
180	7.400	0.800	20.902
190	5.900	0.800	16.619
200	4.600	1.000	12.850
210	3.800	1.200	10.508
220	3.400	1.300	9.338
230	3.200	1.500	8.709
240	3.600	2.900	9.452
250	4.700	17.000	8.567
260	720.000	19.500	2050.401
295	10.000	2.600	27.813
300	3.800	2.600	10.109
310	2.900	3.200	7.367
320	2.670	1.900	7.082
330	2.720	1.300	7.396
340	2.950	1.000	8.138
350	3.400	0.950	9.437

Honeywell Cleaning Procedure

2/1/1970 WINDOW NO 246

START LD 180.00 END LD 180.00
MEAN LD 180.00 E COS(PHI) 188.09

PSI 0 DEGREE

THETA LW*E_3 LB*E_4 (LW-LB)/(E*cos(PHI))*E_5

15	37.000	1.900	19.571
20	29.000	1.900	15.317
30	21.500	2.600	11.293
40	17.900	1.600	9.432
50	16.600	1.200	8.762
60	17.500	1.000	9.251
70	26.700	0.800	14.153
80	41.000	0.800	21.756
100	81.000	0.700	43.028
110	98.000	0.800	52.061
120	115.000	0.900	61.094
130	140.000	1.100	74.375
140	178.000	1.500	94.557
150	242.000	2.100	128.552
160	390.000	10.200	206.808
200	420.000	11.400	222.694
210	262.000	2.600	139.158
(220	187.000	1.600	99.337
230	147.000	1.200	78.091
240	120.000	1.000	63.747
250	100.000	0.900	53.119
260	81.000	0.800	43.022
280	38.000	0.900	20.155
290	25.100	1.000	13.292
300	19.800	1.100	10.469
310	18.600	0.900	9.841
320	20.000	1.500	10.554
330	24.700	2.300	13.010
340	34.000	4.200	17.853
345	43.000	8.400	22.415

2/ 1/1970 WINDOW NO 246
 START LD 178.800 END LD 173.000
 MEAN LD 175.500 E COS(PSI) 180.600

PSI 10 DEGREE

THETA LW*E_3 LB*E_4 (LW-LB)/(E*COS(PSI))*E_5

5	720.000	1.900	398.567
10	770.000	1.900	426357.500
20	55.000	2.600	30.310
30	30.000	1.700	16.517
40	22.700	1.200	12.503
50	20.200	1.000	11.130
60	21.400	0.800	11.805
70	28.800	0.750	15.905
80	50.000	0.700	27.647
100	110.000	0.800	60.864
110	135.000	0.950	74.608
120	160.000	1.100	88.533
130	196.000	1.400	108.450
140	257.000	2.200	142.182
150	390.000	10.200	215.383
190	380.000	11.200	209.790
200	220.000	3.100	121.645
210	160.000	1.800	88.494
220	120.000	1.400	66.368
230	96.000	1.000	53.101
240	79.000	0.900	43.693
250	66.000	0.800	36.501
260	55.000	0.800	30.410
280	27.000	1.100	14.889
290	18.500	1.100	10.183
300	15.200	0.900	8.367
310	14.400	1.500	7.890
320	15.000	2.300	8.178
330	18.000	4.200	9.734
335	19.000	8.500	10.050

2/ 1/1970 WINDOW NO. 246
 START LD 173.000 END LD 175.000
 MEAN LD 174.000 E-COS(PSE) 170.85

PSI 20 DEGREE

THETA	LW×E_3	LB×E_4	(LW-LB)/(E×COS(PSE))×E_5
0	27.000	1.900	15.692
10	72.000	2.600	41.989
20	91.000	1.700	53.262
30	52.000	1.200	30.365
40	30.000	1.000	17.500
50	25.300	0.800	14.761
60	26.000	0.750	15.174
70	35.000	0.700	20.444
80	63.000	0.700	36.833
90	138.000	1.000	80.713
100	170.000	1.200	99.430
110	212.000	1.500	123.995
120	276.000	2.200	161.413
130	400.000	1.200	233.522
140	330.000	11.200	192.493
150	210.000	3.200	122.725
160	168.000	1.800	98.225
170	105.000	1.500	61.368
180	85.000	1.000	49.692
190	70.000	0.900	40.918
200	58.000	0.800	33.900
210	49.000	0.800	28.633
220	40.000	1.000	23.353
230	22.300	1.200	12.982
240	16.100	0.900	9.371
250	13.200	1.500	7.638
260	12.500	2.400	7.176
270	13.000	4.100	7.369
280	14.500	8.400	7.995
290	24.100	1.900	13.994

2/ 1/1970 WINDOW NO 246
 START LD 175.00 END LD 175.00
 4EAN LD 175.00 E-COS(PSI) 158.36

PSI 30 DEGREE

THETA	LW*E-3	LB*E-4	(-LW-LB)-(E*cos(PSI))*E-5
0	18.300	2.600	11.391
10	25.000	1.600	15.685
20	30.000	1.200	56.755
30	178000.000	1.000	1123991.750
40	83.000	0.800	52.360
50	41.000	0.750	25.842
60	40.000	0.600	25.220
70	52.000	0.700	32.792
80	93.000	0.800	58.675
100	210.000	1.100	132.536
110	270.000	1.500	170.398
120	340.000	2.200	214.556
130	500.000	10.200	315.084
170	350.000	11.200	220.302
180	205.000	3.100	129.253
190	138.000	1.900	87.021
200	100.000	1.500	63.051
210	100.000	1.000	63.082
220	60.000	0.800	37.837
230	49.000	0.800	30.891
240	41.000	0.800	25.839
250	36.000	1.000	22.669
260	30.000	1.100	18.874
280	18.300	1.000	11.493
290	13.500	1.500	8.430
300	11.800	2.400	7.300
310	11.000	4.000	6.693
315	11.500	8.200	6.744
345	15.500	1.800	9.674
350	15.000	1.800	9.358

2/ 1/1970 WINDOW NO. 246
 START LD 175.000 END LD 175.00
 MEAN LD 175.000 E COS(PSI) 140.08

PSI 40 DEGREE

THETA LW*E_3 LB*E_4 (LW-LB)/(E*COS(PSI))*E_5

0	13.300	1.600	9.380
10	17.000	1.200	12.050
20	26.000	1.000	18.480
30	130.000	0.800	92.740
40	275.000	0.800	1963145.500
50	133.000	0.600	94.902
60	61.000	0.700	43.496
70	72.000	0.800	51.342
80	120.000	1.000	85.593
100	275.000	1.500	196.207
110	360.000	2.200	256.837
120	520.000	10.200	370.485
160	360.000	11.200	256.194
170	200.000	3.100	142.553
180	133.000	1.800	94.816
190	95.000	1.600	67.704
200	70.000	1.000	49.900
210	55.000	0.800	39.206
220	95.000	0.800	67.761
230	35.000	0.800	24.928
240	30.000	1.000	21.345
250	26.500	1.000	18.846
260	23.300	1.000	16.562
280	15.500	1.500	10.958
290	12.300	2.500	8.602
300	10.800	4.100	7.417
305	10.800	8.000	7.130
335	14.900	1.800	10.508
340	10.900	1.800	7.653
350	11.500	2.600	8.024

2/ 1/1970 WINDOW NO 246
 (START LD 178.000 END LD 175.000
 MEAN LD 176.500 E COS(PSI) 118.55

PSI 50 DEGREE

THETA	LW×E-3	LB×E-4	(LW-LB)/(E×COS(PSI))×E-5
0	10.600	1.200	8.840
10	13.000	1.000	10.882
20	17.700	0.850	14.859
30	31.000	0.800	26.082
40	225.000	0.700	189.735
50	560000.000	0.700	4723758.000
60	330.000	0.800	278.297
70	140.000	0.900	118.018
80	192.000	1.300	161.848
100	420.000	2.200	354.096
110	630.000	9.400	530.630
150	370.000	11.200	311.161
160	200.000	3.100	168.444
170	128.000	1.800	107.820
180	92.000	1.500	77.478
190	64.000	1.000	53.901
200	48.000	0.800	40.422
210	38.000	0.800	31.987
220	33.000	0.800	27.769
230	125.000	1.100	105.348
240	22.600	1.200	18.963
250	19.300	1.400	16.162
260	17.500	1.100	14.669
280	13.500	4.000	11.050
290	11.100	4.700	8.967
295	10.700	8.500	8.309
325	13.500	1.800	11.236
330	9.500	1.800	7.862
340	9.000	2.600	7.372
350	9.500	1.600	7.879

2/ 1/1970 WINDOW NO 246
 START LD 175.00 END LD 178.00
 MEAN LD 176.50 E COS(Psi) 92.22

PSI 60 DEGREE

THETA	LWxE_3	LBxE_4	(LW-LB)/(E*cos(Psi))*E_5
0	11.300	1.000	12.145
10	12.400	0.950	13.344
20	15.000	0.800	16.180
30	23.000	0.800	24.855
40	145.000	0.800	157.154
50	1620.000	0.900	1756.661
60	11000000.000	2.000	11928608.000
70	2020.000	3.900	2190.104
80	380.000	8.200	411.190
100	780.000	12.800	844.459
140	350.000	11.100	378.343
150	195.000	3.200	211.115
160	120.000	1.800	129.935
170	83.000	1.600	89.833
180	58.000	1.100	62.777
190	41.000	0.900	44.364
200	31.000	0.900	33.519
210	25.100	0.900	27.121
220	20.500	1.100	22.111
230	24.000	1.500	25.863
240	232.000	1.800	251.390
250	15.600	2.000	16.700
260	15.000	3.800	15.854
280	11.900	8.200	12.015
285	11.400	10.600	11.213
315	9.200	1.800	9.781
320	8.000	1.800	8.480
330	7.800	2.600	8.177
340	8.200	1.700	8.708
350	9.600	1.200	10.280

2/ 1/1970 WINDOW NO. 246
 START LD 178.000 END LD 182.00
 MEAN LD 180.000 -E-COS(PSI)- 64.33

PSI 70 DEGREE

THETA	LW*E_3	LB*E_4	(LW-LB)/(E*COE(PSI))*E_5
0	9.500	0.950	14.620
10	11.000	0.800	16.975
20	14.500	0.800	22.416
30	20.800	0.800	32.209
40	34.000	0.950	52.705
50	78.000	1.300	121.048
60	500.000	5.000	776.467
70	3800000.000	14.500	59070560.000
80	3000.000	42.000	4656.937
130	360.000	10.900	557.921
140	175.000	3.100	271.554
150	105.000	1.800	162.941
160	69.000	1.600	107.011
170	48.000	1.100	74.144
180	33.000	0.900	51.158
190	25.500	0.800	39.515
200	19.300	0.900	29.862
210	15.500	1.100	23.924
220	13.300	1.300	20.173
230	11.800	1.800	18.063
240	20.300	2.000	31.245
250	450.000	4.000	698.898
260	13.800	10.000	19.897
275	310.000	15.500	479.482
305	8.800	2.200	13.338
310	7.700	2.200	11.628
320	6.900	2.900	10.275
330	6.900	1.700	10.462
340	7.400	1.200	11.317
350	8.300	1.000	12.747

2/ 1/1977 WINDOW NO 246
 START LL 52.000 END LD 180.00
 MEAN LD 151.000 E COS(PSI) 32.84

PSI 80 DEGREE

THETA	LWxE_3	LBxE_4	(LW-LB)/(ExCOS(PSI))*E_5
0	8.000	0.800	24.115
10	9.300	0.800	28.073
20	12.000	0.800	36.294
30	16.000	0.950	48.428
40	26.000	1.000	78.861
50	52.000	1.600	157.844
60	160.000	6.100	485.315
70	820.000	26.000	2488.843
80	890000000.000	139.000	270989696.000
120	320.000	8.500	971.757
130	120.000	3.200	364.405
140	69.000	1.900	209.515
150	43.000	1.600	130.440
160	29.000	1.100	87.965
170	20.500	1.000	62.115
180	14.500	0.800	43.906
190	11.000	0.800	33.250
200	8.600	1.000	25.881
210	7.200	1.200	21.557
220	6.400	1.300	19.091
230	6.300	1.500	17.812
240	6.400	2.900	18.604
250	9.000	17.000	22.227
260	720.000	19.500	2186.339
295	6.700	2.600	19.609
300	6.000	2.600	17.477
310	4.700	3.200	13.336
320	4.400	1.900	12.819
330	4.800	1.300	14.219
340	5.400	1.000	16.138
350	6.300	0.950	18.893

-----After Vacuum Outgas-----

1/12/1970 WINDOW NO. 246

START LD 183.00 END LD 185.00
EAN LD 184.50 E COS(PSI) 192.27

PSI 0 DEGREE

THETA	--LW*E-3--	LB*E-4--	(LW-LB)/(E*COS(PSI))*E-5--
15	48.000	1.900	24.866
20	35.000	1.900	18.105
30	26.000	2.600	13.388
40	22.500	1.600	11.619
50	20.500	1.200	10.600
60	20.700	1.000	10.714
70	23.500	0.800	12.181
80	31.000	0.800	16.082
100	56.000	0.700	29.090
110	67.000	0.800	34.806
120	81.000	0.900	42.082
130	91.000	1.100	47.273
140	110.000	1.500	57.134
150	150.000	2.100	77.907
160	241.000	0.200	124.816
200	225.000	11.400	116.432
210	140.000	2.600	72.680
220	101.000	1.600	52.448
230	82.000	1.200	42.587
240	71.000	1.000	36.876
250	60.000	0.900	31.160
260	55.000	0.800	28.564
280	29.000	0.900	15.036
290	22.500	1.000	11.650
300	19.500	1.100	10.085
310	19.200	0.900	9.939
320	20.800	1.500	10.740
330	19.300	2.300	9.918
340	31.000	4.200	15.905
345	36.000	8.400	18.287

1/13/1970 WINDOW NO 246

START LD 185.00 END LD 185.00
 EAN-LD 185.00 E COS(PSI) 190.30

PSI 10 DEGREE

THETA ----- LW*E_3 ----- LB*E_4 -- (LW-LB)/(E*COS(PSI))*E_5 -----

5	170.000	1.900	89.197
10	1280.000	1.900	672.255
20	193.000	2.600	101.242
30	35.000	1.700	18.295
40	28.500	1.200	14.907
50	25.400	1.000	13.290
60	24.800	0.800	12.985
70	28.500	0.750	14.931
80	39.000	0.700	20.449
100	86.000	0.800	45.132
110	103.000	0.950	54.054
120	111.000	1.100	58.248
130	129.000	1.400	67.687
140	158.000	2.200	82.878
150	266.000	0.200	139.188
190	237.000	11.200	123.902
200	135.000	3.100	70.750
210	97.000	1.800	50.857
220	74.000	1.400	38.797
230	60.000	1.000	31.464
240	52.000	0.900	27.267
250	46.000	0.800	24.121
260	41.000	0.800	21.494
280	25.700	1.100	13.442
290	19.700	1.100	10.290
300	17.100	0.900	8.935
310	17.400	1.500	9.061
320	18.500	2.300	9.597
330	20.300	4.200	10.443
335	22.000	8.500	11.110

1/13/1970 WINDOW NO 246
 START LD 185.000 END LD 185.000
 EAN LD 185.000 E-COS(PST) 181.65

PSI 20 DEGREE

THETA	$LW \times E-3$	$LB \times E-4$	$(LW-LB)/(E \times \cos(PST)) \times E-5$
0	27.500	1.900	15.034
10	44.000	2.600	24.079
20	157.000	1.700	864.185
30	269.000	1.200	148.017
40	38.000	1.000	20.864
50	31.000	0.800	17.021
60	30.000	0.750	16.474
70	34.000	0.700	18.678
80	50.000	0.700	27.486
100	117.000	1.000	64.353
110	141.000	1.200	77.554
120	156.000	1.500	85.795
130	194.000	2.200	106.675
140	285.000	10.200	156.330
180	229.000	11.200	125.447
190	128.000	3.200	70.287
200	100.000	1.800	54.951
210	68.000	1.500	37.351
220	52.000	1.000	28.571
230	42.000	0.900	23.071
240	37.000	0.800	20.324
250	33.000	0.800	18.122
260	31.000	1.000	17.010
280	20.700	1.200	11.329
290	16.800	0.900	9.199
300	15.500	1.500	8.450
310	15.900	2.400	8.621
320	16.500	4.100	8.857
325	17.200	8.400	9.006
355	28.500	1.900	15.585

1/12/1970 WINDOW NO 246
 (START LD 185.00 END LD 188.00
 EAN-LD 186.50 E COS(PSI) 168.77

PSI 30 DEGREE

THETA --- LW * E_3 --- LB * E_4 --- (LW-LB)/(E * COS(PSI)) * E_5 ---

0	21.000	2.600	12.289
10	28.000	1.600	16.496
20	53.000	1.200	31.332
30	265.000	1.000	157.531
40	420.000	0.800	248.811
50	52.000	0.750	30.767
60	46.000	0.600	27.220
70	52.000	0.700	30.770
80	64.000	0.800	37.874
100	185.000	1.100	109.551
110	220.000	1.500	130.265
120	225.000	2.200	133.186
130	370.000	1.200	218.628
170	220.000	11.200	129.691
180	125.000	3.100	73.881
190	86.000	1.900	50.844
200	62.000	1.500	36.647
210	64.000	1.000	37.862
220	38.000	0.800	22.468
230	32.000	0.800	18.913
240	28.000	0.800	16.543
250	26.000	1.000	15.346
260	25.800	1.100	15.222
280	19.000	1.000	11.199
290	15.500	1.500	9.095
300	14.500	2.400	8.449
310	15.000	4.000	8.651
315	15.300	8.200	8.580
345	24.000	1.800	14.114
350	18.200	1.800	10.677

1/13/1970 WINDOW NO 246
 START LD 188.000 END LD 188.000
 EAN LD -188.000 --E-COS(PSI)--150.49

PSI 40 DEGREE

THETA -- -- --LW*E-3 -----LB*E-4 --(LW-LB)/(E*COS(PSI))*E-5-----

0	15.7000	1.6000	10.326
10	19.2000	1.2000	12.679
20	26.8000	1.0000	17.742
30	56.0000	0.8000	37.159
40	74.0000	0.8000	49173.531
50	76.0000	0.6000	504.986
60	73.0000	0.7000	48.463
70	73.0000	0.8000	48.456
80	100.0000	1.0000	66.384
100	250.0000	1.5000	166.027
110	320.0000	2.2000	212.496
120	410.0000	10.2000	271.770
160	225.0000	11.2000	148.770
170	125.0000	3.1000	82.857
180	82.0000	1.8000	54.370
190	58.0000	1.6000	38.435
200	43.0000	1.0000	28.507
210	34.0000	0.8000	22.540
220	62.0000	0.8000	41.146
230	25.5000	0.8000	16.892
240	21.5000	1.0000	14.220
250	20.1000	1.0000	13.290
260	22.0000	1.0000	14.553
280	17.6000	1.5000	11.596
290	19.0000	2.5000	12.460
300	13.5000	4.1000	8.698
305	13.8000	8.0000	8.639
335	17.3000	1.8000	11.376
340	13.9000	1.8000	9.117
350	14.2000	2.6000	9.263

1/13/1970 WINDOW NO 246
 START LD 188.000 END LD 187.000
 LEAN LD 187.500 E-COS(PSI) 125.94

PSI 50 DEGREE

THETA	LW*E-3	LB*E-4	(LW-LB)/(E*COS(PSI))*E-5
0	12.600	1.200	9.910
10	14.900	1.000	11.752
20	19.500	0.850	15.416
30	29.000	0.800	22.964
40	76.000	0.700	60.292
50	183999.969	0.700	146103.500
60	2300.000	0.800	1826.231
70	155.000	0.900	123.005
80	180.000	1.300	142.824
100	420.000	2.200	333.323
110	630.000	0.400	499.500
150	230.000	1.200	181.740
160	123.000	3.100	97.421
170	77.000	1.800	60.998
180	54.000	1.500	42.759
190	39.000	1.000	30.888
200	30.000	0.800	23.758
210	24.000	0.800	18.993
220	20.600	0.800	16.294
230	94.000	1.100	74.553
240	19.300	1.200	15.230
250	15.000	1.400	11.799
260	18.500	1.100	14.602
280	11.200	4.000	8.576
290	13.700	4.700	10.505
295	16.900	8.500	12.744
325	18.200	1.800	14.309
330	11.100	1.800	8.671
340	11.000	2.600	8.528
350	11.500	1.600	9.004

1/13/1970 WINDOW NO 246
 START LD 187.000 END LD 186.000
 EAN LD 186.500 -E-CGS(PSI)- 97.44

PSI 60 DEGREE

THETA	LW*E-3	LB*E-4	(LW-LB)/(E*CGS(PSI))*E-5
0	10.500	1.000	10.673
10	12.400	0.950	12.628
20	15.700	0.800	16.030
30	22.500	0.800	23.009
40	40.000	0.800	40.969
50	124.000	0.900	127.165
60	136000.000	2.000	139572.969
70	41000.000	3.900	4207.320
80	4200.000	8.200	430.193
100	830.000	12.800	850.493
140	265.000	11.100	270.823
150	130.000	3.200	133.067
160	76.000	1.800	77.812
170	50.000	1.600	51.149
180	36.000	1.100	36.833
190	27.700	0.900	28.335
200	21.200	0.900	21.665
210	17.200	0.900	17.560
220	14.700	1.100	14.973
230	14.000	1.500	14.214
240	145.000	1.800	148.625
250	18.800	2.000	19.089
260	16.300	3.800	16.338
280	16.300	8.200	15.887
285	14.500	10.600	13.793
315	13.500	1.800	13.670
320	10.000	1.800	10.078
330	9.400	2.600	9.380
340	9.500	1.700	9.575
350	9.800	1.200	9.934

1/13/1970 WINDOW NO 246
 START LD 186.00 END LD 185.00
 LEAN LD 185.50 E COS(Psi) 66.30

PSI 70 DEGREE

THETA	LW*E=3	LB*E=4	(LW-LB)/(E*cos(Psi)) * E=5
0	9.000	0.950	13.432
10	10.500	0.800	15.718
20	13.000	0.800	19.489
30	18.700	0.800	28.086
40	31.000	0.950	46.617
50	67.000	1.300	100.867
60	230.000	5.000	346.177
70	520.000	14.500	7843671.000
80	1490.000	42.000	2241.179
130	370.000	10.900	556.463
140	123.000	3.100	185.065
150	70.000	1.800	105.316
160	45.000	1.600	67.637
170	31.000	1.100	46.594
180	23.000	0.900	34.557
190	16.800	0.800	25.220
200	13.300	0.900	19.926
210	11.200	1.100	16.728
220	0.000	1.300	14.888
230	9.900	1.800	14.662
240	10.300	2.000	15.235
250	370.000	4.000	557.504
260	19.300	10.000	27.604
275	105.000	15.500	156.044
305	13.700	2.200	20.333
310	9.100	2.200	13.395
320	8.200	2.900	11.931
330	7.500	1.700	11.057
340	7.600	1.200	11.283
350	8.100	1.000	12.067

1/13/1970 WINDOW NO 246
 START LD 185.00 END LD 185.00
 EAN LD 185.00 ---E COS(PSI)- 33.57

PSI 80 DEGREE

THETA	LA*E-3	LB*E-4	(LW-LB)/(E*COS(PSI))*E-5
0	6.400	0.800	18.827
10	8.000	0.800	23.594
20	9.800	0.800	28.956
30	14.100	0.950	41.721
40	22.200	1.000	65.836
50	46.000	1.600	136.557
60	113.000	6.100	334.809
70	480.000	26.000	1422.173
80	1550.000	139.000	4617.401
120	263.000	8.500	780.044
130	90.000	3.200	267.156
140	48.000	1.900	142.426
150	28.600	1.600	84.723
160	19.000	1.100	56.273
170	13.500	1.000	39.919
180	10.500	0.800	31.041
190	8.000	0.800	23.594
200	6.600	1.000	19.363
210	5.900	1.200	17.219
220	5.500	1.300	15.997
230	5.700	1.500	16.533
240	6.100	2.900	17.308
250	7.700	17.000	17.874
260	550.000	19.500	1632.639
295	8.100	2.600	23.355
300	6.700	2.600	19.185
310	5.500	3.200	15.431
320	4.800	1.900	13.733
330	4.600	1.300	13.316
340	4.800	1.000	14.001
350	5.400	0.950	15.804

NASA Cleaning Procedure

12/21/1969 WINDOW NO 244 & 246

START LD 186.00 END LD 186.00

MEAN LD 186.00 E COS(PSI) 194.36

PSI 0 DEGREE

THETA	LW×E_3	LB×E_4	(LW-LB)/(E×COS(PSI))×E_5
15	97.00	1.90	49.81
20	59.00	1.90	30.26
30	36.00	2.60	18.39
40	27.00	1.60	13.81
50	26.00	1.20	13.32
60	27.00	1.00	13.84
70	36.00	0.80	18.48
80	49.00	0.80	25.17
100	105.00	0.70	53.99
110	160.00	0.80	82.20
120	125.00	0.90	64.27
130	150.00	1.10	77.12
140	190.00	1.50	97.68
150	262.00	2.10	134.70
160	940.00	10.20	483.12
200	900.00	11.40	462.48
210	290.00	2.60	149.08
220	200.00	1.60	102.82
230	160.00	1.20	82.26
240	130.00	1.00	66.84
250	110.00	0.90	56.55
260	110.00	0.80	56.56
280	48.00	0.90	24.65
290	53.00	1.00	27.22
300	37.00	1.10	18.98
310	33.00	0.90	16.93
320	32.00	1.50	16.39
330	46.00	2.30	23.55
340	64.00	4.20	32.71
345	64.00	8.40	32.50

12/21/1969 WINDOW NO 244 & 246
 START LD 186.000 END LD 186.000
 MEAN LD 186.000 E COS(PSI) 191.40

PSI 10 DEGREE

THETA	LW*E_3	LB*E_4	(LW-LB)/(E*COS(PSI))*E_5
5	550.000	1.90	287.25
10	1650.000	1.90	862047.75
20	80.000	2.60	41.66
30	41.000	1.70	21.33
40	44.000	1.20	22.93
50	35.000	1.00	18.23
60	36.000	0.80	18.77
70	43.000	0.75	22.43
80	51.000	0.70	26.61
100	120.000	0.80	62.65
110	125.000	0.95	65.26
120	170.000	1.10	88.76
130	210.000	1.40	109.64
140	270.000	2.20	140.95
150	470.000	10.20	245.02
190	800.000	11.20	417.38
200	750.000	3.10	391.68
210	170.000	1.80	88.72
220	130.000	1.40	67.85
230	105.000	1.00	54.81
240	85.000	0.90	44.36
250	70.000	0.80	36.53
260	65.000	0.80	33.92
280	36.000	1.10	18.75
290	20.000	1.10	10.39
300	18.000	0.90	9.36
310	20.000	1.50	10.37
320	25.000	2.30	12.94
330	18.000	4.20	9.18
335	29.000	8.50	14.71

12/21/1969 WINDOW NO 244 & 246
 START LD 188.00 END LD 188.00
 MEAN LD 188.00 E COS(PSI) 184.60

PSI 20 DEGREE

THETA	LW*E_3	LB*E_4	(LW-LB)/(E*COS(PSI))*E_5
0	45.00	1.90	24.27
10	89.00	2.60	48.07
20	170.00	1.70	92.09
30	115.00	1.20	62.23
40	56.00	1.00	30.28
50	45.00	0.80	24.33
60	58.00	0.75	31.38
70	48.00	0.70	25.96
80	78.00	0.70	42.22
100	150.00	1.00	81.20
110	146.00	1.20	79.02
120	153.00	1.50	82.80
130	170.00	2.20	91.97
140	100.00	1.20	54.16
180	79.00	11.20	427.35
190	50.00	3.20	270.68
200	38.00	1.80	205.75
210	25.00	1.50	135.35
220	90.00	1.00	48.70
230	80.00	0.90	43.29
240	85.00	0.80	46.00
250	75.00	0.80	40.59
260	65.00	1.00	35.16
280	38.00	1.20	20.52
290	36.00	0.90	19.45
300	32.00	1.50	17.25
310	30.00	2.40	16.12
320	31.00	4.10	16.57
325	32.00	8.40	16.88
355	44.00	1.90	23.73

12/21/1969 WINDOW NO 244 & 246
 START LD 188.00 END LD 189.00
 MEAN LD 188.50 E COS(PSI) 170.58

PSI 30 DEGREE

THETA	LW*E_3	LB*E_4	(LW-LB)/(E*COS(PSI))*E_5
0	36.00	2.60	20.95
10	48.00	1.60	28.05
20	90.00	1.20	52.69
30	340.00	1.00	1993191.00
40	180.00	0.80	105.47
50	78.00	0.75	45.68
60	80.00	0.60	46.86
70	95.00	0.70	55.65
80	105.00	0.80	61.51
100	380.00	1.10	222.70
110	640.00	1.50	375.10
120	800.00	2.20	468.86
130	1150.00	10.20	673.57
170	780.00	11.20	456.60
180	480.00	3.10	281.21
190	340.00	1.90	199.21
200	240.00	1.50	140.61
210	230.00	1.00	134.77
220	140.00	0.80	82.03
230	110.00	0.80	64.44
240	95.00	0.80	55.65
250	90.00	1.00	52.70
260	62.00	1.10	36.28
280	36.00	1.00	21.05
290	32.00	1.50	18.67
300	30.00	2.40	17.45
310	28.00	4.00	16.18
315	29.00	8.20	16.52
345	34.00	1.80	19.83
350	32.00	1.80	18.65

12/21/1969 WINDOW NO 244 & 246
 START LD 189.00 END LD 189.00
 MEAN LD 189.00 E COS(PSI) 151.29

PSI 40 DEGREE

THETA	LW×E_3	LB×E_4	(LW-LB)/(E×COS(PSI))×E_5
0	31.00	1.60	20.38
10	38.00	1.20	251.10
20	53.00	1.00	34.97
30	150.00	0.80	99.10
40	590.00	0.80	3899852.00
50	280.00	0.60	1850.74
60	130.00	0.70	85.88
70	145.00	0.80	95.79
80	150.00	1.00	99.08
100	600.00	1.50	396.50
110	900.00	2.20	594.75
120	1200.00	10.20	792.52
160	770.00	11.20	508.22
170	460.00	3.10	303.85
180	320.00	1.80	211.40
190	230.00	1.60	151.92
200	160.00	1.00	105.69
210	125.00	0.80	82.57
220	215.00	0.80	142.06
230	86.00	0.80	56.79
240	74.00	1.00	48.85
250	71.00	1.00	46.86
260	95.00	1.00	62.73
280	39.00	1.50	25.68
290	32.00	2.50	20.99
300	29.00	4.10	18.90
305	28.00	8.00	17.98
335	30.00	1.80	19.71
340	27.00	1.80	17.73
350	28.00	2.60	18.34

12/21/1969 WINDOW NO 244 & 246
 START LD 189.00 END LD 189.00
 MEAN LD 189.00 E COS(PSI) 126.95

PSI 50 DEGREE

THETA	LW*E_3	LB*E_4	(LW-LB)/(E*COS(PSI))*E_5
0	37.00	1.20	29.05
10	44.00	1.00	34.58
20	58.00	0.85	45.62
30	83.00	0.80	65.32
40	210.00	0.70	165.37
50	1200.00	0.70	945287.00
60	200.00	0.80	157.48
70	400.00	0.90	315.02
80	530.00	1.30	417.40
100	500.00	2.20	393.70
110	550.00	9.40	432.52
150	800.00	11.20	629.31
160	460.00	3.10	362.12
170	300.00	1.80	236.18
180	220.00	1.50	173.18
190	155.00	1.00	122.02
200	115.00	0.80	90.53
210	87.00	0.80	68.47
220	75.00	0.80	59.02
230	280.00	1.10	220.48
240	72.00	1.20	56.62
250	62.00	1.40	48.73
260	170.00	1.10	133.83
280	66.00	4.00	51.68
290	41.00	4.70	31.93
295	32.00	8.50	24.54
325	32.00	1.80	25.07
330	29.00	1.80	22.70
340	30.00	2.60	23.43
350	32.00	1.60	25.08

12/21/1969 WINDOW NO 244 & 246
 START LD 188.00 END LD 188.00
 MEAN LD 188.00 E COS(PSI) 98.22

PSI 60 DEGREE

THETA	LW*E_3	LB*E_4	(LW-LB)/(E*COS(PSI))*E_5
0	38.00	1.00	38.59
10	46.00	0.95	46.74
20	58.00	0.80	58.97
30	78.00	0.80	79.33
40	115.00	0.80	117.00
50	380.00	0.90	386.78
60	3900.00	2.00	3970.53
70	3500.00	3.90	3562.90
80	850.00	8.20	864.54
100	1800.00	12.80	1831.25
140	840.00	11.10	854.06
150	460.00	3.20	467.99
160	300.00	1.80	305.24
170	200.00	1.60	203.45
180	145.00	1.10	147.51
190	105.00	0.90	106.81
200	83.00	0.90	84.41
210	68.00	0.90	69.14
220	58.00	1.10	58.94
230	57.00	1.50	57.88
240	52.00	1.80	52.76
250	85.00	2.00	86.33
260	380.00	3.80	386.49
280	100.00	8.20	102.60
285	140.00	10.60	141.45
315	33.00	1.80	33.41
320	32.00	1.80	32.40
330	31.00	2.60	31.30
340	32.00	1.70	32.41
350	34.00	1.20	34.49

12/21/1969 WINDOW NO 244 & 246
 START LD 188.00 END LD 188.00
 MEAN LD 188.00 E COS(PSI) 67.19

PSI 70 DEGREE

THETA	LW*E_3	LB*E_4	(LW-LB)/(E*COS(PSI))*E_5
0	32.00	0.95	47.49
10	39.00	0.80	57.93
20	49.00	0.80	72.81
30	64.00	0.80	95.13
40	92.00	0.95	136.79
50	165.00	1.30	245.38
60	540.00	5.00	802.96
70	2350.00	14.50	34976.00
80	2550.00	42.00	37952.50
130	640.00	10.90	950.92
140	340.00	3.10	505.57
150	220.00	1.80	327.17
160	140.00	1.60	208.13
170	105.00	1.10	156.11
180	80.00	0.90	118.93
190	60.00	0.80	89.18
200	48.00	0.90	71.31
210	41.00	1.10	60.86
220	38.00	1.30	56.36
230	37.00	1.80	54.80
240	42.00	2.00	62.21
250	740.00	4.00	1100.78
260	500.00	10.00	742.68
305	35.00	2.20	51.76
310	31.00	2.20	45.81
320	29.00	2.90	42.73
330	27.00	1.70	39.93
340	26.00	1.20	38.52
350	29.00	1.00	43.01

12/21/1969 WINDOW NO 244 & 246
 START LD 188.00 END LD 188.00
 MEAN LD 188.00 E COS(PST) 34.11

PST 80 DEGREE

THETA	LW*E_3	LB*E_4	(LW-LB)/(E*COS(PST))*E_5
0	7.10	0.80	20.58
10	10.00	0.80	29.08
20	11.00	0.80	32.01
30	13.00	0.95	37.83
40	28.00	1.00	81.79
50	100.00	1.60	292.68
60	205.00	6.10	599.16
70	1000.00	26.00	2923.84
80	8400.00	139.00	24624.32
120	380.00	8.50	1111.46
130	180.00	3.20	526.72
140	105.00	1.90	307.25
150	76.00	1.60	222.32
160	54.00	1.10	157.98
170	40.00	1.00	116.97
180	30.00	0.80	87.71
190	26.00	0.80	75.98
200	23.00	1.00	67.13
210	20.00	1.20	58.28
220	20.00	1.30	58.25
230	22.00	1.50	64.05
240	27.00	2.90	78.30
250	43.00	17.00	121.07
260	1250.00	10.50	3658.61
295	34.00	2.60	98.91
300	36.00	2.60	104.77
310	24.00	3.20	69.42
320	22.00	1.90	63.94
330	20.00	1.30	58.25
340	18.00	1.00	52.47
350	19.00	0.95	55.42

Vacuum Contamination of Both

1/15/1970 WINDOW NO 246 & 244
 START LD 171.00 END LD 171.00
 MEAN LD 171.00 E COS(PSI) 178.68

PSI DEGREE

THETA	LW×E_3	LB×E_4	(LW-LB)/(E×COS(PSI))×E_5
15	120.000	1.900	67.052
20	75.000	1.900	41.867
30	45.000	2.600	25.039
40	35.000	1.600	19.498
50	30.000	1.200	16.722
60	31.000	1.000	17.293
70	38.000	0.800	21.222
80	53.000	0.800	29.617
100	18.700	0.700	10.426
110	68.000	0.800	38.011
120	79.000	0.900	44.162
130	96.000	1.100	53.665
140	110.000	1.500	61.477
150	158.000	2.100	88.307
160	310.000	10.200	172.920
200	310.000	11.400	172.853
210	164.000	2.600	91.637
220	110.000	1.600	61.472
230	91.000	1.200	50.861
240	74.000	1.000	41.358
250	56.000	0.900	31.290
260	29.500	0.800	16.465
280	49.000	0.900	27.372
290	37.000	1.000	20.651
300	30.000	1.100	16.728
310	29.500	0.900	16.459
320	33.000	1.500	18.384
330	45.000	2.300	25.055
340	79.000	4.200	43.977
345	130.000	8.400	72.284

1/15/1970 WINDOW NO 246 & 244
 ! TART LD 171.00 -- END LD 172.00
 MEAN LD 171.50 E COS(Psi) 176.48

PSI 10 DEGREE

THETA	LW×E-3	LB×E-4	(LW-LB)/(E×COS(Psi))×E-5
5	5500.000	1.900	3116.335
10	3600.000	1.900	2039853.500
20	360.000	2.600	203.838
30	83.000	1.700	46.934
40	50.000	1.200	28.263
50	40.000	1.000	22.608
60	39.000	0.800	22.053
70	48.000	0.750	27.156
80	68.000	0.700	38.491
100	24.800	0.800	14.007
110	98.000	0.950	55.476
120	110.000	1.100	62.267
130	138.000	1.400	78.115
140	186.000	2.200	105.268
150	310.000	10.200	175.076
190	390.000	11.200	220.349 x
200	150.000	3.100	84.818
210	100.000	1.800	56.561
220	76.000	1.400	42.984
230	63.000	1.000	35.641
240	58.000	0.900	32.813
250	42.000	0.800	23.753
260	23.300	0.800	13.157
280	40.000	1.100	22.603
290	31.000	1.100	17.503
300	25.700	0.900	14.511
310	24.600	1.500	13.854
320	26.800	2.300	15.055
330	33.000	4.200	18.461
335	38.000	8.500	21.050

1/15/1970 WINDOW NO 246 & 244
 TART LD 172.00 END LD 185.00
 MEAN LD 178.50 E COS(Psi) 175.27

PSI 20 DEGREE

THETA	LW*E_3	LB*E_4	(LW-LB)/(E*cos(Psi))*E_5
0	68.000	1.900	38.688
10	58.000	2.600	33.766
20	36.000	1.700	2053952.000
30	49.000	1.200	279.497
40	101.000	1.000	57.568
50	64.000	0.800	36.469
60	58.000	0.750	33.049
70	70.000	0.700	39.898
80	97.000	0.700	55.303
100	47.000	1.000	26.758
110	153.000	1.200	87.225
120	175.000	1.500	99.759
130	234.000	2.200	133.381
140	380.000	1.200	216.224
180	285.000	11.200	161.966
190	145.000	3.200	82.546
200	194.000	1.800	110.582 x
210	75.000	1.500	42.705
220	56.000	1.000	31.893
230	46.000	0.900	26.194
240	45.000	0.800	25.629
250	32.000	0.800	18.212
260	19.000	1.000	10.783
280	34.000	1.200	19.330
290	26.700	0.900	15.182
300	22.000	1.500	12.466
310	20.900	2.400	11.787
320	22.500	4.100	12.603
325	24.300	8.400	13.385
355	58.000	1.900	32.983

1/15/1978 WINDOW NO 245 & 244
TART LD 185.00 END LD 191.00
MEAN LD 188.00 E COS(PST) 170.13

PSI 30 DEGREE

THETA	LW*E_3	LB*E_4	(LW-LB)/(E*cos(PST))*E_5
0	40.000	2.600	23.359
10	73.000	1.600	42.815
20	510.000	1.200	299.703
30	2950.000	1.000	1733.985
40	440.000	0.800	258.581
50	105.000	0.750	61.674
60	80.000	0.600	46.988
70	91.000	0.700	53.448
80	123.000	0.800	72.251
100	68.000	1.100	39.905
110	208.000	1.500	122.173
120	265.000	2.200	155.635
130	460.000	10.200	269.785
170	310.000	11.200	181.557
180	145.000	3.100	85.048
190	92.000	1.900	53.965
200	71.000	1.500	41.645
210	150.000	1.000	88.110 x
220	45.000	0.800	26.404
230	35.000	0.800	20.526
240	38.000	0.800	22.289
250	25.800	1.000	15.106
260	18.500	1.100	10.809
280	30.500	1.000	17.869
290	23.500	1.500	13.725
300	20.000	2.400	11.615
310	19.200	4.000	11.050
315	19.800	8.200	11.156
345	30.000	1.800	17.528
350	28.500	1.800	16.646

1/15/1970 WINDOW NO 246 & 244
 TART LD 182.50 END LD 183.00
 MEAN LD 182.50 E COS(PSI) 146.08

PSI 40 DEGREE

THETA	LW*E_3	LB*E_4	(LW-LB)/(E*COS(PSI))*E_5
0	26.300	1.600	17.894
10	37.000	1.200	25.246
20	70.000	1.000	47.849
30	560.000	0.800	383.284
40	3850.000	0.800	2635.456
50	660.000	0.600	451.751
60	161.000	0.700	110.162
70	144.000	0.800	98.518
80	189.000	1.000	129.308
90	116.000	1.500	79.303
100	330.000	2.200	225.746
120	580.000	10.200	396.331
160	310.000	11.200	211.439
170	146.000	3.100	99.730
180	85.000	1.800	58.062
190	59.000	1.600	40.278
200	44.000	1.000	30.051
210	39.000	0.800	26.642
220	133.000	0.800	90.988
230	29.500	0.800	20.139
240	25.600	1.000	17.456
250	18.900	1.000	12.869
260	15.800	1.000	10.747
280	25.800	1.500	17.558
290	19.500	2.500	13.177
300	17.000	4.100	11.356
305	16.700	8.000	10.884
335	22.000	1.800	14.937
340	18.700	1.800	12.678
350	21.000	2.600	14.197

1/19/1970 WINDOW NO 246 & 244
 TART LD 153.00 END LD 155.00
 MEAN LD 154.00 E COS(PSI) 103.44

PSI 50 DEGREE

THETA	LW×E_3	LB×E_4	(LW-LB)/(E×COS(PSI))×E_5
0	17.900	1.200	17.189
10	23.200	1.000	22.332
20	33.000	0.850	31.821
30	74.000	0.800	71.464
40	610.000	0.700	580.663
50	670000.000	0.700	6477366.000
60	1030.000	0.800	995.697
70	320.000	0.900	309.280
80	330.000	1.300	318.909
100	420.000	2.200	386.496
110	650.000	9.400	627.493
150	261.000	11.200	251.244
160	134.000	3.100	129.248
170	78.000	1.800	75.234
180	51.000	1.500	49.160
190	37.000	1.000	35.674
200	28.000	0.800	26.992
210	23.400	0.800	22.545
220	25.300	0.800	24.382
230	155.000	1.100	149.743 x
240	22.600	1.200	21.733
250	14.000	1.400	13.399
260	15.900	1.100	15.265
280	25.200	4.000	23.976
290	18.100	4.700	17.044
295	17.900	8.500	16.483
325	17.300	1.800	16.551
330	13.100	1.800	12.491
340	13.400	2.600	12.703
350	15.000	1.600	14.347

1/19/1978 WINDOW NO 246 & 244
 TART LD 155.000 END LD 160.000
 MEAN LD 157.500 E COS(PSI) 82.29

PSI 60 DEGREE

THETA	LW*E_3	LB*E_4	(LV-LB)/(E*COS(PSI))*E_5
0	14.800	1.000	17.864
10	19.200	0.950	23.217
20	25.300	0.800	30.648
30	45.000	0.800	54.588
40	133.000	0.800	161.529
50	710.000	0.900	862.709
60	1830.000	2.000	2223.885
70	3000.000	3.900	3645.239
80	1270.000	8.200	1542.355
100	1220.000	12.800	14824.344
140	310.000	11.100	375.375
150	115.000	3.200	139.363
160	76.000	1.800	92.139
170	49.000	1.600	59.352
180	33.000	1.100	39.969
190	25.200	0.900	30.515
200	20.100	0.900	24.317
210	16.700	0.900	20.185
220	14.900	1.100	17.973
230	20.800	1.500	25.095
240	290.000	1.800	352.200 x
250	18.100	2.000	21.753
260	37.000	3.800	44.502
280	54.000	8.200	64.626
285	29.000	10.600	33.954
315	13.100	1.800	15.701
320	11.700	1.800	14.000
330	11.200	2.600	13.295
340	11.700	1.700	14.012
350	12.900	1.200	15.531

1/19/1978 WINDOW NO 246 & 244
 (TART LD 168.88 END LD 159.88
 MEAN LD 159.58 E COS(Psi) 57.88

PSI 70 DEGREE

THETA	LW×E_3	LB×E_4	(LW-LB)/(E×COS(Psi))×E_5
0	13.488	8.958	23.341
10	16.788	8.888	29.156
20	23.188	8.888	40.384
30	34.888	8.888	59.585
40	64.888	8.958	112.187
50	182.888	1.388	319.851
60	1458.888	5.888	2542.831
70	4488888.888	14.588	77188384.888
80	12888.888	42.888	21844.816
130	458.888	18.988	787.515
140	128.888	3.188	289.978
150	78.888	1.888	122.484
160	44.888	1.688	76.988
170	38.888	1.188	52.435
180	22.488	8.988	39.138
190	17.388	8.888	38.289
200	13.888	8.988	24.851
210	12.188	1.188	21.834
220	11.188	1.388	19.244
230	11.688	1.888	28.834
240	15.288	2.888	26.314
250	568.888	4.888	981.696
260	37.888	18.888	63.154
275	149.888	15.588	258.669
305	12.188	2.288	28.841
310	11.888	2.288	18.911
320	9.988	2.988	16.859
330	9.788	1.788	16.718
340	18.388	1.288	17.859
350	11.488	1.888	19.823

1/19/1970 WINDOW NO 246 & 244
TART LD 159.00 END LD 157.00
MEAN LD 158.00 E COS(PSI) 28.67

PSI 80 DEGREE

THETA	LM-E-3	LB-E-4	(LM-LB)/(E×COS(PSI))×E-5
0	10.400	0.800	35.997
10	12.800	0.800	44.368
20	17.300	0.800	60.064
30	24.000	0.950	83.382
40	40.000	1.000	139.174
50	85.000	1.600	295.927
60	350.000	6.100	1218.695
70	4300.000	26.000	14989.609
80	91000000.000	139.000	317413760.000
120	600.000	8.500	2089.874
130	140.000	3.200	487.213
140	57.000	1.900	198.157
150	33.000	1.600	114.548
160	22.600	1.100	78.447
170	16.300	1.000	56.507
180	12.700	0.800	44.019
190	10.600	0.800	34.602
200	8.400	1.000	28.951
210	7.700	1.200	26.440
220	7.400	1.300	25.358
230	7.600	1.500	25.986
240	7.800	2.900	26.195
250	11.300	17.000	33.485
260	600.000	19.500	2086.037
295	11.600	2.600	39.555
300	9.600	2.600	32.579
310	7.800	3.200	26.091
320	7.200	1.900	24.151
330	7.200	1.300	24.661
340	7.700	1.000	26.509
350	8.800	0.950	30.364

Apollo Specimen

11/ 4/1969

WINDOW APOLLO

START LD 250.00 END LD 275.00
 MEAN LD 262.50 E COS(PSI) 274.29

PSI ° DEGREE

THETA	LW×E_3	LB×E_4	(LW-LB)/(E×COS(PSI))×E_5
15	2650.00	98.00	962.54
20	2280.00	60.00	829.04
30	1930.00	28.00	702.60
40	1850.00	21.00	673.69
50	1800.00	18.00	655.57
60	1830.00	20.00	666.44
70	1920.00	23.00	699.14
80	3400.00	1800.00	583.31
100	2040.00	3900.00	601.54
110	2130.00	10.50	776.15
120	2010.00	9.00	732.46
130	1940.00	9.00	706.94
140	2040.00	11.50	743.31
150	2270.00	19.50	826.87
160	2950.00	50.00	1073.44
200	3200.00	215.00	1158.79
210	2220.00	48.00	807.60
220	2000.00	18.00	728.49
230	1900.00	11.50	692.27
240	1920.00	9.50	699.63
250	2130.00	9.00	776.21
260	2850.00	3200.00	922.37
280	5400.00	1800.00	1903.06
290	2380.00	20.50	866.93
300	1830.00	17.00	666.55
310	1640.00	17.00	597.28
320	1600.00	18.00	582.66
330	1610.00	21.00	586.19
340	1750.00	27.50	637.00
345	1900.00	38.00	691.30

11/ 4/1969 WINDOW APOLLO

START LD 250.00 END LD 235.00

LEAN LD 242.50 E COS(PSI) 249.55

PSI 10 DEGREE

THETA	LW*E_3	LB*E_4	(LW-LB)/(E*COS(PSI))*E_5
5	780000.00	65.00	3125669.00
10	55000.00	43.00	22038.27
20	2750.00	22.50	1101.10
30	2050.00	18.00	820.77
40	1880.00	16.00	752.73
50	1800.00	16.50	720.65
60	1840.00	18.00	736.62
70	1960.00	23.50	784.48
80	3400.00	14000.00	801.45
100	2400.00	1550.00	899.63
110	2050.00	6.60	821.23
120	1950.00	6.80	781.15
130	1930.00	8.70	773.05
140	2150.00	17.70	860.85
150	2800.00	59.00	1119.67
190	2860.00	130.00	1140.87
200	1950.00	41.00	779.77
210	1750.00	21.00	700.43
220	1700.00	16.00	680.59
230	1660.00	14.00	664.65
240	1720.00	14.50	688.67
250	2050.00	19.50	820.71
260	2440.00	10000.00	577.05
280	2950.00	4600.00	997.81
290	1930.00	25.50	772.38
300	1630.00	21.00	652.34
310	1480.00	19.50	592.29
320	1450.00	21.00	580.21
330	1450.00	25.50	580.03
335	1500.00	36.00	599.65

11/ 6/1969 WINDOW APOLLO

START LD 250.00 END LD 240.00

EAN LD 245.00 E COS(PSI) 240.57

PSI 20 DEGREE

THETA	LW*E_3	LB*E_4	(LW-LB)/(E*COS(PSI))*E_5
0	16000.00	43.00	6640.11
10	54000.00	23.00	22445.80
20	185000.00	17.00	7690096.00
30	2350.00	16.50	976.16
40	1900.00	16.00	789.13
50	1780.00	17.00	739.21
60	1760.00	19.00	730.81
70	1900.00	26.00	788.71
80	3300.00	16000.00	706.66
100	2200.00	1500.00	852.15
110	2300.00	7.80	955.74
120	2350.00	10.00	976.43
130	2450.00	18.50	1017.65
140	3440.00	63.00	1427.32
180	2650.00	110.00	1096.98
190	1920.00	45.00	796.24
200	1700.00	32.00	705.33
210	1500.00	26.00	622.44
220	1450.00	24.00	601.74
230	1500.00	24.00	622.52
240	1580.00	25.00	655.74
250	1850.00	36.00	767.51
260	2550.00	15300.00	423.99
280	2550.00	6500.00	789.79
290	1650.00	33.00	684.50
300	1350.00	27.00	560.05
310	1290.00	27.00	535.11
320	1260.00	30.00	522.51
325	1250.00	38.00	518.02
355	1400.00	48.00	579.96

11/ 6/1969

WINDOW APOLLO

START LD 250.00

END LD 250.00

EAN LD 250.00

E COS(PSI) 226.23

PSI 30 DEGREE

THETA	LW*E_3	LB*E_4	(LW-LB)/(E*COS(PSI))*E_5
0	1300.00	20.50	573.72
10	1620.00	16.00	715.36
20	6600.00	14.50	2915.69
30	16100.00	14.50	7115.87
40	3400.00	15.00	1502.20
50	2380.00	16.00	1051.30
60	2200.00	19.00	971.60
70	2320.00	27.00	1024.29
80	4000.00	18500.00	950.34
100	3150.00	1800.00	1312.80
110	3300.00	11.00	1458.18
120	3600.00	19.00	1590.43
130	4150.00	70.00	1831.29
170	2830.00	102.00	1246.41
180	1900.00	27.50	838.62
190	1650.00	20.00	728.45
200	1610.00	18.00	710.86
210	1560.00	17.00	688.80
220	1440.00	17.00	635.76
230	1460.00	20.00	644.46
240	1600.00	26.00	706.08
250	1860.00	42.00	820.30
260	2700.00	17000.00	442.02
280	2560.00	2800.00	1007.80
290	1600.00	40.00	705.46
300	1330.00	32.00	586.47
310	1250.00	34.00	551.02
315	1230.00	40.00	541.92
345	1160.00	49.00	510.58
350	1190.00	36.00	524.41

11/ 7/1969 WINDOW APOLLO
 START LD 250.00 END LD 270.00
 JEAN LD 260.00 E COS(PSI) 208.12

PSI 40 DEGREE

THETA	LW*E_3	LB*E_4	(LW-LB)/(E*COS(PSI))*E_5
0	1130.00	14.00	542.28
10	1340.00	12.00	643.28
20	1780.00	12.00	854.70
30	9400.00	12.30	4516.02
40	29600.00	13.00	14221.89
50	4950.00	15.00	2377.71
60	3500.00	19.00	1680.80
70	3500.00	28.50	1680.35
80	5300.00	18500.00	1657.69
100	4600.00	1650.00	2130.97
110	5500.00	18.00	2641.83
120	7100.00	56.00	3408.79
160	2830.00	84.00	1355.75
170	1800.00	21.50	863.85
180	1530.00	11.50	734.60
190	1420.00	12.00	681.72
200	1400.00	12.50	672.09
210	1490.00	13.50	715.28
220	1570.00	17.00	753.55
230	1530.00	22.00	734.09
240	1620.00	28.50	777.02
250	1870.00	46.00	896.31
260	2850.00	15000.00	648.66
280	2420.00	2500.00	1042.66
290	1610.00	44.00	771.48
300	1340.00	38.00	642.03
305	1270.00	42.00	608.20
335	1050.00	50.00	502.11
340	1050.00	36.00	502.79
350	1060.00	19.00	508.41

11/ 7/1969

WINDOW APOLLO

START LD 257.00 END LD 265.00

EAN LD 257.50 E COS(PSI) 172.95

PSI 50 DEGREE

THETA	LW*E_3	LB*E_4	(LW-LB)/(E*COS(PSI))*E_5
0	910.00	10.60	525.54
10	980.00	9.80	566.06
20	1250.00	10.00	722.15
30	2070.00	10.60	1196.23
40	1610.00	12.20	9308.08
50	5000.00	15.40	28908.38
60	6600.00	20.50	3814.84
70	5200.00	34.00	3004.60
80	7100.00	25600.00	2624.96
100	7600.00	2000.00	4278.57
110	3600.00	52.00	2078.46
150	3300.00	118.00	1901.19
160	1800.00	26.00	1039.23
170	1370.00	13.20	791.35
180	1230.00	9.30	710.63
190	1160.00	10.00	670.12
200	1150.00	10.80	664.29
210	1180.00	11.80	681.58
220	1300.00	17.50	750.63
230	1460.00	29.70	842.43
240	1530.00	38.00	882.43
250	1700.00	55.00	979.74
260	2830.00	15000.00	768.99
280	2130.00	6300.00	867.28
290	1430.00	51.00	823.86
295	1350.00	52.00	777.54
325	910.00	52.00	523.14
330	900.00	32.00	518.52
340	860.00	18.20	496.19
350	870.00	13.00	502.27

11/ 8/1969 WINDOW APOLLO

START LD 250.00 END LD 270.00
EAN LD 260.00 E COS(PSI) 135.84

PSI 60 DEGREE

THETA	LW×E_3	LB×E_4	(LW-LB)/(E×COS(PSI))×E_5
0	740.00	9.70	544.04
10	800.00	9.40	588.23
20	1100.00	9.80	809.05
30	1540.00	11.00	1132.87
40	3800.00	13.40	2796.40
50	22500.00	17.70	16562.16
60	183000.00	26.00	134714.22
70	15100.00	46.00	11112.54
80	14700.00	34000.00	8318.54
100	20000.00	3200.00	14487.51
140	3900.00	130.00	2861.43
150	1800.00	33.00	1322.65
160	1350.00	13.80	992.79
170	1150.00	8.70	845.94
180	1050.00	7.60	772.40
190	980.00	8.80	720.78
200	980.00	9.60	720.72
210	1030.00	11.20	757.41
220	1100.00	18.00	808.44
230	1250.00	31.00	917.91
240	1480.00	63.00	1084.87
250	1680.00	80.00	1230.85
260	1870.00	7000.00	861.30
280	2150.00	10400.00	817.13
285	1560.00	980.00	1076.26
315	820.00	59.00	599.30
320	800.00	38.00	586.13
330	760.00	20.00	558.00
340	730.00	14.20	536.35
350	715.00	11.20	525.53

11/ 8/1969

WINDOW APOLLO

START LD 250.00 END LD 250.00

EAN LD 250.00 E COS(PSI) 89.35

PSI 70 DEGREE

THETA	LW*E_3	LB*E_4	(LW-LB)/(E*COS(PSI))*E_5
0	500.00	8.00	558.72
10	530.00	7.80	592.32
20	660.00	8.30	737.76
30	940.00	9.60	1051.00
40	1800.00	12.40	2013.23
50	5200.00	17.40	5818.06
60	37000.00	26.50	41408.62
70	160000.00	53.00	179071.16
80	290000.00	46000.00	27309.26
130	4000.00	108.00	4464.84
140	1570.00	26.00	1754.28
150	1000.00	11.00	1118.00
160	780.00	7.20	872.20
170	660.00	5.50	738.08
180	600.00	5.00	670.98
190	560.00	6.00	626.10
200	560.00	7.30	625.95
210	590.00	9.00	659.34
220	650.00	14.50	725.88
230	740.00	24.50	825.49
240	910.00	43.00	1013.69
250	1200.00	94.00	1332.56
260	2300.00	13800.00	1029.69
275	5600.00	48000.00	895.39
305	680.00	63.00	754.03
310	640.00	39.00	711.94
320	570.00	21.00	635.61
330	530.00	14.50	591.57
340	500.00	10.80	558.41
350	490.00	9.20	547.39

11/ 8/1969

WINDOW APOLLO

START LD 250.00 END LD 250.00

MEAN LD 250.00 E COS(PSI) 45.36

PSI 80 DEGREE

THETA	LW*E_3	LB*E_4	(LW-LB)/(E*COS(PSI))*E_5
0	300.00	5.90	660.04
10	320.00	5.80	704.15
20	400.00	6.80	880.28
30	610.00	8.50	1342.84
40	1130.00	10.70	2488.68
50	2860.00	15.60	6301.31
60	8800.00	27.00	19393.27
70	61000.00	64.00	134457.75
80	550000.00	68000.00	12109520.00
120	7400.00	95.00	16202.04
130	1510.00	25.50	3323.11
140	820.00	11.00	1805.23
150	560.00	7.10	1232.93
160	440.00	5.40	968.77
170	370.00	4.30	814.70
180	340.00	3.90	748.66
190	320.00	5.20	704.28
200	320.00	7.00	703.88
210	335.00	9.10	736.49
220	370.00	14.50	812.45
230	420.00	22.50	920.91
240	510.00	40.00	1115.46
250	700.00	74.00	1526.81
260	2010.00	15200.00	1080.18
295	540.00	79.00	1172.99
300	490.00	50.00	1069.16
310	390.00	25.50	854.12
320	350.00	16.00	768.03
330	310.00	11.00	680.96
340	295.00	8.80	648.37
350	285.00	7.00	626.73

APPENDIX D

INFRARED SCANS AND MASS SPECTROMETER DATA

The sodium chloride flats were mutually contaminated with the Vycor windows in the vacuum system. These flats were removed and placed in a special container for shipment to the facility housing the Beckman spectrophotometer. This instrument was used to run infrared scans from 2.5 to 25 microns to identify collected materials. The test report results are duplicated below for ready reference

No. 1. NaCl Flats - Submitted 1 January 1970

A thin film of a silicone (dimethyl siloxane type) oil was detected on these flats by infrared analysis. No other organics were detected.

No. 2. NaCl Flats - Submitted 14 January 1970

No organics could be detected on the surfaces of these flats by infrared analysis using 10x scale expansion.

The No. 1 NaCl flat contamination was due to the room temperature cured RTV while the No. 2 NaCl flat contamination was due to the high-temperature cured RTV.

The background gas composition present in the vacuum system during the experiment was monitored with a mass spectrometer. A Quad 150 residual gas analyzer manufactured by Electronic Associates Inc. (EAI) was used for this task. The residual gas analyzer has an extended mass range of 1 to about 150 atomic mass units. Data obtained was used to qualitatively identify the residual vapors present before the RTV samples were heated and while the samples were heated. The data also provided a comparison of outgassing rates for the two different samples.

The specific mass spectrometer data obtained during the course of this investigation is presented in Figures D1 through D4. Figure D1 illustrates the relative amounts of residual gas present in the vacuum system during the heating of high-temperature cured RTV-560. The calibration of the system was performed at two different points in time. After 24 hours of pumping on the system while heating without RTV present a mass spectrometer data run was performed. This data is presented in Figure D2. The system was then only pumped for an additional 24 hours. Figure D3 shows the results of the mass spectrometer scan after that time period. It should be noted that the magnitude of the coordinates on the abscissa was chosen for convenience only. Obviously the data in Figure D1 were taken under more severe circumstances than the data in Figures D2 and D3. As a result the gain in the system was drastically reduced for data-gathering purposes in Figure D1. The relative magnitude of each m/e ratio is only of significance in these figures. Finally, the scans taken during the outgassing of the room temperature - cured RTV are presented in Figure D4.

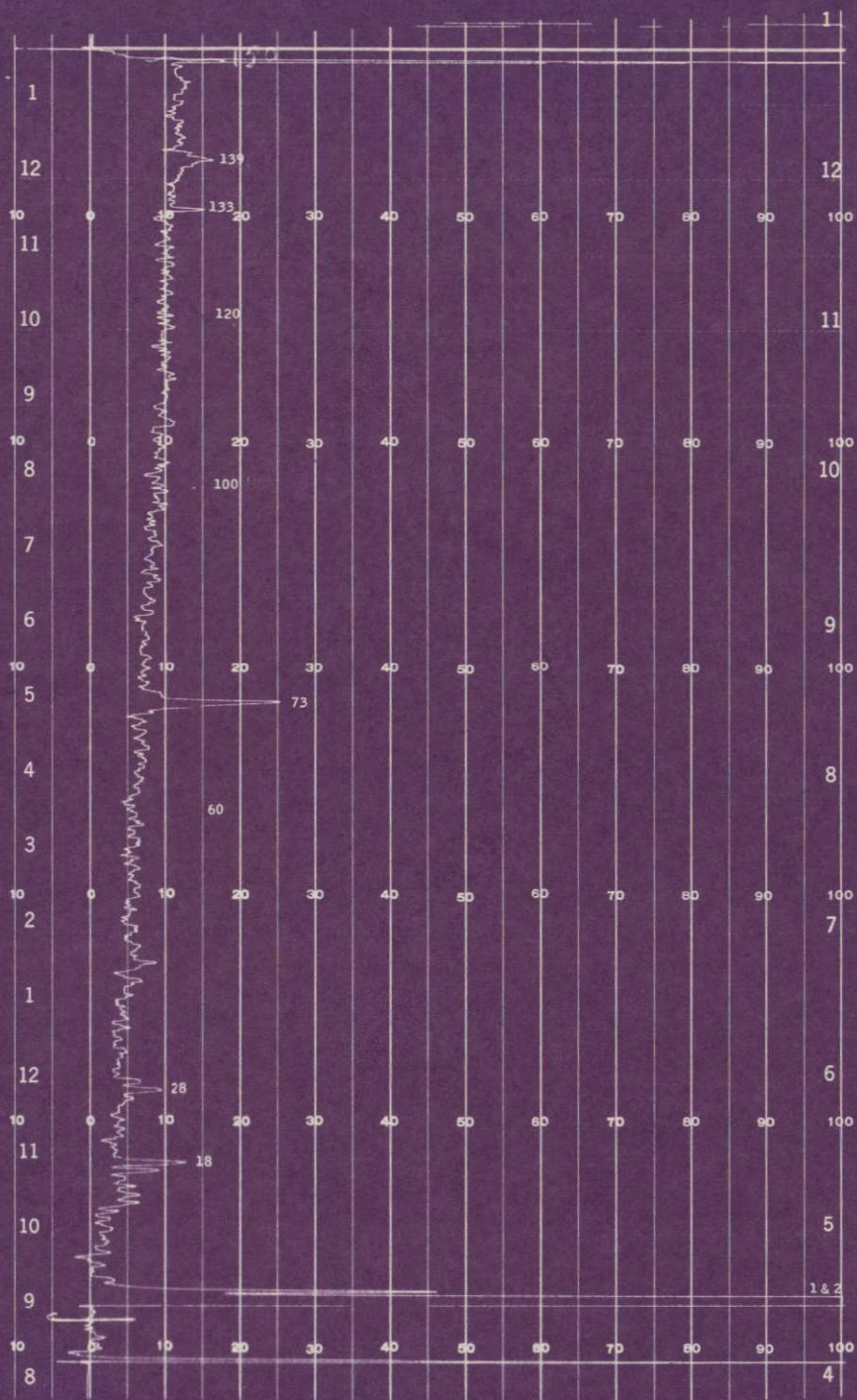


Figure D1. Mass Spectrum Data - High Temperature Cured Rubber (10-9-69)

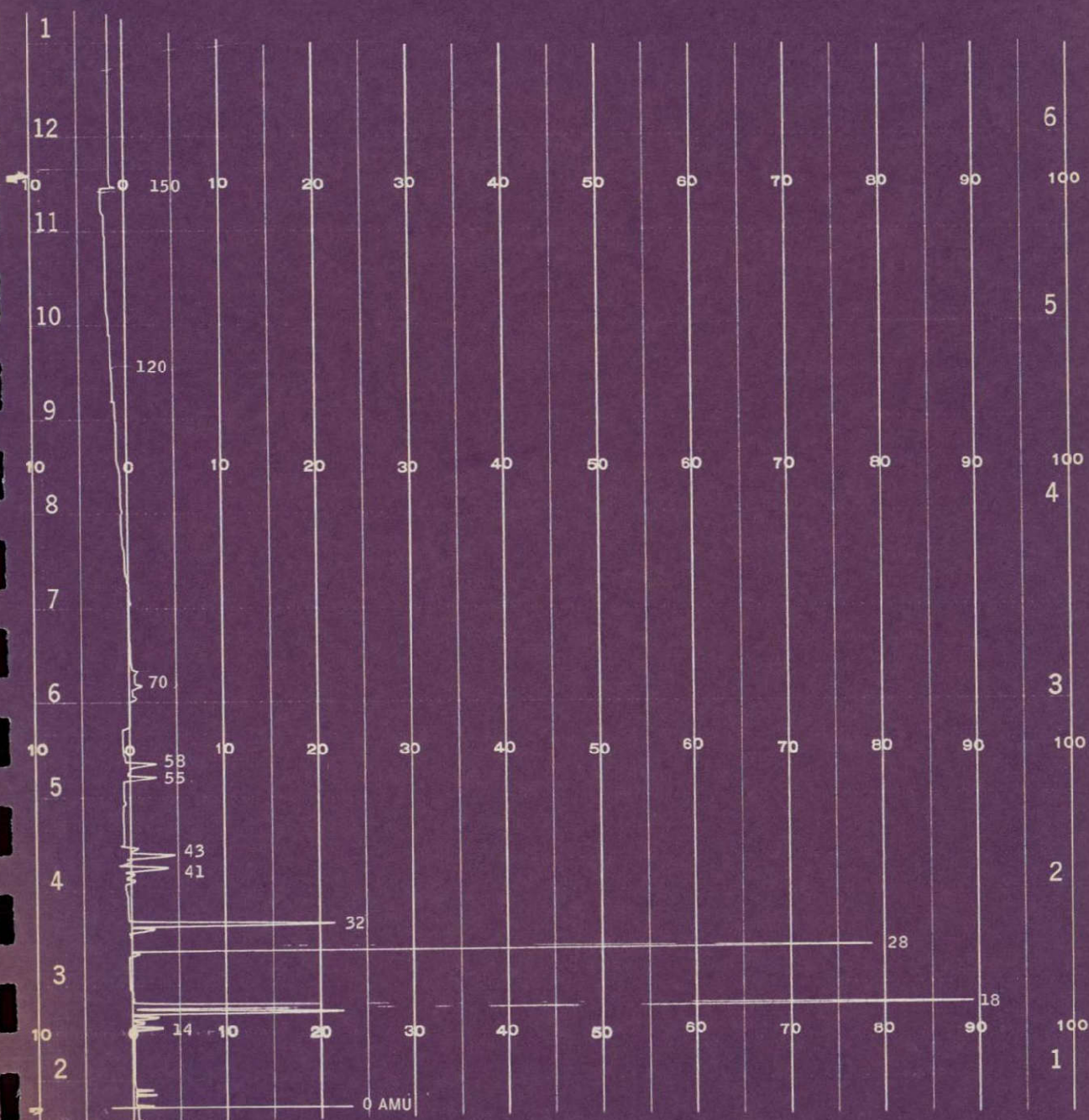


Figure D2. Mass Spectrum Data - 24 Hour Bake of System
Only: Total Pressure 4×7^{-10} Torr
(12-10-69-Morning)

END OF SCAN

PRECEDING PAGE BLANK NOT FILMED.

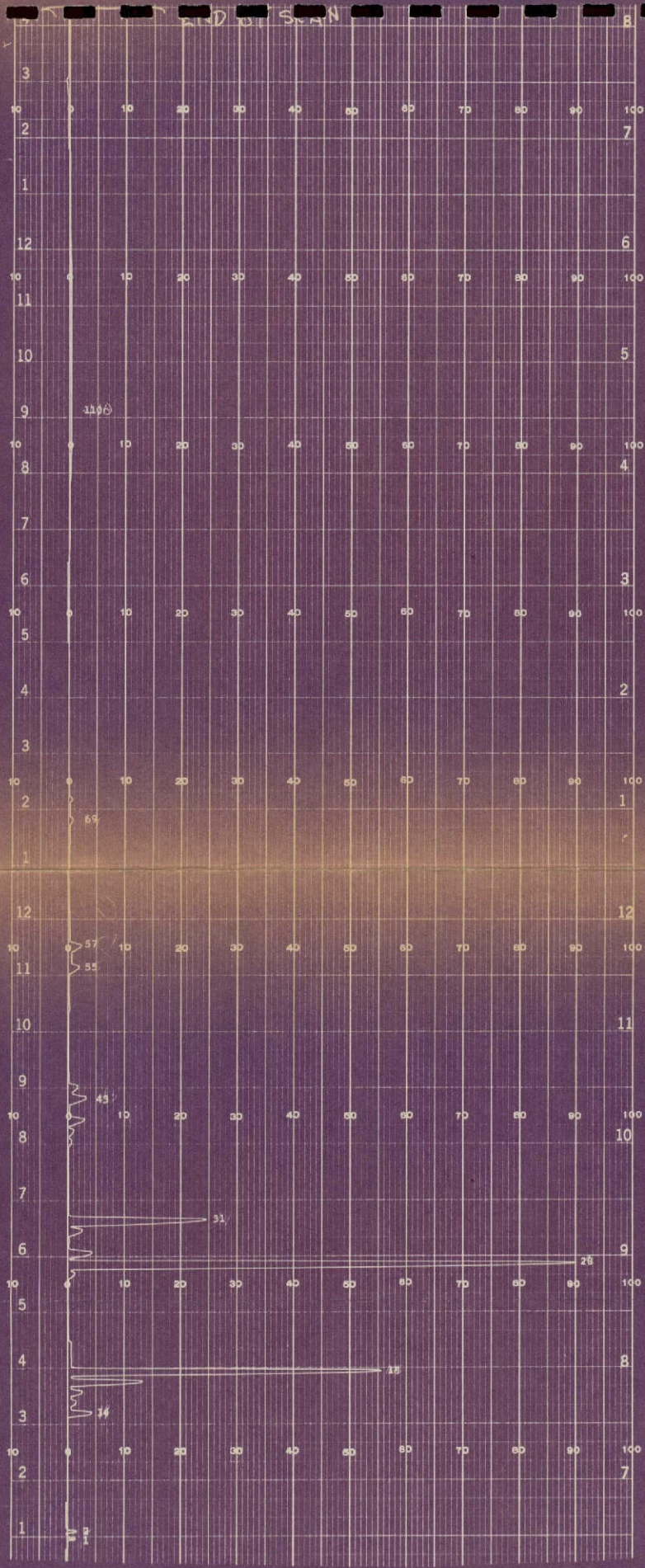


Figure D3. Mass Spectrum Data - Total Pressure
 3.2×10^{-7} ; 48 Hours Pumping System
Only (12-11-69-Morning)

FOLDOUT FRAME

FOLDOUT FRAME

PRECEDING PAGE BLANK NOT FILMED

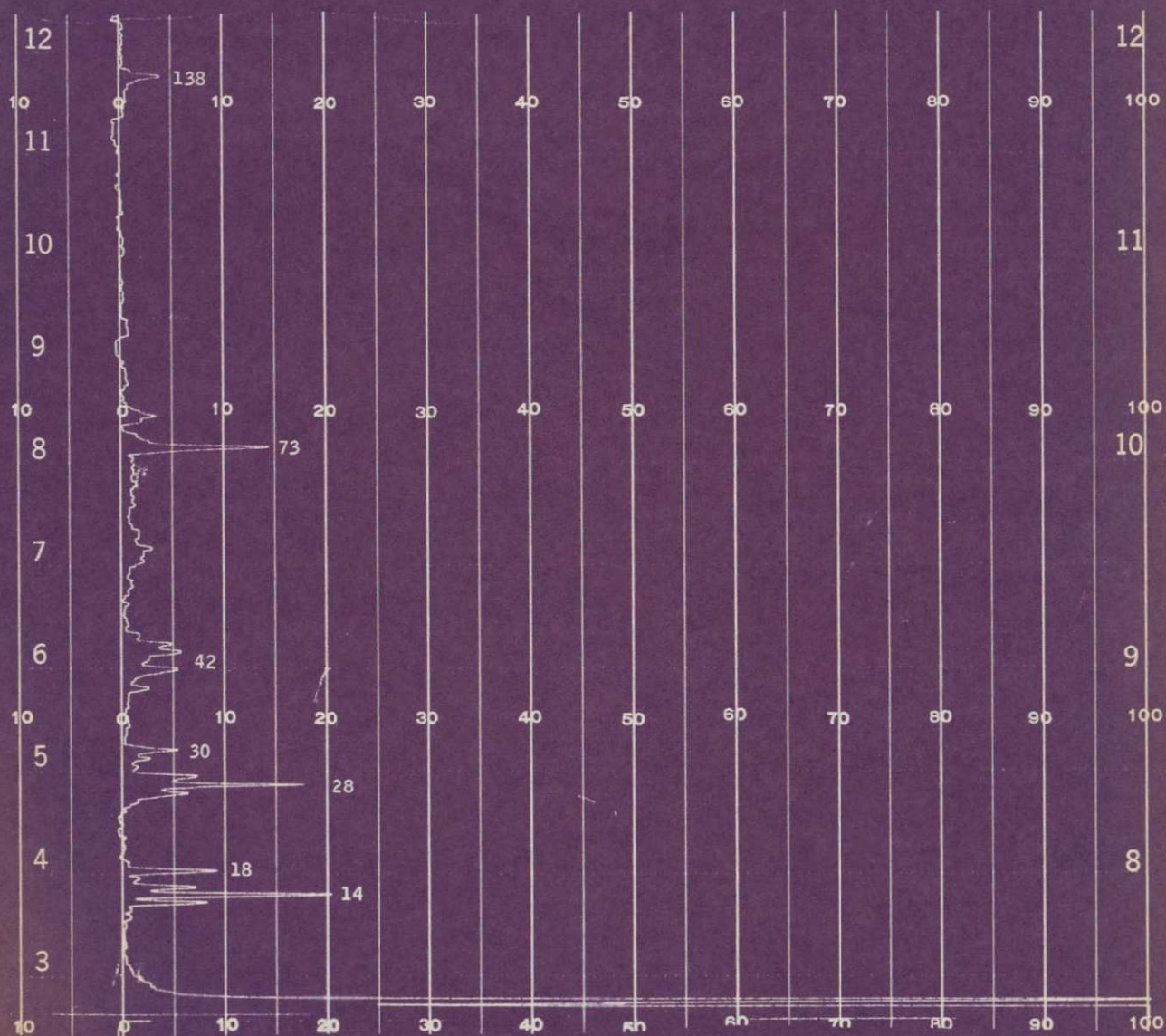


Figure D4. Mass Spectrum Data - Pressure 3.2×10^{-6} ;
Room Temperature Cured Rubber (1-12-70)

To determine the composition of the as-received uncured RTV 560 (resin and hardner), a routine chemical analysis was performed. Three tests were used. Infrared absorption spectra from 2.5 to 15 microns were used to "fingerprint" the materials. X-ray diffraction was used to identify the filler material. Finally, spectrographic tests were used for elemental analysis. The purpose of this data was to fingerprint and characterize the as-received material for reference to the experiment.

The results of the three chemical analysis are given below. The results as given are self-explanatory.

<u>Test</u>	<u>Infrared Identification</u>
Infrared	
<u>Sample</u>	
Resin	Organic (Sn by Spectro) acid salt
Hardner	Silicone (DC200 type) Resin
Spectrographic	
<u>Sample</u>	
Resin	Relatively large amounts of tin
Hardner	Relatively large amounts of iron and silicon
X-ray Diffraction	
The filler in the resin was identified as $\alpha \text{ Fe}_2 \text{ O}_3$	

REFERENCES

1. Heimsch, R P , Jolliffe, C. L , and Schmidt R N , "An Experimental and Analytical Study of Visual Detection in a Spacecraft Environment," NASA CR 1561, March 1970, NASA Contract NASA 2-5015
2. Muraca, R. F , and Whittick, J S , (Stanford Research Institute), "Polymers for spacecraft Applications, Final Report," JPL Contract No. 950745 under NAS 7-100, September 15, 1967.
3. Baker, C A , Visual Capabilities in the Space Environment, Pergamon Press, Oxford, page 7
4. Blackwell, Richard H , "Contrast Thresholds of the Human Eye," J Opt Soc. Am 36, No. 11 (1964)
5. Hardy, A. C , "How Large is a Point Source?" J Opt Soc Am 57, page 44 (1967)
6. Pustinger, J V., and Hodgson, F. N., "Identification of Volatile Contaminants of Space Cabin Materials," AMRL-TR-67-58, Air Force Contract AF 33(615)-3377, June, 1967
7. McPherson, D G. , (Ball Brothers Research Corporation), "Apollo Telescope Mount Extended Applications Study Program, ATM Contamination Study, Final Report," NASA CR-61173, May 25, 1967.
8. Fettes, E , ed , Chemical Reaction of Polymers, Interscience - Wiley Inc., N. Y , Vol 19 in the Interscience High Polymer Series, 1964.
9. Bolstad, L , Crook, T , Loy, J , and Gonnella, N , "Gassing and Flammability Testing of Organic Materials for Apollo C/M Stabilization and Control System," Honeywell Document No. A63777 A22(2), September 25, 1963
10. Crook, T , Personal Communication, Honeywell Inc , 1970
11. Frenkel, J , "Kinetic Theory of Liquids," Clarendon Press, Oxford, 1946
12. Terenin, A , and Solonitzin, Yu , "Discussion of the Faraday Society," Vol 28, 1959.
13. Lange, W J , and Riemersma, H , "American Vacuum Symposium Transaction," p. 167, 1962